Movement of bromide-ion and carbofuran in the humic sandy soil of a potato field with ridges and furrows

Measurements in the field and computations with the PEARL model

M. Leistra
J.J.T.I. Boesten

Movement of bromide-ion and carbofuran in the humic sandy soil of a potato field with ridges and furrows

Movement of bromide-ion and carbofuran in the humic sandy soil of a potato field with ridges and furrows

Measurements in the field and computations with the PEARL model

M. Leistra
J.J.T.I. Boesten

ABSTRACT

In fields with ridges and furrows (like in potato growing), water flow and pesticide transport in soil may be more complicated than in level fields. In a field experiment, movement of bromide-ion (as a tracer) and of the insecticide carbofuran through a sandy soil with humic top layer to the groundwater was measured. About 15% of the dosage was transported along the ridge surface to the furrows by rainfall and sprinkler irrigation. The wide ranges of measured concentrations in soil indicate that transport in soil was highly irregular. In a first period, incidental high concentrations were measured in the groundwater besides a vast majority of much lower concentrations. Substance behaviour in the averaged field and in separate ridge and furrow systems was simulated with the PEARL model. The distribution of the substances in soil indicated that about 20% of the water surface-flowed from the ridges to the furrows in the first month. Downward movement of the substances in soil was distinctly greater for the furrow system than for the ridge system. This increases the risk of pesticide leaching to groundwater, as compared to that for a more level field.

Contents

Preface

Computation models are recognised as efficient tools in the assessment of the environmental risks of the use of crop protection chemicals (pesticides). These models have to be tested against the results of detailed field experiments. The question arises which complications in pesticide behaviour in soil can occur in practice. Such complications can lead to under-estimation of the risk of pesticide leaching to groundwater. Some important crops are grown on ridges in the field. Water flow and pesticide transport in ridged soil can be more complex than in soils with a level surface.

A field experiment with potatoes grown on ridges was carried out near Roswinkel (Drenthe) in the years 2000 to 2002. The aim was to provide a data set on the extent of the complications in pesticide behaviour in ridged soil. Procedures in this field experiment were described by Crum et al. (2004) and many results were included in files on the appended compact disk.

The comprehensive Roswinkel field experiment was carried out by two Alterra teams in the framework of two research projects. Major contributors to the projects were: S.J.H. Crum, L.W. Dekker, D. Hooyer, A.M. Matser, K. Oostindie, L.J.T. van der Pas, J.H. Smelt and K. Trouwborst.

The present work is a follow-up of the experimental work; it deals mainly with computations in which the processes in the Roswinkel field are simulated with the PEARL model. This study was carried out in the framework of the LNV Research Theme BO-06-010: "Risk assessment methodology for pesticide registration" of the Dutch Ministry for Agriculture, Nature and Food Quality. The specific project BTG-4 reads: "Development and improvement of methods and tools for assessment of leaching to ground and surface water in the context of Dutch and EU pesticide registration". The new model version PEARL 3.3.3. used in the computations was made available by F. van den Berg.

Summary

The evaluation of the risk of leaching of pesticides from soil to groundwater usually deals with fields in which water flow and pesticide transport are assumed to be rather uniform. In almost any field experiment with pesticides, the soil surface is level. In computation models, it is usually assumed that water infiltration, water flow in soil and pesticide transport are rather uniform. In field conditions, however, distinct deviations from a level soil surface and the assumed uniform transport in soil may occur. An example is the usual growth of potatoes on ridges in a field. A fraction of the water from rainfall and sprinkler irrigation may flow over the soil surface from the ridges to the furrows. This may be attended by pesticide runoff from the ridges to the furrows. Thus transport below the furrows can be more extensive than expected for a level field, thus increasing the risk of pesticide leaching to groundwater.

In the field experiment near Roswinkel (2000-2002), dealing with a ridged potato field, rainfall was supplemented by sprinkler irrigation. The tracer bromide-ion and the example pesticide carbofuran were sprayed uniformly on the soil of the field. Water, bromide-ion and carbofuran were measured in the soil profile of both the ridges and the furrows. Computer simulations were carried out with the PEARL model for both the averaged field (ridges and furrows pooled), and for the ridge and furrow systems separately. Most of the input data were taken from the measurements in the field and in the laboratory; these were supplemented by literature data where needed. Adsorption of carbofuran to soil was measured in the laboratory, but its rate of transformation in soil had to be estimated from the field experiment.

First of all, water flow in soil had to be simulated with the PEARL-SWAP combination of models. The hydraulic relationships measured for a few soil columns in the lab were not representative for the averaged Roswinkel field, so they were not used in the further computations. Although representative hydraulic relationships (topsoil, subsoil) were taken from the Staring Series, substantial calibration to the Roswinkel field was found to be needed. The parameters in the function for groundwater discharge were also obtained by calibration. In this way reasonable simulations of the soil moisture profiles in the field and of the fluctuating depth of the groundwater table were obtained.

Bromide-ion served as a tracer for water flow and substance transport along the soil surface and in soil. The measurements at each depth were represented by their SD range: the average ± the standard deviation. The SD ranges for the averaged field were very wide, partly because the systematic differences between the ridges and furrows were not accounted for. Sometimes, the fraction of (almost) zero concentrations was unexpectedly high. A substantial amount of bromide-ion was taken up by the crop and released from the crop later in the growing season (so bromide-ion is a non-conservative tracer for cropped soil). It was difficult to sample the wet soil deeper in the profile, so only a limited number of deeper soil

measurements were available (incomplete concentration profiles). For all these reasons, the computations can only be compared with tendencies in the measurements.

Both the computed and measured distributions of carbofuran largely remained in the soil profile during the growing season. Again, the SD range of the measurements averaged for the field were very wide, partly because the systematic differences between the ridges and furrows were not taken into account.

The simulations for the averaged field allowed comparison of computed and measured concentrations of the substances at some depths in the groundwater, as a function of time. In the first period after application, incidentally high concentrations were found in the water samples, besides a vast majority of very low concentrations. This may be the result of preferential fast transport through the soil in the field. The wave of bromide-ion in the groundwater at two depths appeared somewhat earlier than simulated by the model. The onset of accelerated transformation of carbofuran in soil after the growing season and its instability in water samples interfered with the comparison of computations and measurements in the groundwater.

In the second series of comparisons between computations and measurements, the ridge and furrow systems were distinguished. Although the ranges of the measurements (average ± standard deviation) for the separate ridge and furrow systems were smaller than those for the averaged field, they were still very wide. This hampers a close comparison between computations and measurements. In the computations it was assumed that 20% of the amount of rainfall + sprinkler irrigation surface-flowed from the ridges to the furrows. The measurements indicated that about 15% of the dosage of the substances on the ridges was transported to the furrows by the surface flow of water. Comparison of computed and measured distributions of the substances in the soil profiles indicates that this surface flow-off of water was restricted to a first period of e.g. a month after application of the substances. In this period the above-ground plant parts were absent or still small. After the initial period, flow pathways of the water through the crop canopy may play a distinct role.

The complex measuring results for both the ridge and furrow systems can be explained by distinguishing three zones in the soil. In the first zone, water flow and substance transport proceed faster than corresponds to uniform transport. In the second zone, water flow and substance transport approximate chromatographic (uniform) transport, as described by the model. The third soil zone is found outside the main pathways of water flow and substance transport. A fraction of both bromide-ion and carbofuran moved faster to the subsoil than the wave computed by the model (uniform chromatographic transport). Another fraction, especially of carbofuran in the top layer, moved more slowly than computed. This distinction in three zones can also explain the very wide variation in the concentration measurements at a certain depth in soil.

Finally, the breakthrough curves of the substances at 1 m depth in soil were computed for the ridge and furrow systems separately. Breakthrough of bromide-ion from the furrow system was much earlier than that from the ridge system. The maximum concentration of bromide-ion leaching from the ridge system was not much lower than that leaching from the furrow system. There was a distinct breakthrough of carbofuran from the furrow system, but no breakthrough from the ridge system in the cropping period. This large difference is explained by the much longer time available for pesticide transformation in the ridge system. The simulation for the furrow system showed a much higher maximum leaching concentration of carbofuran than that for the all-time averaged field system.

The comparatively high leaching of carbofuran from the furrow system can be explained by a combination of factors:
    a) the rooting zone of the furrow system is 0.2 m thinner that that of the ridge system (due to hilling-up);
    b) the surface flow of water from rainfall and sprinkler irrigation from the ridges to the furrows;
    c) the run-off of pesticide from the ridges to the furrows;
    d) the shorter time available for transformation of the pesticide in the thin topsoil of the furrows;
    e) the lower plant root activity (uptake of water and pesticide) in the furrow systems.

The risk of pesticide leaching from a field with ridges and furrows to groundwater is distinctly higher than that from a similar field with a level surface. The first period with (largely) uncovered ridges seemed to be most vulnerable for non-uniform infiltration. In the case of the Roswinkel field, much additional sprinkler irrigation was given in the first period. Further, the rooting zone in this field was comparatively shallow. Possibly, these factors exaggerated the increase in leaching from the furrow systems. In practice, however, water flow-off from the ridges to the furrows can also occur later in the potato growing season. For a more general assessment of the increase in leaching risk, a wider range of field situations has to be studied and simulated.

1   Introduction

In the registration procedures for agricultural pesticides (European, National), the risk of leaching of the pesticides to groundwater is being evaluated. The maximum permissable concentration of a pesticide in groundwater is 0.1 µg/L (or lower), in view of the use of groundwater as a source of drinking water. The computation model PEARL (Pesticide Emission Assessment at Regional and Local scales) for the behaviour of pesticides in soil-plant systems is an important tool in evaluating the risk of leaching. The first version of the model was described by Tiktak et al. (2000; Manual) and Leistra et al. (2001; Processes). The role of PEARL in the Dutch decision tree for the evaluation of pesticide leaching was described by van der Linden et al. (2004).

The PEARL model makes simplifying assumptions, like those on uniform water flow and substance movement through the soil profile (chromatographic transport). It has to be investigated to what extent this type of simplifying assumption can lead to incorrect estimates of the risk of pesticide leaching to groundwater.

Growing potatoes is an example of a culture that occurs on fields with ridges and furrows. Such a ridged soil surface can have consequences for the uniformity of water infiltration into the soil surface and of water flow through the soil profile. Rain water can flow along the ridge surfaces to the furrows, followed by local infiltration. As the crop develops, more rain water lands on the crop with a chance of localised downward flow though the canopy (e.g. along stems and leaves) and local infiltration into the soil.

In a field experiment near Roswinkel (Province of Drenthe, The Netherlands), carried out in the years 2000 to 2002, the movement of the tracer bromide-ion and of the insecticide carbofuran in a humic sandy soil profile was studied (Crum et al., 2004). The conditions in the field (soil, weather, crop, cultural measures) were characterised. Movement of bromide-ion and carbofuran through the soil profile and to the groundwater were followed by sampling and chemical analysis. In laboratory experiments, adsorption and transformation of carbofuran in the Roswinkel soil were measured.

The first aim of the present report is to give a condensed survey of the field and laboratory experiments, with their results. The input data for the PEARL computations are collected both from the experiments of Crum et al. (2004) and from the literature. The results of the field experiment are prepared in a format in which they can be used for comparison of computations and measurements.

The second aim of this study is to carry out computations with the model PEARL, to simulate the processes in the Roswinkel field. The computed results have to be compared with the measured results, with a thorough analysis, if possible, of the causes of the differences. The three stages in this work deal with: a) simulation of

water flow in soil, b) simulation of the behaviour of the tracer bromide-ion, and c) simulation of the behaviour of the insecticide carbofuran, as example pesticide.

Building-up ridges above the rows of planted potatoes leads to two sub-systems in the potato field:
- the ridges with a comparatively thick humic-sandy rooting zone and containing most of the plant mass;
- the furrows with a thinner humic-sandy rooting zone containing a lower fraction of the plant mass.

Some water from rainfall and sprinkler irrigation can be expected to flow down the surfaces of the ridges to the furrows, resulting in higher infiltration in the latter. A fraction of the pesticide dosage could be transported via the soil surface from the ridges to the furrows. As a whole, the study should give insight into the effect of building ridges and furrows, with the attendant complications in water flow, on the movement of pesticides in soil, and thus on the risk of leaching to groundwater.

2 Field experiment

2.1 General description

The field experiment, with application of carbofuran and bromide-ion (as a tracer), was carried out on an arable field with humic sandy soil near Roswinkel (Province of Drenthe, The Netherlands). The soil profile consisted of a humic fine-sandy plough layer (0.3 m thick), with a fine-sandy subsoil in which the organic matter content decreased with depth. The groundwater table fluctuated around 1 m depth.

Potatoes were planted on the field on 20 April 2000, in rows 0.75 m apart. On 8 May, the ridges above the rows with potatoes were hilled up with soil from the furrows to their final height. The difference in height between the top of the ridges and the bottom of the furrows was 0.20 m.

In the morning of 10 May 2000, carbofuran (formulated as Curater-liquid) was sprayed broadcast on the soil surface (with ridges and furrows), using a tractor-mounted boom sprayer. The dosage of 4.63 kg ha^{-1} was applied in 617 L spray liquid per ha. Subsequently, KBr solution was sprayed at a dosage corresponding to 64.7 kg bromide-ion per ha, also in 617 L ha^{-1}. The size of the sprayed area was 21 m (boom width) x 100 m.

The potato plants emerged around the 22nd of May 2000. Soil cover by the plants increased roughly linearly, until almost complete soil cover on the 10th of July (Crum et al., 2004). Rooting depth is assumed to be restricted to the top 0.5 m of the soil profile, because of the dense sandy layer below that. The potatoes were harvested by the end of November 2000, but well before that the leaves will have died-off. In the next year 2001 the field was kept fallow.

Natural rainfall was supplemented by sprinkler irrigation and the total amount of water was measured with rain gauges. Air and soil temperatures were followed via measurements. The depth of the groundwater table was measured via six filter tubes, installed before pesticide spraying.

At three times after application of the substances, soil samples were taken with long tubes. The soil columns were divided into 0.1 m layers for extraction and chemical analysis. Soil moisture content was measured in the same samples. The upper groundwater was sampled via a grid of 64 tubes (0.9 to 2.0 m deep) on a subplot of the sprayed area. Carbofuran and bromide-ion in soil and water extracts/samples were analysed via HPLC.

An outline of the experimental field is given in Figure 2.1. Details on the procedures in the field experiment were described in an internal report by Crum et al. (2004). Some results were presented briefly in their report, while many raw data on the results were given on the appended CD. In the present report a condensed

description of procedures and results is given, and results were prepared for comparison with the PEARL computations in this study. Besides, additional input data on bromide-ion and carbofuran were collected from the literature.
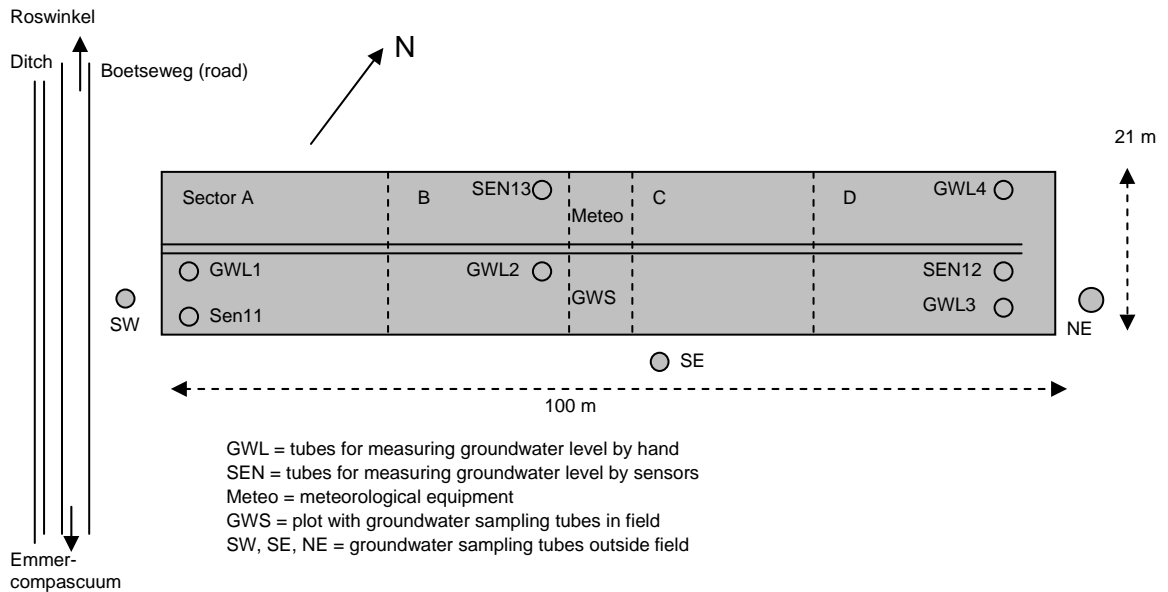
Figure 2.1. Outline of the Roswinkel experimental field. Ridges and furrows lengthways of the field.

2.2   Soil characteristics

The soil profile of the Roswinkel field consists of a fine-sandy aeolic deposit, in which a humic top layer has developed. The profile description is given in Table 2.1. The Dutch soil classification is: veldpodzol (de Bakker et al., 1989). The FAO soil classification is: gleyic podzol (FAO, 1988).

Table 2.1. Description of the soil profile of the Roswinkel experimental field.

Layer (m)	Soil horizon	Material
0 – 0.3	Ap	Humic, slighly loamy, moderately fine sand
0.3 – 0.4	Bh	Moderately humic, slight loamy, moderately fine sand
0.4 – 0.6	BC	Low humic, moderately fine sand
0.6 – 1.5	Cg	Moderately fine sand

The composition of the soil and the pH in various layers were measured by the Laboratory for Soil and Crop Testing, Oosterbeek, The Netherlands. The results are given in Table 2.2.

Table 2.2. Characteristics of the soil of the Roswinkel field. Sand, silt and clay are given in percentage of the mineral fraction.

Soil layer (m)	Sand (> 50 μm; %)	Silt (2-50 μm; %)	Clay (< 2 μm; %)	Organic matter (%)	Organic carbon (%)	pH-KCl
0-0.2	88.3	8.5	3.2	4.9	3.24	4.5
0.3-0.4	92.0	5.4	2.6	1.7	0.93	4.7
0.6-1.0	95.5	2.3	2.2	0.3	0.12	5.0
0-0.3	87.6	8.4	4.0	4.3	3.26	4.4
0.5-0.7	94.7	3.5	1.8	0.6	0.25	4.8

2.3   Weather conditions

Precipitation and evaporation

Rainfall was recorded continuously with a tipping-bucket rain gauge (aperture 400 cm^2 at a height of 0.5 m), connected to a data logger. The rainfall data could be checked on the basis of the KNMI measurements on the nearest surrounding rainfall stations Ter Apel, Emmen and Klazinaveen (KNMI, 2000a, 2001a). Rainfall before May 2000 and after September 2001 (outside the period with own measurements) was taken from the nearest KNMI rainfall station of Ter Apel (KNMI, 2000a, 2001a). The latter data were used to complete the meteorological input file of PEARL to data for full calendar years.

At nine times distributed over the period 10 May to 23 June 2000, the field was sprinkler irrigated. The slowly-driving sprinkler car was connected to a groundwater source 30 m deep. The sprinkler covered the whole width (21 m) of the sub-field. The amount of irrigation water per gift was measured by 24 rain gauges, distributed over the sub-field. The total amount of sprinkler irrigation was 136 mm. Details are given by Crum et al. (2004).

The daily values of rainfall plus irrigation in the period with own measurements are given in Figure 2.2. It shows that substantial amounts of water fell on the field throughout the experimental period.

The daily values of reference crop evaporation were taken to be the average of the values calculated by KNMI (2000a, 2001a) for the weather stations at the nearest airports of Eelde and Hoogeveen. This evaporation is calculated by Makkink's method.

The cumulative amounts of rainfall plus irrigation and of reference crop evaporation in the first 17 months after application are given in Figure 2.3. Again it is shown that substantial amounts of water fell on the field. The cumulative reference crop evaporation clearly shows the course of this evaporation over the seasons.
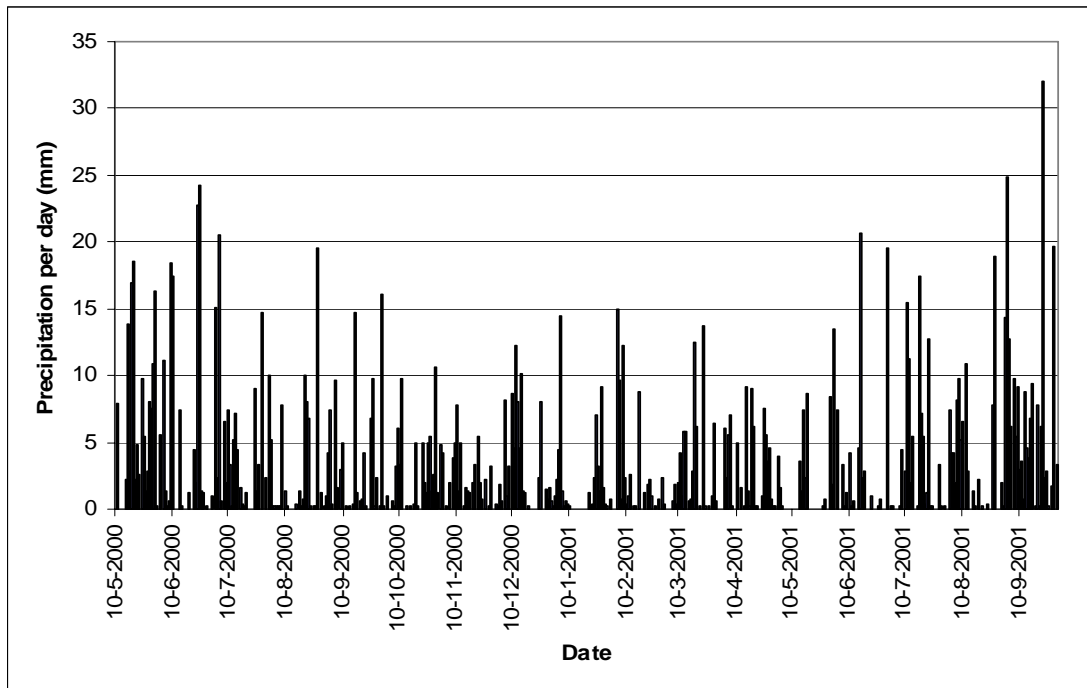
Figure 2.2. Daily values of rainfall plus irrigation on the Roswinkel field after application of the substances on 10 May 2000.
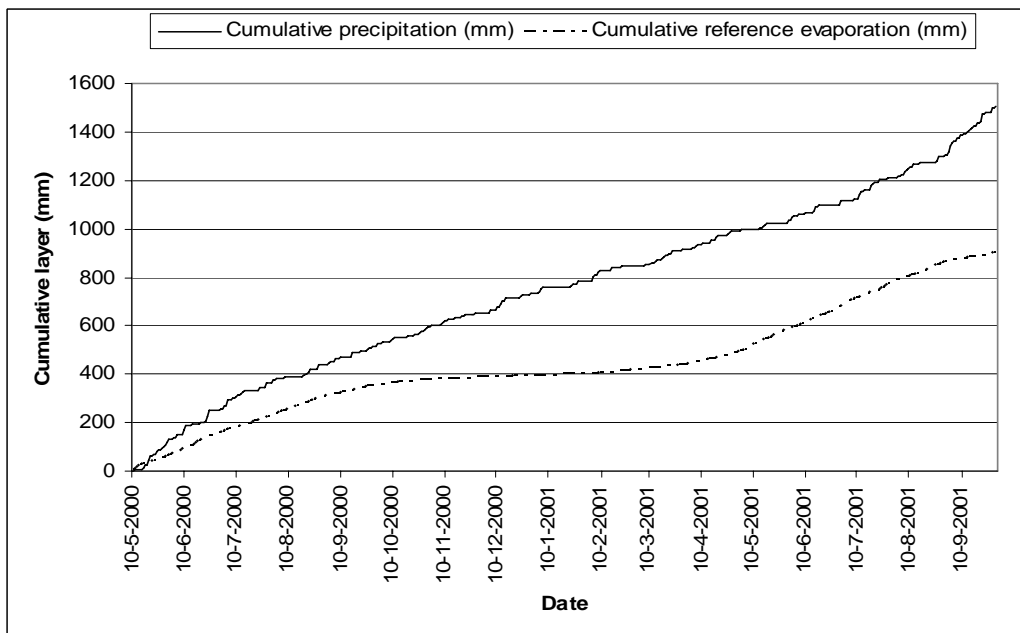
Figure 2.3. Cumulative precipitation (= rainfall + irrigation) and cumulative reference crop evaporation for the field experiment.

Temperatures

Daily minimum and maximum air temperatures could be used as measured at the Roswinkel field (1.5 m high, shaded) in the period 12 May to 20 September 2000. Outside this period, the air temperatures measured at the weather station Eelde

(KNMI, 2000b, 2001b) were used. These air temperatures are used by the PEARL model to calculate soil temperatures.

2.4   Soil moisture flow

Moisture flow in soil is calculated by the Richards equation, as described by Tiktak et al. (2000) and Leistra et al. (2001). Two soil hydraulic relationships are needed for the calculations with this equation:
   a) the moisture retention curve;
   b) the hydraulic conductivity curve.
These relationships were measured for a few columns from four layers of the Roswinkel soil, by using the Evaporation Method. The results are presented by Crum et al. (2004).

In the computations, the hydraulic relationships were described by the Van Genuchten-Mualem equations, as given by Tiktak et al. (2000) and Leistra et al. (2001). The parameters in these equations were fitted to the experimental curves using the APPIA optimisation program (Crum et al., 2004). The resulting values of the Van Genuchten-Mualem parameters for each of the layers are given in Table 2.3. The description of the symbols is as follows:

Θ_{res} = residual volume fraction of moisture in soil (-).
Θ_{sat} = saturated volume fraction of moisture in soil (-).
α, n, m, λ = Van Genuchten-Mualem parameters, with m = 1 – 1/n.
K_{sat} = saturated hydraulic conductivity (m d^{-1}).

Table 2.3. Parameters of the Van Genuchten-Mualem equations fitted to the moisture retention and hydraulic conductivity curves measured for four soil layers of the Roswinkel field (Crum et al., 2004).

Layer	Θ_{res} (-)	Θ_{sat} (-)	α (cm^{-1})	n	λ	K_{sat} (m d^{-1})
Ridge, 0 - 0.1 m	0.045	0.403	0.0123	2.317	-2.068	0.257
Furrow, 0 - 0.1 m	0.045	0.368	0.0123	1.816	-1.516	0.24
0.3 - 0.4 m	0.041	0.314	0.0129	2.513	-0.762	0.21
0.6 - 0.7 m	0.022	0.270	0.0122	4.125	-1.661	0.10

These measurements were carried out for only one soil column per (type of) soil layer. Consequently, the representativeness of these values for the average situation in the Roswinkel field is questionable. Experiences with the use of the parameters in Table 2.3 in the SWAP-PEARL computations are described in Appendix D. Substantial calibration of these hydraulic relationships was found to be needed. In the main part of this study, the most relevant hydraulic relationships from the Staring Series are used (Wösten et al., 2001). The latter relationships are the average of the relationships measured for many similar Dutch soils, so they are considered to be more representative for the average situation in the Roswinkel field.

2.5 Soil sampling and soil conditions

Separate samples of the top soil (0.2 m deep; three layers) of the ridges and furrows were taken at 6 h after application of the substances (10 May 2000), to measure the initial contents of bromide-ion and carbofuran. At three times thereafter, the soil was sampled to about 1 m depth: on 29 May, 13 July and 18 September 2000. The field was divided into four sections (Figure 2.1) and in each section four long soil cores were taken from both the ridges and furrows. So a total of 32 soil cores was taken at the field each time.

The soil was sampled with a long stainless steel tube (with PVC liner), which was pressed hydraulically into the soil with an excavation machine. It was attempted to sample the soil to 1 m depth. However, this depth could not always be attained because of the high density of the subsoil and because some wet subsoil flowed from the tubes when pulling them up. The soil cores (diam. 9.4 cm; length about 1 m) in the PVC liners were transported to the laboratory, where they were divided into 0.1 m layers. Details on the soil samplings are given by Crum et al. (2004).

The dry bulk density of the soil was determined from the mass of moist soil sampled per layer of 0.1 m, soil moisture content and volume of the sample. The averages of the several tens of values for each layer are given in Table 2.4. The measurements for the top layers were sometimes disturbed by the presence of loose soil, potato tubers or stones (Crum et al., 2004). The top of the ridges, formed by hilling up, was comparatively loose. The sandy subsoil was dense.

Table 2.4. Averaged dry bulk densities of the soil in the Roswinkel profile.

Depth (m)	Bulk density (kg dm^{-3}) below	
	ridges	furrows
0 – 0.1	1.08	1.21
0.1 – 0.2	1.19	1.36
0.2 – 0.3	1.26	1.55
0.3 – 0.4	1.45	1.63
0.4 – 0.5	1.62	1.72
0.5 – 0.6	1.69	1.78
0.6 – 0.7	1.79	1.83
0.7 – 0.8	1.82	1.81
0.8 – 0.9	1.83	1.77
0.9 – 1.0	1.80	1.88

A subsample of the soil core sections was used to measure soil moisture content. Multiplication of this content with soil bulk density gives the volume fraction of moisture in soil (Table 2.5). In almost all cases, volume fraction of water below the ridges was lower than that below the furrows at the same depth and time. This may have been caused by surface flow of water from the ridges to the furrows and by higher water uptake from the ridges by the potato plants. The spreading in soil moisture was greatest at depths around 0.2 m, possibly due to differences in water flow and water uptake by plant roots.

Table 2.5. *Volume fractions of moisture in the soil of the Roswinkel potato field in the growing period in 2000. Averages with their standard deviation (s.d.).*

Depth in soil (m)	8th May, furrow	10th May, ridge	10th May, furrow	29th May, ridge	29th May, furrow	13th July, ridge	13th July, furrow	18th Sept., ridge	18th Sept., furrow
0-0.1	0.195 (s.d.=0.026	0.159 (s.d.=0.046)	0.195 (s.d.=0.046)	0.180 (s.d.=0.024)	0.240 (s.d.=0.032)	0.172 (s.d.=0.024)	0.229 (s.d.=0.030)	0.178 (s.d.=0.022)	0.240 (s.d.=0.038)
0.1-0.2	0.236 (s.d.=0.023	0.187 (s.d.=0.034)	0.218 (s.d.=0.040)	0.220 (s.d.=0.038)	0.267 (s.d.=0.035)	0.185 (s.d.=0.024)	0.247 (s.d.=0.023)	0.202 (s.d.=0.024)	0.255 (s.d.=0.036)
0.2-0.3	0.259 (s.d.=0.038)			0.217 (s.d.=0.020)	0.235 s.d.=0.058)	0.177 (s.d.=0.025)	0.207 (s.d.=0.062)	0.217 (s.d.=0.031)	0.227 (s.d.=0.071)
0.3-0.4	0.245 (s.d.=0.063)			0.234 (s.d.=0.034)	0.250 (s.d.=0.043)	0.215 (s.d.=0.029)	0.210 (s.d.=0.038)	0.236 (s.d.=0.046)	0.244 (s.d.=0.054)
0.4-0.5	0.242 (s.d.=0.042)			0.229 (s.d.=0.039)	0.251 (s.d.=0.016)	0.213 (s.d.=0.057)	0.224 (s.d.=0.016)	0.232 (s.d.=0.058)	0.250 (s.d.=0.028)
0.5-0.6	0.242 (s.d.=0.025)			0.241 (s.d.=0.041)	0.272 (s.d.=0.025)	0.219 s.d.=0.031)	0.249 (s.d.=0.029)	0.245 (s.d.=0.037)	0.259 (s.d.=0.011)
0.6-0.7	0.248 (s.d.=0.019)			0.270 (s.d.=0.029)	0.301 (s.d.=0.025)	0.232 (s.d.=0.018)	0.244 (s.d.=0.033)	0.253 (s.d.=0.019)	0.263 (s.d.=0.026)
0.7-0.8	0.249 (s.d.=0.042)			0.271 (s.d.=0.025)	0.289 (s.d.=0.024)	0.251 (s.d.=0.022)	0.258 (s.d.=0.033)	0.255 (s.d.=0.012)	0.275 (s.d.=0.030)
0.8-0.9	0.248 (s.d.=0.054)			0.286 (s.d.=0.019)	0.294 (s.d.=0.008)	0.263 (s.d.=0.038)	0.331 (n=1)	0.283 (s.d.=0.007)	0.326 (s.d.=0.021)
0.9-1.0	0.301 (s.d.=0.037)			0.307 (s.d.=0.013)	0.310 (n=1)	0.283 (s.d.=0.042)		0.295 (s.d.=0.010)	0.320 (n=1)
1.0-1.1	0.283 (n=1)			0.304 (s.d.=0.033)	0.363 (n=1)	0.320 (s.d.=0.016)		0.296 (s.d.=0.043)	
1.1-1.2						0.290 (n=1)		0.293 (s.d.=0.026)	

2.6 Groundwater flow and water table

The experimental field and its surroundings are underlain with a phreatic aquifer, 25 to 30 m thick (Crum et al., 2004). Earlier geohydrological surveys showed that the aquifer material ranges from fine to coarse sands. The groundwater in the aquifer is expected to flow globally in North-West direction, with a gradient in pressure head in the range of 0.2 to 0.4 m km^{-1}. The hydraulic conductivity in the aquifer was estimated to be in the range of 1.9 to 6.0 m d^{-1}. The resulting rate of horizontal groundwater flow is in the range of 0.4 to 3.8 m year^{-1}. Much of the horizontal flow is expected to occur in deeper coarse-sandy layers. Presumably, the groundwater in the moderately fine sand of the upper part of the aquifer, with comparatively low hydraulic conductivity, mainly flows in vertical direction.

The water percolating through the soil profile is discharged via the upper part of the groundwater zone. In dry periods, water may flow upward through the upper groundwater zone. The depth of the groundwater table is an important indicator for these processes. In the present field experiment, the depth of the groundwater table was measured in two ways:
   a) by hand in four groundwater tubes with filter at 4.5 m depth (at 13 days distributed over the experimental period);
   b) by pressure sensors in three groundwater tubes with filter at 3 m depth, connected to a data logger (hourly measurements in intermittent periods).
The location of the groundwater tubes is given in Figure 2.1. The raw data on the measured groundwater levels are given by Crum et al. (2004) on their CD.

In some respects, the results on the groundwater depths were conflicting, so the most reliable results had to be selected. The depths measured by Sensor 11 were systematically greater than those measured by the two other sensors (on average 0.19 m deeper) and those measured by hand. For that reason, the data of Sensor 11 were not included in the present results. At the time of the hand measurements, the results of the two remaining Sensors 12 and 13 (if available) and the four hand measurements can be compared. These results are shown in Table 2.6.

Table 2.6. Depths of the groundwater table in the Roswinkel field, measured by sensors and by hand on the days of the hand measurements. Depths below soil surface around the groundwater tube.

Measuring date	Depth (m) of the water table measured by:					
	Sensor 12	Sensor 13	Hand 1	Hand 2	Hand 3	Hand 4
29th May 2000	0.83	0.87	0.97	0.99	0.81	0.82
28th June 2000	1.25	1.25	1.28	1.39	1.23	1.25
19th July 2000	1.02	1.04	1.15	1.20	1.02	1.03
18th August 2000	1.23	1.24	1.32	1.41	1.23	1.23
31st August 2000	1.03	1.05	1.16	1.22	1.03	1.03
18th October 2000	0.98	1.00	1.10	1.17	0.99	0.97
24th November 2000	0.74	0.77	1.13	1.22	1.01	1.02
27th December 2000	0.86	0.89	1.04	1.07	0.87	0.86
2nd February 2001	0.69	0.72	0.46	0.42	0.28	0.20
4th April 2001	-	-	1.06	1.02	0.80	-
17th May 2001	-	-	1.25	1.32	1.15	1.19
18th July 2001	1.27	1.29	1.30	1.35	1.15	1.25
24th Sept. 2001	-	-	0.53	0.47	0.31	0.27

In most of the measurements in the year 2000, the values of Sensors 12 and 13 were close to those for Hand 3 and Hand 4 (Table 2.6). The levels for Hand 1 and Hand 2 were somewhat deeper. However, on the 24th of November, the table depths for Sensors 12 and 13 were less than those for the Hand measurements. The values of 2nd February 2001 show the problem of the limited measuring range for the Sensors: they could not measure the very shallow depths of the groundwater table. The Sensor values for 18th July 2001 were again close to the average of the Hand measurements.

Results of at least three daily-averaged measurements per month of the groundwater depth by Sensors 12 and 13 are shown in Figure 2.4. They give an impression of the fast variation in groundwater table of some decimetres under the influence of rainfall/irrigation and groundwater discharge. The course in the year, with deeper levels in summer and shallower levels in winter, is clearly shown. At most of the comparison days there is reasonable agreement between the sensor and hand measurements (Figure 2.4). The difference in sensor and hand measurements for 24th November 2000 is clearly shown (no explanation available). The pressure sensors could not measure groundwater depths shallower than about 0.6 m, as this was outside the measuring range. So the sensor results for the corresponding periods with much rain (e.g. midwinter 2000/2001) are not usable. In the spring of 2001 there was a substantial gap in the sensor measurements.

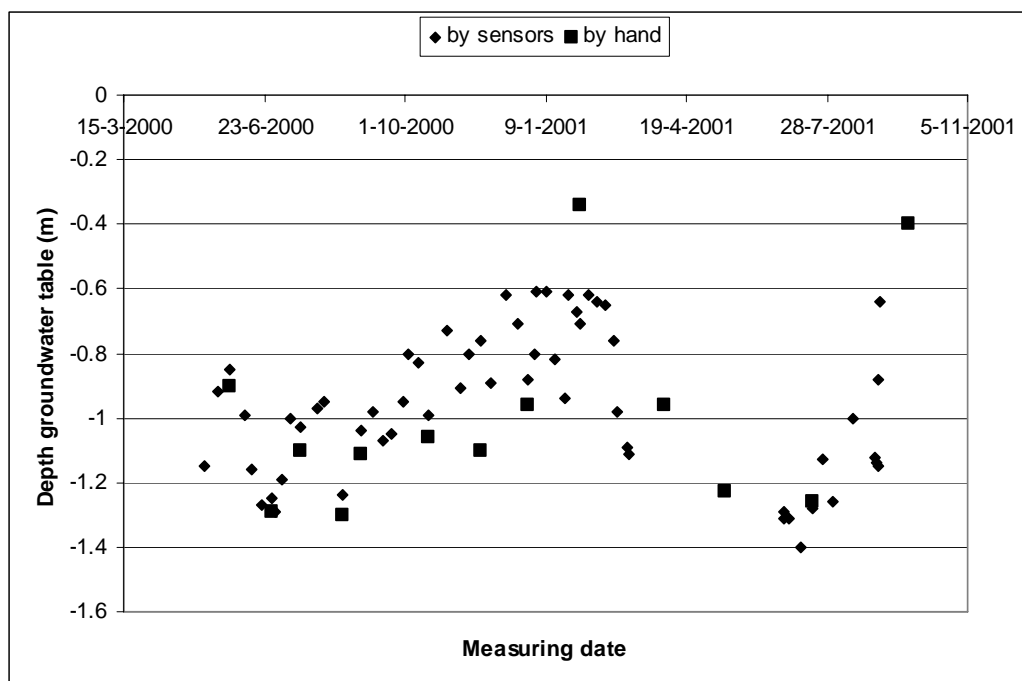*Figure 2.4. Depths of the groundwater table in the Roswinkel field measured by pressure sensors and by hand.*

When installing the groundwater tubes, only sandy material was encountered (no water-flow disturbing layers). The vertical water flux (downward seepage) from the field was estimated from the difference between the water level in a 30 m deep groundwater tube and that in the 5 m deep tubes (Crum et al., 2004). The hydraulic

conductivity in the top of the sandy phreatic aquifer was taken to be 0.1 m d^{-1}. For the period between June and the end of August 2000, the downward water flux was estimated to be of the order of 0.5 mm d^{-1}. Due to the higher water tables in the winter half-year, this flux could be higher then.

2.7   Soil analyses

The soil core sections were analysed separately for bromide-ion, so there were 16 analyses per depth and per sampling time (both for ridges and furrows). The four soil samples from each depth in a field section were combined to one sample for the analysis of carbofuran. So the pesticide was measured in quadruplicate for each depth in soil (both for ridges and furrows). In various cases, two adjacent 0.1 m soil sections from the subsoil were combined to one 0.2 m section.

Bromide-ion was extracted by shaking 45 g moist soil with 40 mL water (containing 0.01 mol CaCl$_2$ per L) for 1 hour. A subsample of the water layer was filtered (0.45 μm) and subjected to HPLC. Bromide-ion was separated in an anion-exchange column, with buffered water as mobile phase. Bromide was measured by UV detection, at a wavelength of 210 nm. The efficiency of the extraction from soil was 93%; the results were not corrected for this. The limit of quantification for the soil samples was 0.4 mg/kg. Details of the HPLC analyses of bromide-ion were given by Crum et al. (2004).

Carbofuran was extracted by shaking 100 g moist soil samples with 100 mL methanol in 250 mL flasks for 1 hour. After centrifugation, the extracts were diluted with water or concentrated by evaporation, if needed. The concentrations of carbofuran were measured by HPLC. The compound was separated in a C18 column, with water/acetonitrile (30/70) as mobile phase. Carbofuran was measured by UV detection, at wavelengths of 230 or 280 nm. The recovery from topsoil material was on average 98% and that from subsoil material on average 85%; the results were not corrected for this. The limit of quantification for soil was 0.0008 mg/kg. Details on the HPLC analysis of carbofuran were given by Crum et al. (2004).

2.8   Groundwater sampling and analysis

The upper groundwater was sampled shortly before the application of the substances and at 14 times after application (period 29 May 2000 to 7 May 2002). It was sampled from a grid of 64 groundwater tubes installed in a section of the experimental field (Figure 2.1). Half of the tubes was installed in the ridges and the other half in the furrows. The original soil was refilled and tamped around the tubes, but there is no information on sealing with swelling clay (as required). The sampling depths were 0.9, 1.3, 1.6 and 2.0 m. The first two depths could not be sampled when the groundwater table was deeper. The groundwater tubes were emptied (one or three times; conflicting information) before the water sample was taken. The water sample

was sucked from the tubes via a narrow stainless-steel tube into a glass bottle with under-pressure realised by a battery-driven air pump.

The groundwater samples were filtered (0.45 μm) and subjected to the HPLC method for bromide-ion, as described for the water extracts of the soil samples. The limit of quantification of bromide-ion in the water samples was 0.3 mg L^{-1}.

Carbofuran in a 300 mL water sample was extracted by the solid-phase extraction technique. After elution with methanol, the solvent was largely evaporated and the compound taken up in water. Carbofuran was analysed by the HPLC method as described above for the soil extracts. Recovery of carbofuran from water was on average 89%; the measured concentrations were not corrected for recovery. The limit of quantification of carbofuran in groundwater was 0.05 μg L^{-1}.

2.9   Crop sampling and analysis

Potato crop samples were collected to measure bromide-ion content and total amount taken up. On 10 July and 18 September 2000, whole-plant samples were taken consisting of a) the leaves plus stems, and b) the tubers plus main roots. Besides, separate samples of potato tubers were collected then. Four plant samples were taken at each time. On 24 November 2000 only tuber plus main root samples were taken, as hardly any green foliage was left. The plant samples were rinsed, chopped, mixed, dried and then stored at –25 °C until chemical analysis of bromide-ion.

The dried crop samples were pulverised in a cross mill with 1 mm bottom sieve. A sample of 4 g was combined with 50 mL of an aqueous solution of HCl (0.01 mol L^{-1}) and the mixture was boiled for 10 min. After standing overnight, a subsample of the water layer was filtered (0.45 μm) and subjected to HPLC, as described for the water extracts of soil. The recovery of bromide-ion from two spiked potato tuber samples was low (38 and 57%). The limit of quantification of bromide-ion had to be set at the high value of 12 mg kg^{-1}, because of interfering substances in the crop extracts.

 Fresh mass of the crop samples and sampled area were measured and used to calculate the total areic mass of bromide-ion taken up in the crop parts. Moisture content of the crop samples was measured by drying to constant mass at 105 °C. This allowed calculation of dry mass crop production.

3 General information on the substances

3.1 Bromide-ion

Bromide-ion was selected as a tracer for water flow because it shows minimal interactions with the soil. The ionic mass of bromide is 79.9 g mol^{-1}. The vapour pressure of bromide-ion is extremely low. The solubility of bromide-ion in water is very high. The octanol/water partitioning can be expected to be very low. The coefficient of diffusion of bromide-ion in water (Lide, 1999), translated to 20 $^{\circ}$C, is taken to be 1.6 10^{-4} m^2 d^{-1}. The diffusion coefficient in air was set at 1.6 m^2 d^{-1} (but virtually no bromide-ion in the gas phase).

Adsorption of bromide as an anion to soil can be assumed to be nil. The half-life of transformation of bromide in soil is very long (possibly some incorporation into organic matter). The concept of the Transpiration Stream Concentration Factor (TSCF) for uptake by plant roots does not hold for ionic species. As there is no alternative in the model and as no quantitative information is available, TSCF was tentatively set at 0.5.

In the computations, arbitrarily very low (e.g. for vapour pressure) or very high (e.g. for half-life) values can be introduced for the extreme properties of bromide-ion; their precise value will have hardly any effect on the results.

3.2 Carbofuran

Carbofuran is an insecticide used internationally in various crops, by application to both plants and soil (Tomlin, 2003). In 2000, various approvals were terminated in the Netherlands, because of toxic risks to birds (NL-Ctgb, 2007). Only some applications in glasshouses were maintained. In the registration procedure of the EU (2007) it has been decided that carbofuran will not be placed on the Annex I of Guideline 91/414/EEG. As a result, the approval of carbofuran in The Netherlands has been finished in December 2007 (NL-Ctgb, 2007). Nevertheless cabofuran remains an interesting example compound for studying pesticide movement through the soil to groundwater, in view of its properties (see below).

Computations with the PEARL model ask for input of essential physico-chemical properties of the pesticide. Various characteristics can be collected from the literature and from registration sources, as shown for carbofuran in Table 3.1. Different values are stated for the vapour pressure of carbofuran, in a range of moderate to low values. Solubility in water and octanol/water partitioning point to intermediate polarity of the carbofuran molecules.

The coefficient for diffusion of carbofuran in air at the reference temperature (20 $^{\circ}$C) was estimated to be 0.44 m^2 d^{-1}, using the FSG method described by Tucker &

Nelken (1982). Using the method of Hayduk & Laudie described by Tucker & Nelken (1982), the diffusion coefficient of carbofuran in water was estimated to be $0.44 \cdot 10^{-4} \, m^2 \, d^{-1}$.

Table 3.1. Physico-chemical characteristics of carbofuran, collected from the literature and from registration reviews.

Characteristic	Value, unit, condition	Reference
Molar mass	$221.3 \, g \, mol^{-1}$	Tomlin (2003)
Melting range	151-154 ºC	Tomlin (2003); EU (2007)
Vapour pressure	0.031 mPa at 20 ºC	Tomlin (2003)
	0.072 mPa at 20 ºC	
	0.23 mPa at 20 ºC	EU (2007)
	0.08 mPa at 25 ºC	
Solubility in water	320-351 mg L^{-1} (20 ºC)	Tomlin (2003)
	315-322 mg L^{-1} (20 ºC)	EU (2007)
Octanol/water partitioning	$\log(P_{ow}) = 1.52$ (20 ºC)	Tomlin (2003)
	$\log(P_{ow}) = 1.8$ (20 ºC); 1.62 (22 ºC)	EU (2007)
Diffusion coefficient in air	$0.44 \, m^2 \, d^{-1}$ (20 ºC)	Estimated (Tucker & Nelken, 1982)
Diffusion coefficient in water	$0.44 \cdot 10^{-4} \, m^2 \, d^{-1}$ (20 ºC)	Estimated (Tucker & Nelken, 1982)

Hydrolysis and photolysis
Carbofuran is reported to be stable to hydrolysis at pH 4, while the rates of hydrolysis in water (25 ºC) at higher pH values correspond to 28-46 days (pH 7), 2.7 days (pH 8) and 0.1 day (pH 9) (EU, 2007).

The rate of photolysis (wavelengths 300-400 nm) of carbofuran in water (pH 7) corresponded to a half-life of 5.6 days (NL-Ctgb, 2007). EU (2007) gives a half-life for photolysis in aqueous solution of 33 days (pH 5, 22 ºC).

Adsorption to soils
Using the results of a series of soil adsorption and soil column experiments, the average sorption coefficient K_{om} of carbofuran (for adsorption to soil organic matter) was calculated to be 19.5 L kg^{-1} (n = 9; s.d. = 8.9 L kg^{-1}) (NL-Ctgb, 2007). The results of adsorption measurements for four soils corresponded to a mean K_{oc} value (for adsorption to soil organic carbon) of 22 L kg^{-1} (range 17 to 28 L kg^{-1}) (EU, 2007), which matches a K_{om} value of 13 L kg^{-1}. These data indicate that adsorption of carbofuran to soils is moderate to weak.

Transformation rate in/on soil
On the basis of insufficient research data, the half-life of carbofuran in soil (20 ºC) was estimated (for the time being) to be on average 28 days (NL-Ctgb, 2007). Microbial transformation is predominant. The overall geometric mean of the half-life of carbofuran incubated in soils in the laboratory (temperature and moisture not specified) was 29.3 days (very wide range from 6 to 444 days) (EU, 2007). The overall geometric mean value for the half-life derived from field studies was 20.8 days (very wide range; normalisation to reference temperature and moisture was not possible).

The rate of phototransformation of carbofuran on a soil surface corresponded to a half-life of 30.1 days (25 ºC; natural light, summer time) (EU, 2007).

In general, it can be stated that the moderate to low volatility, the moderate to low adsorption to soils and the substantial half-life of transformation in soils makes carbofuran a suitable model compound for a leaching experiment in the field. However, the chance of accelerated transformation of carbofuran in soils by microbial adaptation (e.g. Karpouzas et al., 2001) is an unpredictable factor.

Uptake by plants
The uptake of carbofuran by the roots of the potato crop was described according to Briggs et al. (1982). They derived a relationship between the Transpiration Stream Concentration Factor (TSCF) and the $\log(P_{ow})$ value for octanol/water partitioning of the compound. Using this relationship, the TSCF for carbofuran was calculated to be 0.78 (high uptake).

4 Laboratory experiments on carbofuran

4.1 Adsorption to soil

Soil was collected from the top 0.25 m layer of the field on 10 July 2002. A mass of 50 g moist soil was added to a series of centrifugation tubes (80 mL). Soil moisture content was 15.2%, so the moist soil corresponded to 43.4 g dry soil. Aqueous solution (50 mL, with 0.01 mol $CaCl_2$ per L) of carbofuran was added to each of the tubes, with concentrations of 0.0092, 0.0227, 0.091 and 0.455 mg L^{-1}, respectively. The measurements were carried out in triplicate for each concentration. The centrifugation tubes were closed with ground-glass stoppers and slowly rotated on an inclined disk for 24 hours. Adsorption was measured in temperature cabinets at 5, 15 and 25 °C, respectively. After equilibration, the stoppers were replaced by aluminium foil and the tubes were centrifuged at 33 s^{-1} for 20 min (at the equilibration temperature). The concentration of carbofuran in the water layer was measured by HPLC, as described for the water samples from the field experiment (Section 2.8). The adsorption to soil was calculated from the difference between initial and final concentration in the water layer. Further details of the adsorption measurement have been given by Crum et al. (2004).

The results of the measurements of carbofuran concentration in water and of the calculations of its content adsorbed to soil (both after 24 h equilibration) are given in Table 4.1.

Table 4.1. Results of the measurements of the adsorption of carbofuran to Roswinkel topsoil at the three temperatures.

Temperature					
5 °C		15 °C		25 °C	
Concentration in water (mg L^{-1})	Content on soil (mg kg^{-1})	Concentration in water (mg L^{-1})	Content on soil (mg kg^{-1})	Concentration in water (mg L^{-1})	Content on soil (mg kg^{-1})
0.0032	0.0064	0.0033	0.0063	0.0038	0.0057
0.0026	0.0072	0.0028	0.0070	0.0028	0.0069
0.0033	0.0062	0.0027	0.0071	0.0053	0.0037
0.0111	0.0119	0.0093	0.0141	0.0132	0.00893
0.0118	0.0106	0.0097	0.0133	0.0164	0.00472
0.0132	0.0087	0.0092	0.0143	0.0152	0.00645
0.0397	0.0527	0.0420	0.0499	0.0608	0.0256
0.0407	0.0519	0.0409	0.0504	0.0598	0.0267
0.0411	0.0511	0.0418	0.0501	0.0607	0.0258
0.212	0.247	0.216	0.243	0.308	0.123
0.215	0.239	0.231	0.222	0.310	0.119
0.213	0.239	0.207	0.251	0.295	0.139

The points for the adsorption of carbofuran at 15 °C are given in Figure 4.1 (linear scales). At the lower concentrations, the three points per concentration level (almost) coincide.
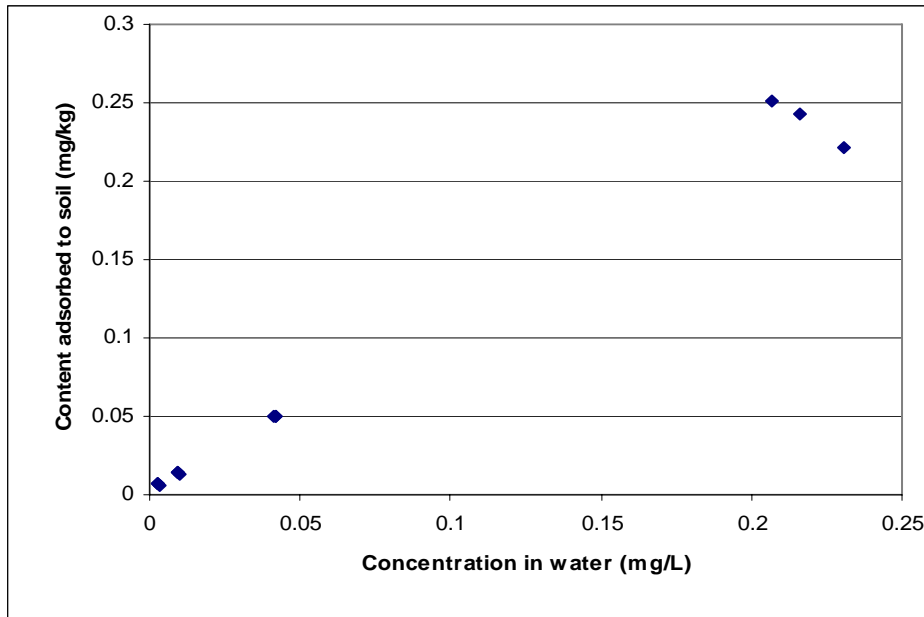

Figure 4.1. Points for the adsorption of carbofuran to Roswinkel topsoil at 15 °C, plotted on linear scales. Three points at each of the four concentration levels.

The Freundlich plot for the adsorption of carbofuran at 15 °C is given in Figure 4.2 (log-log scales). Again, various points (three per concentration level) are very close to each other or even coincide. The Freundlich parameters calculated by linear regression with Excel are: coefficient $K_F = 0.77$ L kg^{-1} and exponent $n_F = 0.83$.
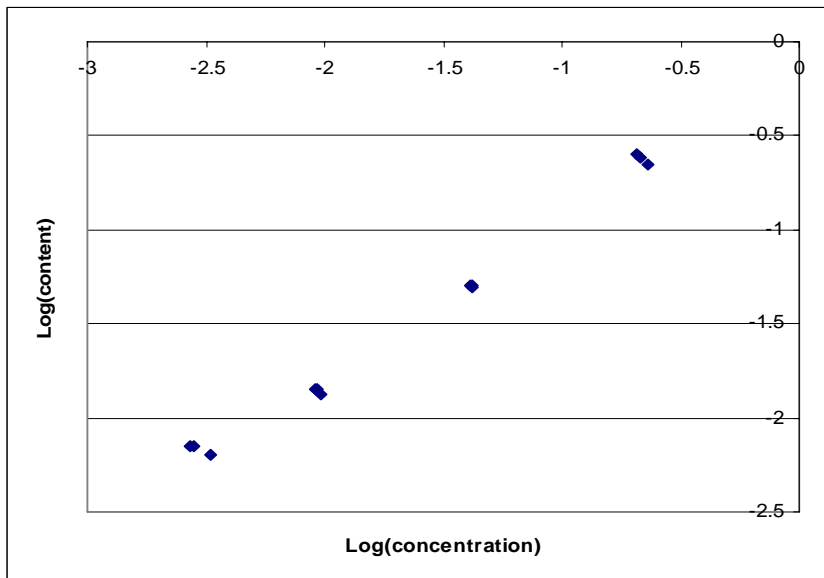

Figure 4.2. Points for the adsorption of carbofuran to Roswinkel topsoil at 15 °C, plotted on log-log scales (Freundlich plot).

The plots for the adsorption of carbofuran to the Roswinkel topsoil at 5 and 25 ºC are given in Appendix A.

The Freundlich parameters calculated for the adsorption of carbofuran to Roswinkel topsoil at all three temperatures are given in Table 4.2.

Table 4.2. Freundlich parameters calculated for the adsorption of carbofuran
to Roswinkel topsoil at the three temperatures.

Temperature (ºC)	Freundlich coefficient K_F (L kg^{-1})	Freundlich exponent n_F (-)
5	0.84	0.89
15	0.77	0.83
25	0.24	0.75

Figure 4.2 shows that the three points for the lowest concentration level are somewhat above the imaginary line through the points for the three higher concentration levels. For the measurements at 5 and 25 ºC, this phenomenon is even stronger (see figures in Appendix A). It is one of the causes of the low (extrapolated) value of K_F obtained for 25 ºC. As the data for 15 ºC show the least complicated picture, the parameter values for this temperature were selected for input in the PEARL computations.

The coefficient K_{om} for the adsorption of carbofuran to soil organic matter can be calculated by: $K_{om} = K_F/om$, with om = organic matter content (0.049 kg kg^{-1}; Table 2.2). This yields $K_{om} = 16$ L kg^{-1}. The coefficient K_{oc} for the adsorption of carbofuran to organic carbon (0.0324 kg kg^{-1}; Table 2.2) is calculated to be 24 L kg^{-1}. These values indicate that the adsorption of carbofuran to soil is moderate to weak. It is possible that some transformation of carbofuran occurred in the 24-hour equilibration time. This would result in some over-estimation of adsorption by the present measurements. Values for K_{om} derived in registration procedures are 13 L kg^{-1} and 19.5 L kg^{-1} (Section 3.2).

An attempt was made to measure long-term sorption kinetics of carbofuran in Roswinkel topsoil at 25 ºC. Carbofuran was incubated in the soil as described in the transformation study (Section 4.2). At various times, pore water was isolated from the moist soil by centrifugation on a glass filter plate. Only at day 3, carbofuran could be detected in the pore water; from day 7 on, its concentration in pore water was below detection limit. So transformation of carbofuran was too fast to measure sorption kinetics via the pore water.

4.2   Rate of transformation in soil

On 10 July 2002 (so about 2 years after the start of the field experiment), soil materials for the transformation study were collected from the 0 to 0.25 m and 0.5 to 0.8 m layers of the Roswinkel experimental field. Moist soil batches (equivalent to 100 g dry soil) were weighed into 250 mL glass jars and pre-incubated at the relevant temperature for 5 days. A volume of 1 mL aqueous solution of 200.5 µg carbofuran

per mL was added to each top-layer batch and mixed with the soil. 1 mL solution with 10.0 µg carbofuran per mL was added to the 0.5 to 0.8 m soil batches and mixed-in. The top-soil batches were incubated in constant-temperature cabinets at 5, 15 and 25 °C, respectively. The soil batches from the 0.5 to 0.8 m layer were incubated at 15 °C. The moisture contents of the soils were 18% (0 to 0.25 m layer) and 14% (0.5 to 0.8 m layer). At various time intervals, duplicate flask contents from each series were subjected to extraction with methanol and chemical analysis, as described for the soil samples from the field experiment (Section 2.7). Crum et al. (2004) presented further details on the transformation study.

The percentages of the dose of carbofuran remaining in the soil after different times of incubation at the three temperatures are given in Table 4.3.

Table 4.3. Percentages of the dose of carbofuran remaining in the soil after different times of incubation at 5, 15 and 25 ºC in soil from Roswinkel.

Layer (m)	Temperature (ºC)	Replicate	Percentage remaining after incubation for:						
			1 day	3 days	7 days	14 days	28 days	64 days	87 days
0 to 0.25	5	No 1	109.3	103.2	103.7	102.9	36.0	5.4	2.8
		No 2	108.1	105.3	103.6	92.6	38.3	5.5	2.8
	15	No 1	108.0	99.7	28.0	4.5	1.8	0.72	0.44
		No 2	105.3	99.9	30.0	4.3	1.9	1.28	0.38
	25	No 1	104.0	67.5	3.8	1.5	0.51	0.65	<0.2
		No 2	104.4	68.8	3.8	1.5	1.07	1.95	<0.2
0.5 to 0.8	15	No 1	88.9	83.7	77.8	29.4	4.6	<0.2	<0.2
		No 2	80.4	82.9	79.4	60.2	8.6	<0.2	<0.2

The measured course in time of the transformation of carbofuran in topsoil material at 15 °C is shown in Figure 4.3. Various duplicate points coincide in the figure. The transformation proceeded quickly: after 14 days only 4% of the dose was left. Transformation in this soil material collected in 2002 was much faster than that in the soil of the experimental field in 2000 (half-life of about a month; Section 5.2). In registration procedures, an average half-life of about 29 days in soil (20 °C) was derived from lab incubations of carbofuran (Section 3.2). Apparently, the soil micro-organisms had adapted to carbofuran, resulting in accelerated transformation. Consequently, these laboratory results cannot be used as input for the PEARL simulations of the field experiment in 2000 (before the adaptation).
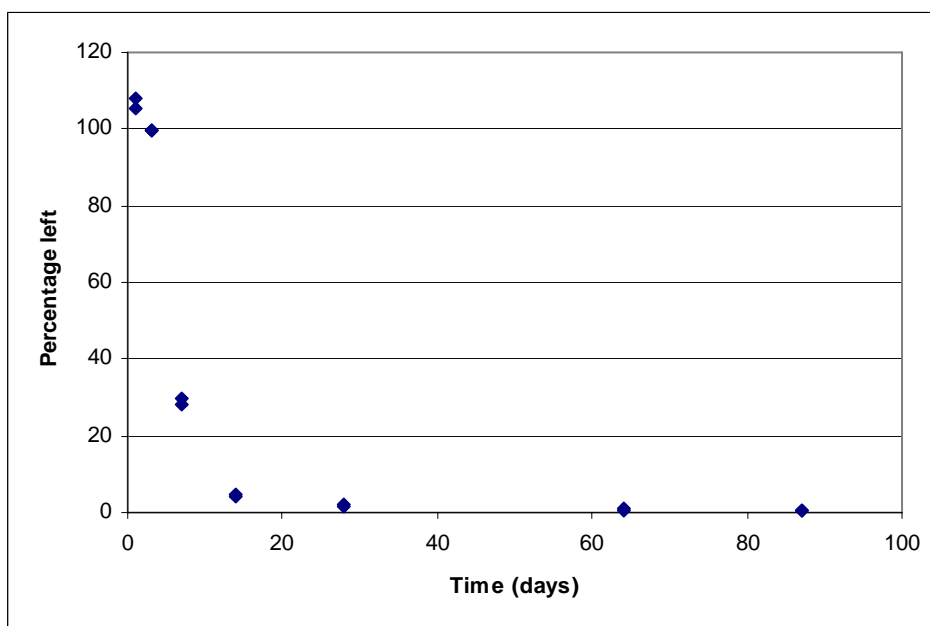
Figure 4.3. Course of the transformation of carbofuran in Roswinkel topsoil at 15 °C (linear scales). Duplicate poins at each time.

The course of carbofuran transformation in Roswinkel topsoil at 15 °C is also represented in a log-linear plot (Figure 4.4) for clarifying the transformation kinetics. Transformation in the first three days was comparatively slow, which is followed by a period with substantially faster transformation. After the first two weeks, the rate coefficient of transformation decreases. The last residue of about 1% of the dose seems to be poorly available for microbial transformation. Further, the analysis at this low level may be influenced by background substances. Transformation in the first 14 days was approximated by first-order kinetics, by regression in Excel of ln(percentage left) against time. This resulted in the rate coefficient $k_r = 0.26$ d^{-1}, which corresponds to a half-life of 2.7 days for carbofuran in Roswinkel topsoil at 15 °C .

The course of transformation of carbofuran in topsoil material at 5 °C shows a first period of 14 days with comparatively slow transformation (Appendix B, Figure B.1). After that, the rate coefficient of transformation increased substantially. In the period 14 to 87 d, transformation was approximated by first-order kinetics, with a rate coefficient $k_r = 0.049$ d^{-1}. This corresponds to a half-life of 14 days for carbofuran in Roswinkel topsoil at 5 °C in this period.
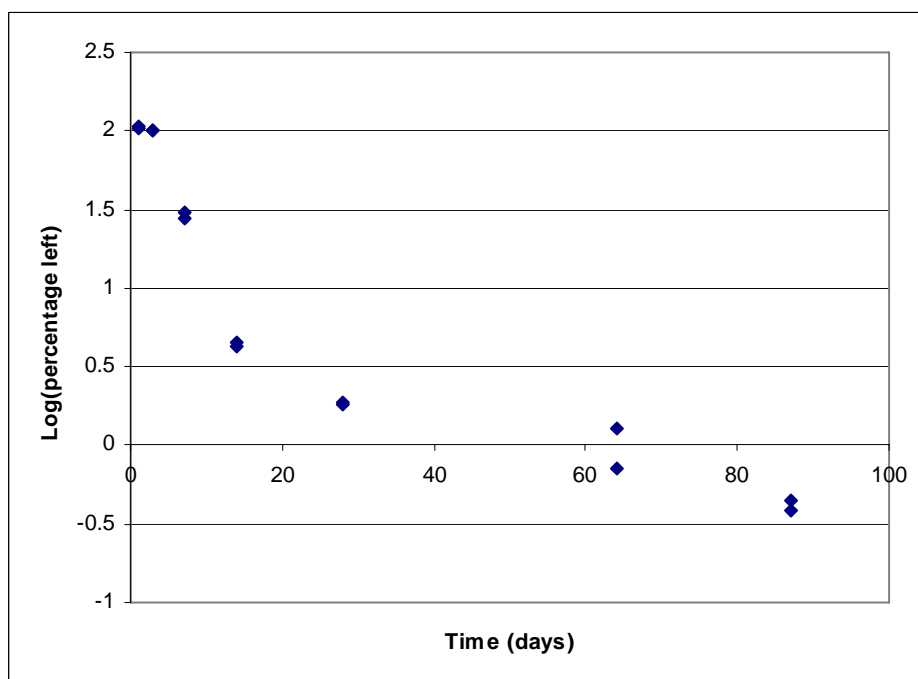
Figure 4.4. Course of the transformation of carbofuran in Roswinkel topsoil at 15 ºC (log-linear scales). Duplicates at each time.

In the incubation of carbofuran in soil at 25 ºC, the initial period with comparatively slow transformation was very short and the rate of transformation was high (Appendix B, Figure B.2). The course of transformation in the first 14 days was approximated by first-order kinetics. The rate coefficient was calculated to be $k_r = 0.34$ d^{-1}, which corresponds to a half-life of 2.0 d in Roswinkel topsoil at 25 ºC.

The results of the regression calculations for first-order transformation kinetics of carbofuran in Roswinkel topsoil are collected in Table 4.4.

Table 4.4. Results of the regression calculations for periods in which carbofuran transformation in topsoil could be approximated by first-order kinetics.

Incubation temperature (ºC)	Period (days)	Rate coefficient (d^{-1})	Half-life (d)
5	14 to 87	0.049	14
15	0 to 14	0.26	2.7
25	0 to 14	0.34	2.0

Initially, the transformation of carbofuran in subsoil material (0.5 to 0.8 m layer) at 15 ºC (Table 4.3) was substantially slower than that in topsoil material at the same temperature. In an initial period of less than 2 weeks there was gradual transformation. After that, the transformation rate coefficient increased drastically. After 28 d only 5 to 9% of the dose was left, while from 64 d onwards carbofuran could not be detected anymore.

5 Measured concentrations in the soil profile

5.1 Bromide-ion in the soil profile

The contents of bromide-ion measured in soil were multiplied with bulk density of the soil layer, to obtain the concentration of bromide-ion in soil. The concentrations of bromide-ion in the topsoil just after application on 10 May 2000 are given in Table 5.1. The average amount of bromide-ion measured in the top 0.2 m of the soil profile amounted to 68.4 mg dm^{-2}, which corresponds to 105.6% of the calculated dosage (Table 5.3) .

Table 5.1. *Concentrations of bromide-ion in the topsoil of the Roswinkel field just after application on 10 May 2000. Average of n = 15 or 16 measurements. s.d. = standard deviation.*

Soil layer	Concentration in soil (mg dm^{-3})	
(m)	Ridges (n = 15)	Furrows (n = 16)
0-0.05	119 (s.d.= 22)	143 (s.d. = 29)
0.05-0.10	2.0 (s.d. = 1.7)	3.1 (s.d. = 3.6)
0.10-0.20	1.0 (s.d. = 0.5)	2.1 (s.d. = 1.6)

The average concentrations of bromide-ion per layer in the soil profile at three times in the growing period of the potato crop are given in Table 5.2. On 29 May most of the dosage of bromide-ion was still present in the top metre of the soil profile. Movement below the furrows was deeper (peak in 0.3 to 0.5 m layer) than that below the ridges (peak in 0.1 to 0.2 m layer). The wide variation in concentration per layer is shown by the fact that standard deviations are of the same order of magnitude as the average concentrations. Sampling of the greatest depths was difficult due to limited power of the machine (29 May) or wet subsoil condition.

Table 5.2. *Concentrations of bromide-ion in the soil profile of the Roswinkel field at three times in the growing period of the potato crop in 2000. Averages of 16 measurements per layer, with standard deviation (s.d.). n = lower number of measurements.*

Soil layer	Concentration in soil (mg dm^{-3}) on					
(m)	29 May		13 July		18 September	
	ridges	furrows	ridges	furrows	ridges	furrows
0-0.1	6.4 (s.d. = 3.3)	1.7 (s.d. = 3.8)	0.4 (s.d.= 0.3)	0.4 (s.d. = 0.3)	2.5 (s.d = 1.8)	3.8 (s.d.= 1.7)
0.1 – 0.2	11.5 (s.d = 7.5)	4.6 (s.d = 5.6)	0.8 (s.d = 0.7)	0.3 (s.d = 0.3)	0.9 (s.d = 1.2)	2.8 (s.d. = 2.0)
0.2 – 0.3	5.5 (s.d = 5.7)	7.0 (s.d = 6.5)	1.3 (s.d. = 1.3)	0.2 (s.d. = 0.3)	0.3 (s.d. = 0.5)	2.2 (s.d. = 2.0)
0.3 – 0.5	1.2 (s.d. = 2.9)	11.0 (s.d = 7.1)	3.9 (s.d = 2.4)	0.4 (s.d. =0.4)	2.2 (s.d = 1.7)	2.3 (s.d. = 2.6)
0.5 – 0.7	1.5 (s.d. = 3.7)	2.6 (s.d = 2.5)	6.0 (s.d. = 3.4)	4.6 (s.d. = 3.6)	5.3 (s.d = 2.3)	5.5 (s.d.= 3.0)
0.7 – 0.9	< 0.7	< 0.7	8.7 (s.d = 6.8)	11.6 (n = 2)	7.2 (s.d. = 3.3)	7.1 (s.d = 4.9)
0.9 – 1.1			12.0 (n = 3)		8.3 (s.d = 7.7)	5.0 (s.d. = 4.6)

It seems that a substantial fraction of the bromide-ion had moved out of the top metre of the soil profile on 13 July (Table 5.2). Again, downward movement below the furrows was more extensive than that below the ridges.

On 18 September, the concentrations of bromide-ion below the ridges (Table 5.2) were only slightly lower that those on 13 July. It is remarkable that the concentrations below the furrows had increased in summer. The concentrations in the top layers below the furrows had become even higher than those in the top layers below the ridges.

The areic masses of bromide-ion in the soil profile on the sampling days, as calculated from the results in Table 5.2, are given in Table 5.3. The amounts are expressed also in percentage of the dosage (which corresponded to 64.7 mg dm^{-2}).

Table 5.3. *Amounts of bromide-ion measured in the soil profile of the Roswinkel field.*

Sampling date:		10 May	29 May	13 July	18 September
No of days after application:		0	19	64	131
Areic mass (mg dm^{-2}) for:	ridges	61.5	29.2	36.8	53.5
	furrows	75.2	39.2	10.5	53.5
	whole field	68.4	34.2	23.6	53.5
Percentage of dosage in:	whole field	105.6	52.9	36.5	82.7

The overall amount of bromide-ion measured in soil shortly after application (Table 5.3) was slightly higher than the calculated dosage. The amount measured below the ridges was distinctly lower than that below the furrows. On 29 May only about half of the dosage of bromide-ion was measured in soil. This is remarkable as there was hardly any leaching from soil (Table 5.2; Table 6.1) and hardly any uptake by the very small plants (just emerged; Section 2.1). The amount of bromide-ion below the ridges was smaller than that below the furrows. On 13 July the overall amount of bromide-ion corresponded to 36.5% of the dosage (Table 5.3), but now the amount below the ridges was distinctly higher than that below the furrows. This can be the result of more leaching from the furrows (Table 5.2). Surprisingly, the amount of bromide-ion in soil had increased strongly on 18 September, with equal amounts below the ridges and furrows. Substantial amounts of bromide-ion taken up by the potato crop may have been released from the plants in the last part of the growing period.

5.2   Carbofuran in the soil profile

Four soil columns were taken in each of four sections of the experimental field (Figure 2.1). The four soil samples for each layer in a field section were combined and mixed for the analysis of carbofuran (Section 2.5). So four measurements of carbofuran in a soil layer are available (one for each field section). The measured contents of carbofuran in soil were multiplied by soil bulk density of the layer to obtain its concentrations in soil.

The results of the measurements of carbofuran in the topsoil (three layers), shortly after application on 10 May, are given in Table 5.4. By far most of the carbofuran was measured in the top 0.05 m layer. The amount of carbofuran of 4.90 mg dm^{-2} measured in the top 0.2 m of the soil profile corresponds to 105.8% of the dosage (Table 5.6).

Table 5.4. Concentrations of carbofuran measured in the topsoil of the Roswinkel field shortly after application on 10 May 2000. Averages of four measurements. s.d. = standard deviation.

Soil layer (m)	Concentration in soil (mg dm^{-3})	
	Ridges	Furrows
0-0.05	9.35 (s.d. = 2.43	9.50 (s.d. = 0.65)
0.05-0.10	0.15 (s.d. = 0.09)	0.19 (s.d. = 0.07)
0.10-0.20	0.08 (s.d. = 0.02)	0.13 (s.d. = 0.05)

The average concentrations of carbofuran per layer in the soil profile, at three times in the growing season of the potato crop, are given in Table 5.5. On 29 May, the major part of the carbofuran distribution in soil was still present in the top 0.5 m of the soil profile. Below the furrows, the insecticide had moved deeper into the soil than below the ridges.

Table 5.5. Concentrations of carbofuran in the soil profile of the Roswinkel field at three times in the potato growing season of 2000. Averages of four measurements per layer, with standard deviation (s.d.). n = lower number of measurements.

Soil layer (m)	Concentration in soil (mg dm^{-3}) on					
	29 May		13 July		18 September	
	ridges	furrows	ridges	furrows	ridges	furrows
0-0.1	2.87 (s.d. = 0.68)	2.46 (s.d.= 0.14)	0.58 (s.d.= 0.14)	0.21 (s.d.= 0.04)	0.073 (s.d.= 0.043)	0.078 (s.d.= 0.045)
0.1-0.2	0.24 (s.d. = 0.07)	2.43 (s.d.= 0.14)	0.22 (s.d.= 0.03)	0.23 (s.d.= 0.08)	0.098 (s.d.= 0.080)	0.055 (s.d.= 0.025)
0.2-0.3	0.094 (s.d.= 0.171)	0.55 (s.d.= 0.44)	0.13 (s.d.= 0.08)	0.16 (s.d.= 0.17)	0.046 (s.d.= 0.030)	0.025 (s.d.= 0.036)
0.3-0.5	0.001 (s.d. = 0.003)	0.18 (s.d.= 0.11)	0.045 (s.d.= 0.026)	0.15 (s.d.= 0.09)	0.010 (s.d.= 0.018)	0.019 (s.d.= 0.014)
0.5-0.7	< 0.001	0.002 (s.d. = 0.002)	0.011 (s.d.= 0.008)	0.14 (s.d.= 0.10)	0.022 (s.d.= 0.032)	0.038 (s.d.= 0.067)
0.7-0.9	< 0.001	< 0.001	0.007 (s.d. = 0.008)	0.020 (n = 1)	0.005 (s.d. = 0.006)	0.022 (s.d.= 0.043)
0.9-1.1			0.029 (n = 2)		0.001 (s.d. = 0.001)	<0.001

The concentrations of carbofuran in the top layer decreased substantially in the period between 29 May and 13 July (Table 5.5). Still, movement below the furrows had been more extensive than that below the ridges. The concentrations at depths around 1 m indicate that some leaching of carbofuran had occurred. This is confirmed by the measurements in groundwater (Table 6.5).

On 18 September, carbofuran was distributed throughout the soil profile at a comparatively low level, both below the ridges and furrows (Table 5.5). In the summer of 2000, carbofuran could be measured in groundwater (Tables 6.5 and 6.6).

The areic masses of carbofuran in the soil profile on the sampling days, as calculated from the results in Table 5.5, are given in Table 5.6. The amounts are expressed also in percentage of the dosage (which corresponds to 4.63 mg dm^{-2}). Just after application (10 May), the amounts of carbofuran below the ridges and furrows were similar. The amount measured for the whole field was somewhat above the calculated dosage. On 29 May, the amount of carbofuran measured below the furrows was much higher than that below the ridges. This is an indication of surface runoff of water and pesticide from the ridges to the furrows. The amount of carbofuran in the whole field had only decreased to a limited extent in the first 19 days. In the period 29 May to 18 September there was a distinct further decrease of carbofuran in soil. On 13 July and 18 September, the amounts of carbofuran below the ridges and furrows were almost the same.

Table 5.6. Amounts of carbofuran in measured in the soil profile of the Roswinkel field.

Sampling date:		10 May	29 May	13 July	18 September
No of days after application:		0	19	64	131
Areic mass (mg dm^{-2}) for:	ridges	4.83	3.20	1.10	0.30
	furrows	4.98	5.79	1.19	0.32
	whole field	4.90	4.50	1.14	0.31
Percentage of dosage in:	whole field	105.8	97.1	24.7	6.6

The decrease in time of the amount of carbofuran in the soil profile is given on linear-linear scales in Figure 5.1.
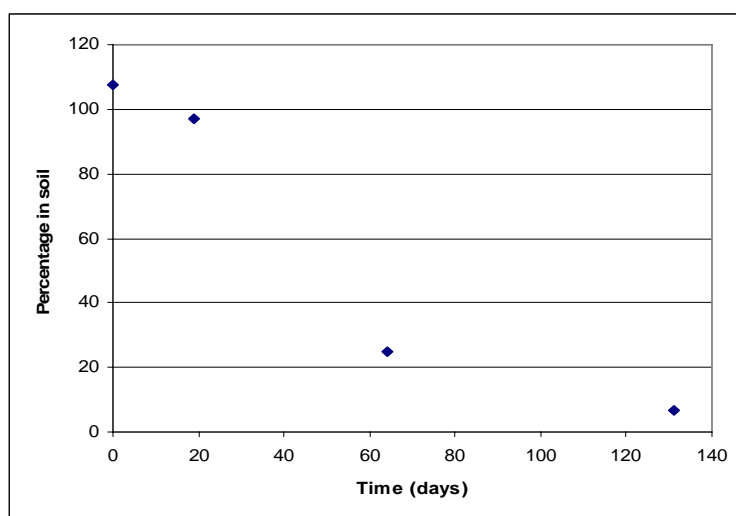

Figure 5.1. Decrease with time of the amount of carbofuran in the soil profile, expressed as percentage of the dosage. Linear-linear scales.

The natural logarithm of the percentages of carbofuran remaining in soil is plotted against the time in Figure 5.2. The decrease was approximated by first-order kinetics, by linear regression of this plot in Excel. The resulting rate coefficient is 0.0224 day^{-1}, which corresponds to a half-life of 30.9 days. It should be noted that this decrease is caused by different processes: 1) transformation in soil, 2) uptake by the plants, and

3) leaching from the soil profile. So the half-life of transformation of carbofuran in soil was longer.
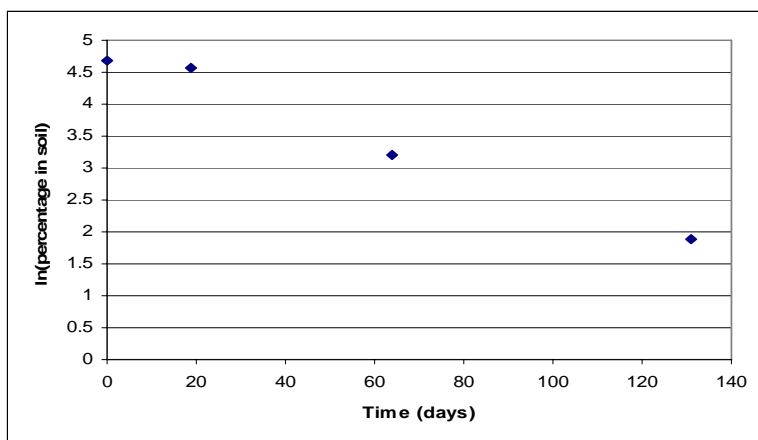

Figure 5.2. Decrease with time of the amount of carbofuran in the soil profile, on natural logarithmic – linear scales.

6 Measured concentrations in groundwater

6.1 Bromide-ion in groundwater

Groundwater samples could be collected via tubes from a maximum of four depths: 0.9 m, 1.3 m, 1.6 m and 2.0 m (Section 2.8). Only at three sampling times (out of 14) groundwater could be collected from 0.9 m depth, because groundwater level was above this level at these times. Sampling of groundwater at 1.3 m depth was possible at six times. Samples of groundwater at 1.6 and 2.0 m depth could be taken at all the 14 sampling times.

Six groundwater samples (three from 1.6 m and three from 2.0 m depth) were taken as blank samples on 8 May, before the applications (10 May 2000). The response of the analytical method was equivalent to a maximum of 0.3 mg bromide-ion per L. This value was taken to be the limit of quantification of bromide-ion applied as a tracer in the present experiment.

Especially in the first few months after application and after more than 1.5 years, bromide-ion was only quantifiable in a small fraction of the groundwater samples from a certain depth. In some early samples, one or a few concentrations were much higher than the others. Nevertheless, the concentrations were averaged per combination of sampling time and depth in the subsoil, to obtain a first survey of the results. The fraction of quantifiable concentrations is indicated by n_q/n_t, with n_q = number of quantifiable concentrations and n_t = total number of analyses. The standard deviation is only given in cases with a substantial number of quantifiable concentrations, with a roughly normal distribution. In the other cases, "skew" indicates a skew distribution with one or a few comparatively high concentrations, beside a vast majority of very low concentrations.

The results of the measurements of bromide-ion in the groundwater at depths of 0.9 m and 1.3 m are summarised in Table 6.1. Substantial concentrations of bromide-ion were measured in the shallow groundwater that could be sampled in the first few months of 2001. In September 2001, the concentrations had become lower. From January 2002 on, bromide-ion could not be quantified anymore in the groundwater at these shallow depths.

Table 6.1. *Averages of the concentrations of bromide-ion measured in groundwater at 0.9 and 1.3 m depth. s.d. = standard deviation. skew = skew distribution of the concentrations.*

Sampling depth (m)	Date	Days after application	Quantifiable ratio n_q/n_t	Average concentration (mg L^{-1})
0.9	6 February 2001	272	12/15	3.2 (s.d. = 2.5)
	24 September 2001	502	8/8	0.51 (s.d. = 0.69)
	31 January 2002	631	2/16	< 0.3
1.3	29 May 2000	19	0/16	< 0.3
	6 February 2001	272	16/16	8.4 (s.d. = 3.5)
	4 April 2001	329	16/16	9.0 (skew)
	24 September 2001	502	16/16	2.5 (s.d. = 1.5)
	31 January 2002	631	6/16	< 0.3
	7 May 2002	727	0/16	< 0.3

The results of the measurements of bromide-ion in the groundwater at 1.6 m depth are summarised in Table 6.2. In the period end-June to mid-August 2000, bromide-ion could only be quantified in a limited number of the groundwater samples, with one or a few comparatively high concentrations. Average concentration was low in this period. From end-August 2000 on, bromide-ion could be quantified in most of the groundwater samples, with a roughly normal distribution of the concentrations. The average concentration increased to a maximum of 14.8 mg L^{-1} in February 2001, after which it decreased gradually to below quantifiable level in May 2002.

Table 6.2. *Averages of the concentrations of bromide-ion measured in groundwater at 1.6 m depth. s.d. = standard deviation. skew = skew distribution of the concentrations.*

Date	Days after application	Quantifiable ratio n_q/n_t	Average concentration (mg L^{-1})
29 May 2000	19	1/16	<0.3
28 June 2000	49	3/16	0.3 (skew)
19 July 2000	70	4/16	0.5 (skew)
18 August 2000	100	5/16	0.5 (skew)
31 August 2000	113	12/16	1.0 (s.d. = 1.7)
26 September 2000	139	10/16	1.0 (s.d. = 1.9)
18 October 2000	161	13/16	3.2 (s.d. = 4.7)
6 February 2001	272	16/16	14.8 (s.d. = 3.0)
4 April 2001	329	16/16	7.8 (s.d. = 1.3)
17 May 2001	372	16/16	6.1 (s.d. = 1.9)
18 July 2001	434	4/4	6.6 (s.d. = 1.2)
24 September 2001	502	16/16	5.0 (s.d. = 1.3)
31 January 2002	631	10/16	0.3 (s.d. = 0.3)
7 May 2002	727	2/16	< 0.3

The results of the measurements of bromide-ion in the groundwater at 2.0 m depth are summarised in Table 6.3. After the low concentrations at the end of May 2000, the average concentration of bromide-ion was below quantifiable level until mid-October 2000. In this period, only a few individual concentrations were above the quantification limit. From begin-February 2001 onwards, substantial concentrations were measured in almost all groundwater samples. Average concentration increased to a maximum of 12.6 mg L^{-1} on 4 April 2001, after which it gradually decreased to below quantifiable level on 7 May 2002.

Table 6.3. Averages of the concentrations of bromide-ion measured in groundwater at 2.0 m depth. s.d. = standard deviation. skew = skew distribution of the concentrations.

Date	Days after application	Quantifiable ratio n_q/n_t	Average concentration (mg L^{-1})
29 May 2000	19	13/16	0.4 (s.d. = 0.2)
28 June 2000	49	0/16	< 0.3
19 July 2000	70	0/16	< 0.3
18 August 2000	100	2/16	< 0.3
31 August 2000	113	3/16	< 0.3
26 September 2000	139	0/16	< 0.3
18 October 2000	161	1/16	< 0.3
6 February 2001	272	16/16	10.1 (s.d. = 7.2)
4 April 2001	329	16/16	12.6 (s.d. = 4.0)
17 May 2001	372	16/16	11.6 (s.d. = 2.0)
18 July 2001	434	16/16	11.8 (s.d. = 2.2)
24 September 2001	502	16/16	9.5 (s.d. = 2.8)
31 January 2002	631	14/16	1.5 (s.d. = 1.3)
7 May 2002	727	3/16	< 0.3

It can be assumed that the dosage of bromide-ion reaching the soil surface in the small part of the experimental field with the many groundwater tubes was lower than the average dosage on the field (Crum et al., 2004). Further the dosage on the soil surface may have been more irregular than in the main part of the field. The plastic bags covering the top of the groundwater tubes increased the interception area. Some of the intercepted bromide-ion may have been washed-off afterwards.

The general picture in the groundwater measurements for bromide-ion is that there was a first period with incidentally occurring comparatively high concentrations besides a great majority of much lower concentrations. In a second period, the major leaching wave of bromide-ion appeared. This indicates that there was preferential water flow and substance transport in the sandy soil. However, in the case of incidentally occurring high concentrations, it is difficult to assess the possible contribution of incidental complications related to the experimental procedures, such as short-circuit transport of water and substance around the groundwater tubes and contamination during sampling and analysis. A literature study may reveal whether preferential water flow and substance transport in sandy soils has been measured also in other cases.

6.2 Carbofuran in groundwater

At two days before the application on 10 May 2000, the concentration of carbofuran in six groundwater samples (three from 1.6 m and three from 2.0 m depth) was below the limit of quantification (0.05 µg L^{-1}).

The results of the measurements of carbofuran in the groundwater at depths of 0.9 and 1.3 m (when the groundwater table was high enough to be sampled) are summarised in Table 6.4. At both depths, the highest concentrations were measured in February 2001; they tended to be lower in September of that year. In January 2002, traces of carbofuran were measured in some samples, but the average concentration was below quantifiable level.

Table 6.4. Averages of the concentrations of carbofuran measured in groundwater at 0.9 and 1.3 m depth. s.d. = standard deviation.

Sampling depth (m)	Date	Days after application	Quantifiable ratio n_q/n_t	Average concentration ($\mu g\ L^{-1}$)
0.9	6 February 2001	272	13/15	0.26 (s.d. = 0.27)
	24 September 2001	502	4/8	0.10 (s.d. = 0.13)
	31 January 2002	631	4/16	< 0.05
1.3	29 May 2000	19	3/16	<0.05
	6 February 2001	272	15/16	0.16 (s.d. = 0.08)
	24 September 2001	502	13/16	0.13 (s.d. = 0.10)
	31 January 2002	631	6/16	< 0.05

The results of the measurements of carbofuran in the groundwater at 1.6 m depth are summarised in Table 6.5. Already at the end of May 2000, low concentrations of carbofuran were measured in the groundwater. At several times after that, a comparatively high average concentration resulted from one or a few very high concentrations, while the other values were much lower. The highest average concentration resulting from skew concentration distributions was 17.0 µg L^{-1}. The maximum value of the averages of concentrations at roughly the same level was only 0.84 µg L^{-1}. It is remarkable that the concentrations were very low at some of the sampling times, amidst substantially higher values. Such a pattern does not correspond to that for bromide-ion (Section 6.1).

Table 6.5. Averages of the concentrations of carbofuran measured in groundwater at 1.6 m depth. s.d. = standard deviation. skew = skew distribution of the concentrations.

Date	Days after application	Quantifiable ratio n_q/n_t	Average concentration ($\mu g\ L^{-1}$)
29 May 2000	19	10/16	0.07 (s.d. = 0.07)
28 June 2000	49	5/16	12.6 (skew)
19 July 2000	70	15/16	17.0 (skew)
18 August 2000	100	13/16	2.3 (skew)
31 August 2000	113	13/16	0.22 (s.d. = 0.23)
26 September 2000	139	12/16	8.7 (skew)
18 October 2000	161	14/16	0.10 (s.d. = 0.08)
6 February 2001	272	16/16	3.9 (skew)
17 May 2001	372	2/16	< 0.05
18 July 2001	434	4/4	0.84 (s.d. = 0.68)
24 September 2001	502	16/16	0.15 (s.d. = 0.07)
31 January 2002	631	3/16	< 0.05

The results of the measurements of carbofuran in the groundwater at 2.0 m depth are summarised in Table 6.6. At this depth too, low concentrations were already measured on 29 May 2000. There are two very skew concentration distributions for this depth, so the effect of incidental very high concentrations was less than at 1.6 m depth (Table 6.5). The maximum average concentration at 2 m depth of 11.6 µg L^{-1} in July 2001 (Table 6.6) was the result of many concentrations at this level. Again there were very low average concentrations, alternated with distinctly higher values.

Table 6.6. Averages of the concentrations of carbofuran measured in groundwater at 2.0 m depth. s.d. = standard deviation. skew = skew distribution of the concentrations.

Date	Days after application	Quantifiable ratio n_q/n_t	Average concentration (µg L^{-1})
29 May 2000	19	11/16	0.09 (s.d. = 0.07)
28 June 2000	49	1/16	< 0.05
19 July 2000	70	14/16	0.14 (s.d. = 0.07)
18 August 2000	100	16/16	0.14 (s.d. = 0.05)
31 August 2000	113	7/16	0.10 (skew)
26 September 2000	139	12/16	0.36 (s.d. = 0.54)
18 October 2000	161	9/16	0.09 (s.d. = 0.10)
6 February 2001	272	16/16	5.0 (skew)
17 May 2001	372	1/16	< 0.05
18 July 2001	434	14/16	11.6 (s.d. = 18.5)
24 September 2001	502	13/16	0.09 (s.d. = 0.07)
31 January 2002	631	3/16	< 0.05

The possible causes of incidental high concentrations of carbofuran in groundwater are the same as those for bromide-ion (Section 6.1).

At various times there is a very low groundwater concentration of carbofuran in between times with much higher concentrations. Examples are:
1.6 m deep; 31 August 2000;
1.6 m deep; 18 October 2000;
1.6 m deep; 17 May 2001
2.0 m deep; 17 May 2001.
Bromide-ion does not show such much lower concentrations in groundwater at these depths and times (Tables 6.2 and 6.3). It seems that carbofuran was subject to transformation in the samples/extracts during storage (Crum et al., 2004). One of the possible causes is that the pH became rather high in the non-buffered aqueous solutions, leading to hydrolysis of carbofuran at a substantial rate (Section 3.2).

6.3 Additional groundwater measurements

One-half of the groundwater tubes was placed in the ridges and the other half was placed in the furrows (Section 2.8). The concentrations of bromide-ion at 0.9 and 1.3 m beneath the furrows were mostly higher than those beneath the ridges (in three out of four samples). In a first period, the concentrations at 1.6 m beneath the furrows (total of 11 samples) were mostly lower than those beneath the ridges, but in a second period they were higher. At 2.0 m depth (total of 12 samples), the

concentrations of bromide-ion beneath the furrows and ridges were mostly at the same level.

The concentrations of carbofuran at 0.9 and 1.3 m depth beneath the furrows (total of three samples) were at the same level as those beneath the ridges. At 1.6 m beneath the ridges, there were some very high concentrations, which were not measured beneath the furrows. At 2.0 m depth, carbofuran concentrations (total of 11 samples) beneath the furrows and the ridges were mostly at the same level. There are two major uncertainties with the carbofuran concentrations in groundwater: 1) the risk of contamination of the samples and 2) the possible degradation of carbofuran during storage of the samples. So the results for carbofuran do no seem to be suitable for comparing the concentrations in groundwater beneath furrows an ridges.

One may wonder whether differences in concentration can be expected in the groundwater beneath ridges and furrows (e.g at 1.6 and 2.0 m depth). It seems that groundwater can easily have a horizontal flow component over short distances, such as the 0.38 m between the ridges and the furrows. Further, water was pumped from the groundwater tubes, both before sampling (as prescribed) and during sampling. It can be expected that this withdrawal induced a horizontal flow component. Even a small horizontal flow component of the groundwater makes the origin (ridges, furrows) of a residue measured in groundwater questionable. It is assumed that little weight can be given to the differences in concentration in the groundwater sampled below the ridges and furrows.

Groundwater tubes were installed also on three places outside the sprayed part of the field, to the South-West (SW), South-East (SE) and North-East (NE) sides, respectively (Figure 2.1). In a period of two years after application, water samples were taken via the tubes from depths of 1.3 (once), 1.6 and 2.0 m. The concentrations of bromide-ion and carbofuran in these samples were measured. In 70% of the water samples, the concentration of bromide-ion was below the quantification limit. For carbofuran, 34% of the concentrations was below this limit. The SW tubes had the highest number of positive measurements for bromide-ion, while the NE tubes had most positive measurements for carbofuran. The highest average concentration of bromide-ion was measured in the SW tubes, while the highest average concentration of carbofuran was measured in the SE tubes. These measurements do not give a coherent picture about a predominant flow direction of the upper groundwater below the field. The global groundwater flow in the region is expected to be in the North-West direction (Section 2.6), without concentration measurements in the present experiment.

7 Measured bromide-ion contents in the crop

The results of the measurements on bromide-ion in the crop parts are summarised in Table 7.1. The contents of bromide-ion in the leaves + stems were higher than those in the tubers + main roots. As expected, the mass of leaves + stems of the full-grown crop remained at the same level, while the mass of tubers + main roots increased substantially. The percentage of bromide-ion in the leaves + stems was highest at the first sampling time. However, the percentage in the tubers + main roots increased in time.

Table 7.1. Average contents (on dry mass basis) and total amounts of bromide-ion in the potato-crop parts in 2000. s.d. = standard deviation. n.d. = not determined.

Sampling date	Plant parts	Content of bromide (mg kg^{-1})	Dry matter of plant parts (kg ha^{-1})	Areic mass of bromide in plant parts	
				in kg ha^{-1}	in percentage of dosage
10 July	Leaves + stems	4107 (s.d. = 1113)	2470 (s.d. = 69)	10.1 (s.d. = 2.8)	15.7 (s.d. = 4.3)
	Tubers + main root	295 (s.d. = 84)	1733 (s.d. = 80)	0.51 (s.d. = 0.14)	0.79 (s.d. = 0.21)
18 September	Leaves + stems	2121 (s.d. = 153)	2602 (s.d. = 274)	5.5 (s.d. = 0.7)	8.5 (s.d. = 1.2)
	Tubers + main root	237 (s.d. = 38)	8833 (s.d. = 369)	2.1 (s.d. = 0.4)	3.2 (s.d. = 0.6)
24 November	Tubers + main root	274 (s.d. = 48)	n.d.	n.d.	n.d.

It should be noted that the recovery of bromide-ion was only measured for two potato-tuber samples. The recoveries were 38 and 57% (Section 2.9); the cause of these low recoveries is not known.

The content of bromide-ion in the tubers + main roots remained at the same level in the measuring period. Assuming that the mass of tubers + main roots increased with 15% after 18 September, the amount of bromide-ion removed with the harvested tubers at the end of November is estimated to be 4.3% of the dosage. Much of the bromide-ion taken up by the plants may have been released from the crop remnants (leaves, stems, roots) to the soil in the last part of the growing season.

Bromide-ion content in two tuber samples taken from the small field section with many groundwater tubes (24 November) was on average 55% of that of the content in the samples from the other parts of the field. Presumably, much of the dosage of bromide-ion sprayed on this section was intercepted by the many plastic bags covering the top of the groundwater tubes to prevent contamination.

8 Set up of the computations

8.1 Soil system

The computation period started on 1 January 2000 to minimise the effect of the selected initial conditions on simulated soil moisture and temperature on the day of application of the substances (10 May 2000). The initial depth of the groundwater table was set at 0.8 m. The temperature at the bottom end of the soil system was set at 10 °C in the beginning.

The first computations with the PEARL model (version 3.3.3) were set up for the averaged situation at the Roswinkel field. For this purpose, the soil characteristics measured separately for ridges and furrows were pooled and then averaged. Later on in this report, computations are presented for the ridge and furrow systems separately (Chapter 12 etc.)

The soil-groundwater system was simulated to a depth of 3.0 m. From top to bottom, the following soil horizons were distinguished in the averaged soil system:
- ten horizons 0.1 m thick, each with five computation compartments;
- one horizon 1.1 m thick, with 55 computation compartments;
- one horizon 0.9 m thick, with 18 computation compartments.

The properties of the soil horizons were obtained by interpolation and extrapolation of the measurements for the Roswinkel field. The resulting values for each of the soil horizons are given in Table 8.1. The bulk densities are averages for the whole field (ridges and furrows). The depth factor f_z for the effect of soil depth on the rate of pesticide transformation was derived from the Dutch Standard Scenario.

Table 8.1. Properties of each soil horizon, most of them derived from the measurements for the soil of the Roswinkel field.

Depth soil horizon (m)	Sand (> 50 μm) (%)	Silt (2-50 μm) (%)	Clay (< 2 μm) (%)	Organic matter (%)	Bulk density (kg m^{-3})	pH	Depth factor f_z (-)
0-0.1	87.9	8.5	3.6	4.9	1150	4.5	1.0
0.1-0.2	87.9	8.5	3.6	4.9	1270	4.5	1.0
0.2-0.3	87.9	8.5	3.6	3.1	1410	4.5	1.0
0.3-0.4	92.0	5.4	2.6	1.7	1540	4.7	0.98
0.4-0.5	93.1	4.6	2.3	1.2	1670	4.8	0.91
0.5-0.6	94.5	3.5	2.0	0.6	1730	4.8	0.80
0.6-0.7	95.1	2.9	2.0	0.5	1810	5.0	0.67
0.7-0.8	95.7	2.3	2.0	0.3	1810	5.0	0.50
0.8-0.9	95.7	2.3	2.0	0.3	1810	5.0	0.33
0.9-1.0	95.7	2.3	2.0	0.3	1810	5.0	0.10
1.0-2.1	95.7	2.3	2.0	0	1810	5.0	0
2.1-3.0	95.7	2.3	2.0	0	1810	5.0	0

Default values were used for some transport parameters in all the computations. The dispersion length for the spreading of the substance distribution during transport with water was set at 0.05 m. Substance diffusion in the water and gas phases was described by Currie's method.

8.2   Water flow

Water flow in the Roswinkel soil was simulated starting from the hydraulic relationships presented by Wösten et al. (2001). The use of these averaged relationships is preferred over the use of the single lab measurements for some soil layers of the Roswinkel field, in the framework of the study of Crum et al. (2004). Experiences with the use of the latter relationships in the simulation of water flow with the SWAP-PEARL model combination are presented in Appendix D.

Wösten et al. (2001) collected soil moisture retention and hydraulic conductivity curves measured in the laboratory for many Dutch topsoils and subsoils. Average relationships were derived for several topsoil and subsoil classes. The soil classes most relevant for the Roswinkel field are topsoil B1 and subsoil O1. The hydraulic relationships are the averages of measurements for many soils, which showed a wide variation within the soil classes. The laboratory measurements start with wet soils, so the drying curves are measured. With the alternate wetting and drying in the field, wetting-drying scanning curves apply. For these reasons it can be expected that calibration of the hydraulic relationships is needed, to describe the water flow in the Roswinkel field. This calibration is described in Section 9.2.

The flow of groundwater through the simulated soil system (3 m deep) is considered to be vertical. The horizontal component of regional flow in the groundwater zone is estimated to be in the order of a few metres per year (Section 2.6). The horizontal flow is expected to occur mainly in the deeper coarse-sandy layers.

A selection has to be made from the boundary conditions for groundwater flow at the bottom end of the soil system, provided by the SWAP-PEARL model combination. Here the option "Flux boundary condition" is selected, in which the downward groundwater flux q is an exponential function of the groundwater level h (q-h relationship). This option is valid for deep sandy subsoils (van Dam et al., 1997). The starting values for the empirical coefficients in the equation (a_{fb} = -0.0112 $m^3 m^{-2}$ d^{-1}) en b_{fb} = -2.5 m^{-1}) were taken from the Dutch Standard Scenario.

Relationships between water discharge q and groundwater level h were measured by Massop & de Wit (1994) for a series of sandy soils with shallow water table. In the description of the relationships with the exponential q-h function, they found a wide range of values for the coefficients a_{fb} and b_{fb}. So it can be expected that calibration of these coefficients to the Roswinkel field situation is needed. This calibration is described in Section 9.2.

Rainfall plus sprinkler irrigation was introduced as measured at the Roswinkel site (Section 2.3). Rainfall was supplemented (for the periods without measurements) with data from surrounding rainfall stations of KNMI. Potential evapotranspiration, as calculated by KNMI using Makkink's method, was introduced into the Meteo file ("Input" option in PEARL). Daily minimum and maximum air temperatures (Section 2.3) were introduced into the Meteo file, for calculation of soil temperatures by the model.

8.3   Crop development and water uptake

The development of the potato crop on the Roswinkel field was defined by using the "fixed crop cycle" option in PEARL. The emergence of the potato crop was set at 22 May 2000. Three crop growth periods were distinguished. In the first period (22 May to 10 July), soil cover by the plants increased linearly until full cover was reached (Section 2.1). In the second period (10 July to 18 September), a full-grown potato crop was simulated to be present. The height of the full-grown crop was taken to be 0.5 m and its Leaf Area Index was set at 4 in this period (Feddes, 1987; Pinto, 1988). In the third period (19 September to 16 October), the green plant parts were assumed to die-off linearly, until no active canopy was left. The time remaining to the harvest of the potato tubers (end of November) was left out of the crop growing period, because there was hardly any above-ground crop activity. The soil was kept fallow during the next year 2001.

Rooting depth of the potato plants was taken to increase linearly from 0.1 m (at emergence) to the final depth of 0.5 m (reached at the end of the first crop growth period). In the top half of the root zone, root activity was taken to be constant with depth; in the lower half it decreased linearly with depth to zero at the lower end of the rooting zone (Pinto, 1988; Gregory & Simmonds, 1992).

Plant transpiration is calculated by multiplying the reference crop evapotranspiration with a crop factor. An averaged crop factor of 1.1 was used for the whole growth period (Feddes, 1987).

Water uptake by the plant roots at a certain depth in soil was dependent on the pressure head h of the water at that depth, as proposed for a potato crop by van Dam et al. (1997). The characteristic points from very wet to very dry soil are:
- start of water uptake (oxygen supply) at h_1 = -0.1 m;
- start of optimal water uptake at h_2 = -0.25 m;
- start of decrease of water uptake under high evaporative demand at $h_{3, high}$ = -3.2 m;
- start of decrease of water uptake under low evaporative demand at $h_{3,low}$ = -6.0 m;
- permanent wilting point at h_4 = -160 m.

8.4 Input data for the substances

Bromide-ion

Bromide-ion was selected as a tracer for water flow because it shows minimal interactions with the soil. The ionic mass of bromide is 79.9 g mol^{-1}. In various cases, arbitrarily very low or very high values can be used for the properties of bromide-ion; they were introduced for 20 ºC. The vapour pressure of bromide-ion is very low; it was set at 10^{-6} mPa. The solubility of bromide-ion in water is very high; it was set at 10^5 mg L^{-1}. The coefficient of diffusion of bromide-ion in water (Lide, 1999) was set at 1.6 10^{-4} m^2 d^{-1} (20 ºC). The diffusion coefficient in air was taken to be 1.6 m^2 d^{-1} (but there was virtually no bromide present in the gas phase).

Adsorption of bromide as an anion to soil can be assumed to be zero. The half-life of transformation of bromide in soil was set at the very high value of 10^5 days. The concept of the Transpiration Stream Concentration Factor (TSCF) for uptake by plant roots does not hold for ionic species. As there is no alternative in the model and as no quantitative information is available, TSCF was tentatively set at 0.5 for bromide-ion.

The crop measurements indicate that substantial amounts of bromide-ion were taken up by the potato plants (Chapter 7). Further, it seems that bromide-ion was released from the plants to the soil in the last part of the growing season. These processes make bromide-ion less suitable as a tracer of water flow in soil in the presence of a crop. They have to be considered when using the measurements of bromide-ion in the soil profile, carried out during the growing season (up to 18 September 2000) for testing the computations. Bromide-ion can be used well as a tracer in periods without a crop (winter half-year), but then there are no ridges and furrows anymore.

In the field study described by Scorza Júnior et al. (2004), bromide-ion was used as a tracer on a field with clay soil grown with winter wheat. Application of bromide in spring, in the presence of a young wheat crop, was followed by a rapid and high uptake by the crop and a rapid decline in the soil. In the course of the growing season, bromide-ion was gradually released from the crop to the soil. It was concluded that bromide-ion is not an ideal tracer for water flow in soil grown with a crop.

Carbofuran

Vapour pressure of carbofuran was set at the low value of 0.1 mPa at 20 ºC (a kind of average value for a range of reported data; Section 3.2). The Freundlich adsorption coefficient was set at 16 L kg^{-1} at 15 ºC and the exponent at 0.83 (based on the lab measurement; Section 4.1). Only equilibrium adsorption/desorption was considered.

The laboratory measurements of the transformation rate of carbofuran in the Roswinkel soil (collected after the field experiment) are not representative, because the soil micro-organisms had adapted to the pesticide (Section 4.2). The half-life of 30.9 d for carbofuran in the field soil (Section 5.2) was the result of various

processes, like transformation in the soil, uptake by the crop and leaching from the soil. So the half-life of transformation of carbofuran will have been longer than 30.9 days. In the computations, the starting value for the half-life of carbofuran transformation in topsoil (moist, 15 $^{\circ}$C) was taken to be 35 days. It can be attempted to get a closer approximation to the transformation rate coefficient by comparing the computed and measured amounts of carbofuran in the soil

8.5 Preliminary computations

The first computations were carried out for bromide-ion and carbofuran in the Dutch Standard Scenario (application in spring), as presented by the PEARL model. The aim of these runs is to get an impression of the material balance of the substances in a situation which is considered to be 80% vulnerable with respect to soil properties and also 80% vulnerable with respect to amount of rainfall. Later on, the vulnerability of the Roswinkel situation can be compared with that of this standard scenario.

As expected, computed volatilisation of bromide-ion from the soil system was nil. Similarly, transformation of bromide-ion in the soil was nil. The computed uptake of bromide by the crop amounted to 57% of the dosage. The percentage leached to the upper groundwater was computed to be 43% of the dosage. The maximum average concentration of bromide-ion in the upper groundwater was 95.9 μg L^{-1} (reached at 0.95 year after application). For a dosage of 64.7 kg bromide-ion per ha as in the Roswinkel experiment (instead of 1 kg ha^{-1} in the standard scenario), the maximum average concentration would be 6.2 mg L^{-1}. This is of the same order of magnitude as measured in the groundwater of the Roswinkel field (Section 6.1).

For the standard dosage of 1 kg ha^{-1}, the maximum average concentration of carbofuran in the upper groundwater was calculated to be 0.34 μg L^{-1} (at 1.6 year after application). Accounting for the field dosage of 4.63 kg ha^{-1}, the maximum average concentration becomes 1.58 μg L^{-1}. The highest average concentration of carbofuran measured in the upper groundwater of the Roswinkel field (for approximately normal concentration distributions) was 11.6 μg L^{-1} (at 1.2 year after application; Section 6.2). This higher measured maximum concentration appearing earlier is possibly related to the comparatively high amount of rainfall plus sprinkler irrigation in combination with the ridge-furrow system.

Computed volatilisation of cabofuran from the soil was only 0.0024% of the dosage. Most of the applied carbofuran was computed to be transformed in the soil system: 86.5% of the dosage. The computed uptake by the crop roots amounted to 13.4% of the dosage. The percentage of the dosage computed to be leached to the upper groundwater amounted to 0.15%. So it seems justified to ascribe most of the decline of carbofuran in field soil to transformation and a minor part to uptake by plants.

9 Simulation of water flow in the averaged field

9.1 Moisture retention, hydraulic conductivity and groundwater discharge

Computations with the SWAP-PEARL combination are carried out with the hydraulic relationships given by van Dam et al. (1997). Parameter values for these Van Genuchten-Mualem equations are given by Wösten et al. (2001) in the Staring Series. A high number of moisture retention curves were measured in the course of years and they were averaged per soil class. The soil classes most relevant for the Roswinkel field are humic sandy topsoil B1 and sandy subsoil O1. The parameter values in the Van Genuchten-Mualem equations for the soil classes B1 and O1, used as starting point in the present computations, are given in Table 9.1. The symbols in this table are defined in Section 2.4.

Table 9.1. Parameters values of the Van Genuchten-Mualem equations for the hydraulic relationships of the soil classes B1, O1 and O2, as defined by Wösten et al. (2001).

Soil class	Θ_{res} ($m^3\,m^{-3}$)	Θ_{sat} ($m^3\,m^{-3}$)	α (cm^{-1})	n	λ	K_{sat} ($m\,d^{-1}$)
Topsoil B1	0.02	0.43	0.0234	1.801	0.0	0.234
Subsoil O1	0.01	0.36	0.0224	2.286	0.0	0.152
Subsoil O2	0.02	0.38	0.0213	1.951	0.168	0.127

On the basis of the measurements of soil moisture profiles in the field samples (Table 2.5), the volume fraction of water $\Theta_{(-1.0)}$ in the topsoil at a pressure head h_p of -1.0 m (pF =2) is expected to be in the range of 0.20 to 0.25 $m^3\,m^{-3}$. The question is now whether the moisture retention curve for Topsoil B1 (Table 9.1) can be expected to describe the field situation. To check this, moisture retention by the topsoil at h_p = - 1.0 m was calculated and found to be $\Theta_{(-1.0)}$ = 0.21 $m^3\,m^{-3}$.

The parameter values used for the hydraulic conductivity curves for topsoil and subsoil were also taken from Wösten et al. (2001); they are included in Table 9.1. The parameter values for the topsoil were assigned to the top 0.5 m of the Roswinkel soil system; those for the subsoil to the soil system below 0.5 m.

Groundwater flow was taken to proceed in vertical direction. The groundwater flux q_{bot} at the bottom of the soil system (3 m deep) was calculated using an exponential function of the depth of the groundwater table ("flux boundary condition" in SWAP-PEARL; van Dam et al., 2001). This boundary condition is considered to be suitable for deep sandy subsoils. The initial values of coefficient a_{fb} = - 0.0112 $m^3\,m^{-2}\,d^{-1}$ and exponent b_{fb} = - 2.5 m^{-1} were taken from the Dutch Standard Scenario in PEARL.

9.2 Calibration of water flow

Run W1 with the SWAP-PEARL combination of models was carried out with the initial values of the parameters for water flow, as given in Table 9.1 (B1 and O1). The calculated volume fractions of water in soil were much higher than those measured in the field. Further, the calculated depth of the groundwater table was much shallower than measured. At five measuring times in the growing season of 2000, calculated depth of the groundwater table was on average only 0.72 times the measured depth. As a first step in the calibration, the flow of groundwater from the bottom of the soil system had to be increased.

In Run W2, the coefficient a_{fb} in the exponential groundwater discharge equation was doubled to $-$ 0.0224 $m^3 m^{-2} d^{-1}$. This increased the average value of the ratio computed/measured for the depth of the groundwater table to 0.95. On the basis of this, the value of a_{fb} was rounded off to $-$ 0.025 $m^3 m^{-2} d^{-1}$ (slightly greater discharge) in Run W3 (b_{fb} was maintained at - 2.5 m^{-1}). Then the ratio between computed and measured groundwater level was on average 0.99 (n = 5; s.d. =0.18), which was considered to be acceptable at this stage.

The volume fractions of water in the top 0.5 m of the soil, computed with Run W3, were mostly higher than the averages from the field measurements. This indicates that moisture retention in the top layer was over-estimated. The moisture retention curve for topsoil B1 was measured in the laboratory as the drying curve for well-wetted soil columns. Due to hysteresis in the field, with alternating wetting and drying, moisture retention can be expected to be lower. To simulate the wetting-drying scanning curves in a simplified way with a single retention curve, Θ_{sat} of the top layer was set at the lower value of 0.40 $m^3 m^{-3}$ in the next Run W4.

There was a clear dip in the volume fraction of water computed in Run W3 for the layers just below the 0.5 m top layer. Such a dip did not show up in the measurements. This indicates that moisture retention at a pressure head of about – 0.5 m was underestimated by the computation, using the parameters of Subsoil O1. Therefore, the parameters for related Subsoil O2 (Wösten et al., 2001), with a somewhat higher moisture retention, were introduced for the subsoil in Run W4. The parameter values for Subsoil O2 are included in Table 9.1.

The saturated volume fraction of water Θ_{sat} in the subsoil was too high in Run W3, using Θ_{sat} = 0.36 $m^3 m^{-3}$ for Subsoil O1 (Table 9.1). According to the field measurements, average Θ_{sat} in the Roswinkel subsoil was 0.31 $m^3 m^{-3}$. To account for this, the Θ_{sat} value of Subsoil O2 was adjusted to 0.31 $m^3 m^{-3}$ in computer Run W4. Further, Θ_{res} was maintained at 0.01 $m^3 m^{-3}$, a value which holds for almost all sandy subsoils (Wösten et al., 2001).

In Run W4, volume fraction of water in the top layer was still over-estimated in most cases. Therefore, Θ_{sat} in the top layer was lowered somewhat to 0.38 $m^3 m^{-3}$ in Run W5, to account for a somewhat greater hysteresis effect. In Run W4, there was still a dip in the volume fraction of water in the upper part of the subsoil (such a dip was

not measured). Thus, moisture retention at these depths was still under-estimated. To remedy this, the α value for Subsoil O2 was lowered to $\alpha = 0.015$ cm^{-1} in Run W5. This moves the reflection point in the moisture retention curve to a lower pressure head: from about $h_p = -0.47$ m to about $h_p = -0.67$ m (Wösten et al., 2001).

The parameter values obtained in the calibration and used for the hydraulic relationships in the further simulations of water flow in the Roswinkel soil are presented in Table 9.2.

Table 9.2. Calibrated parameter values used in the hydraulic relationships for the further simulations of water flow in the Roswinkel soil

Layer	Θ_{res} (m^3 m^{-3})	Θ_{sat} (m^3 m^{-3})	α (cm^{-1})	n	λ	K_{sat} (m d^{-1})
Topsoil, 0-0.5 m	0.02	0.38	0.0234	1.801	0	0.234
Subsoil, > 0.5 m	0.01	0.31	0.015	1.951	0.168	0.127

The calibration of the hydraulic relationships for water flow in soil can have an effect on the calculated depth of the groundwater table. The depths of the groundwater table computed in Run W5 (with $a_{fb} = -0.025$ m^3 m^{-2} d^{-1} and $b_{fb} = -2.5$ m^{-1}) were compared with the measurements. The ratio between the calculated and mean measured groundwater depths in the growing season was on average 1.10 (n = 5; s.d. = 0.21). Groundwater discharge was over-estimated, so some further calibration was needed.

The value of a_{fb} represents the rate of groundwater discharge when the groundwater table is at the soil surface. The value of b_{fb} describes the curvature of the q-h relationship with depth in the soil system. In the next Run W6, the value of a_{fb} was increased to -0.02 m^3 m^{-2} d^{-1}, while b_{fb} was maintained at -2.5 m^{-1}. This lowered the groundwater discharge rate over the whole soil profile. In Run W6, the ratio between the calculated and measured groundwater levels was on average 1.02 (n = 5; s.d. = 0.20).

It was checked whether a lower value of $a_{fb} = -0.03$ m^3 m^{-2} d^{-1} in combination with a lower value of $b_{fb} = -3.0$ m^{-1} improved the simulated of the depth water table.
These parameter values correspond to a higher groundwater discharge with the water table at the soil surface, in combination with a stronger curvature to low discharge rates with depth in the soil. In this Run W7, the ratio between the calculated and measured groundwater levels was on average 0.99 (n = 5; sd = 0.19). This is considered to be satisfactory, so the soil moisture profiles computed with Run W7 (Section 9.3) are compared with the profiles measured for the averaged Roswinkel soil.

9.3 Computed soil moisture profiles

The volume fractions of water (VFW's) calculated with Run W7 for the five soil measuring times in the summer of 2000 are given in the Figures 9.1 to 9.4 and in Table 9.1. They are compared with a range of measured values, represented by 1) the average minus the standard deviation and 2) the average plus the standard deviation (called SD range). This range is close to the 67% confidence interval of the measured data. For 8 May, measurements were only available for the furrows (Table 2.5). For the other four dates, the measurements for ridges and furrows were pooled here to calculate averages and standard deviations for the averaged field (Appendix C, Table C.1).

The soil moisture profile calculated for the averaged field on 8 May is given in Figure 9.1 and can be compared with the SD range of profiles measured for the furrows (Table 2.5). Most of the calculated VFW values were near the lower side of the SD range of measured values. This can be related to the fact that the calculations were carried out for the averaged field (ridges + furrows). At this date, the measurements were confined to the soil below the furrows, just made up to their final depth.
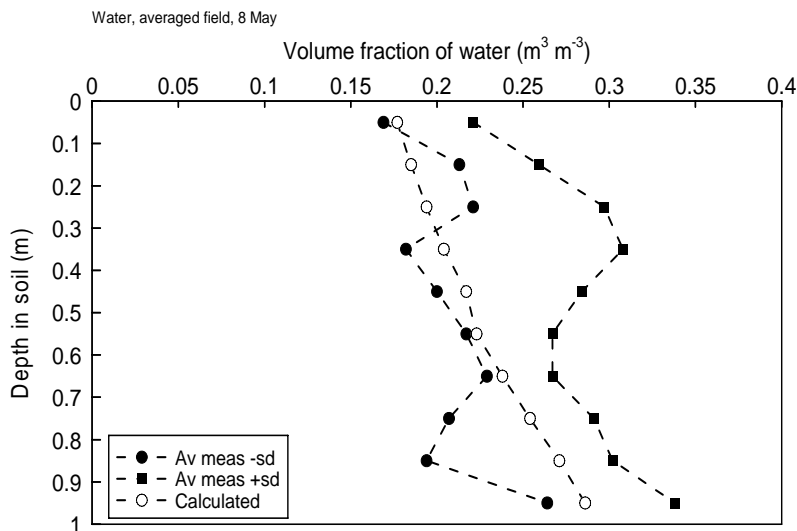
Figure 9.1. Comparison of computed (averaged field) and measured (furrows) volume fractions of water in soil on 8 May 2000.

The comparison of VFW values in soil for 10 May, given in Table 9.1, shows that the computed values (Run W7) are well within the SD range of the measurements (both for the averaged field).

Table 9.1. Comparison of computed (Run W7) and measured volume fractions of water in the top of the averaged Roswinkel soil for 10 May 2000.

Layer (m)	Volume fraction of water (m³ m⁻³)	
	Computed	SD range of measurements
0-0.1	0.16	0.13-0.23
0.1-0.2	0.18	0.16-0.24

For 29 May, the calculated VFW's (Figure 9.2) are partly well within the SD range of measured values. However, some values are close to the upper limit of the range.

Water, averaged field, 29 May
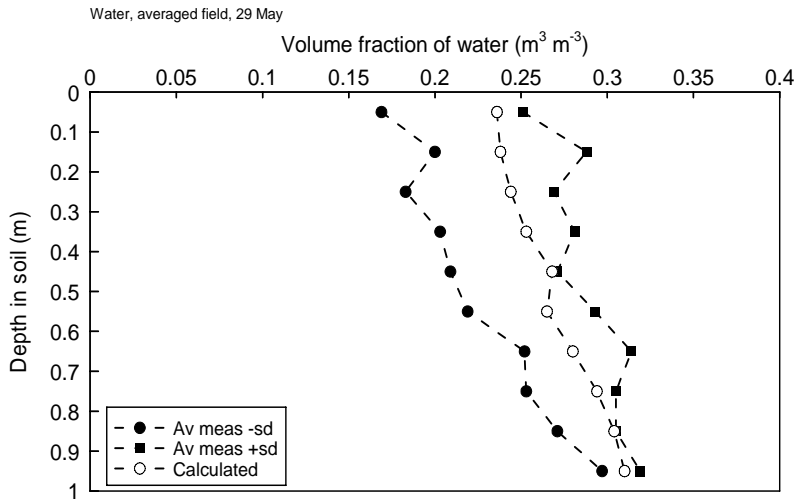
Figure 9.2. Comparison of computed and measured volume fractions of water in the averaged soil on 29 May 2000.

The VFW's calculated for 13 July (Figure 9.3) are close to or even somewhat above the upper limit of the SD range of measurements.

Water, averaged field, 13 July
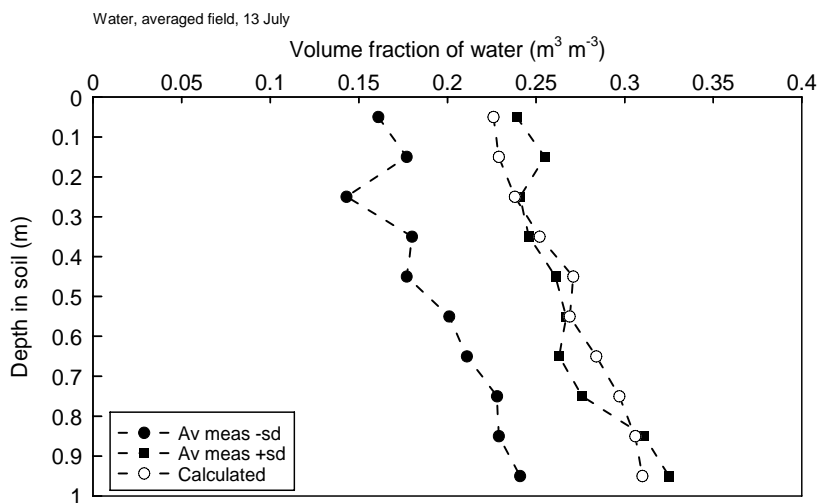
Figure 9.3. Comparison of computed and measured volume fractions of water in the averaged soil on 13 July 2000.

The calculations for 18 September (Figure 9.4) gave VFW values around the lower side of the SD range of the measurements.

Water, averaged field, 18 Sept
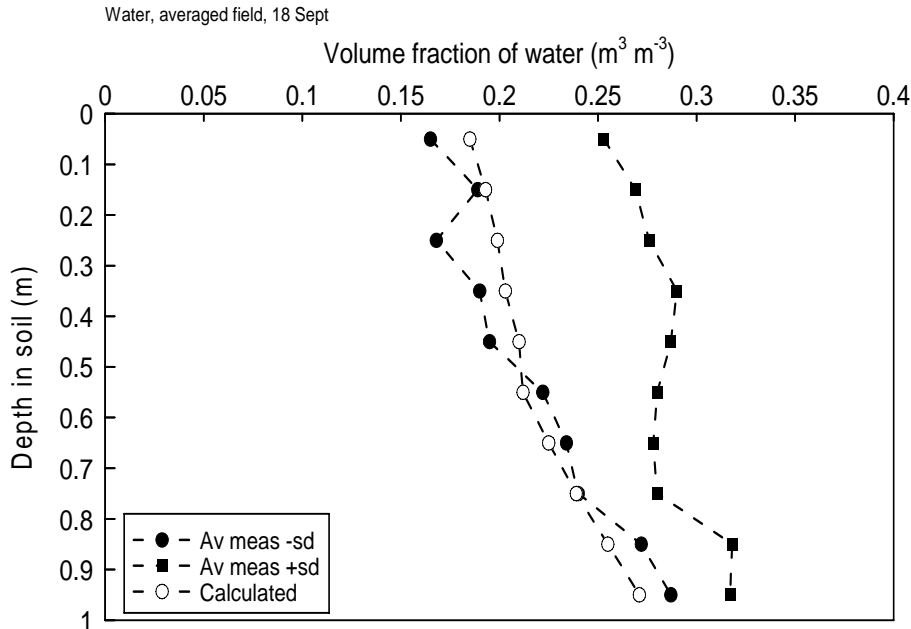
Figure 9.4. Comparison of computed and measured volume fractions of water in the averaged soil on 18 September 2000.

In summary, there were wide ranges of VFW values measured at a certain depth in the Roswinkel soil. This is partly caused by pooling the measurements for the ridges and furrows, thus neglecting the systematic differences. The calculated VFW's were 1) well within the SD range, 2) close to its lower limit or 3) close to its upper limit.

The calculated depths of the groundwater table can be compared with the ranges of measured depths. The comparison for the summer of 2000 is given in Table 9.2. At three times, calculated groundwater is within or close to the SD range of measured levels. At one time calculated depth is distinctly shallower and at one time it is distinctly deeper than the SD range of measurements. The average of the ratio (computed depth)/(measured depth) was 0.99 (n = 5; s.d. = 0.19).

Table 9.2. Comparison of the computed and measured depths of the groundwater table in the summer of 2000. Four hand measurements at each time. SD range = average ± standard deviation.

Date in 2000	Depth of groundwater table (m)		
	Hand-measured		Computed
	Average	SD range	
29 May	0.90	0.80-0.99	0.99
28 June	1.29	1.22-1.36	0.95
19 July	1.10	1.01-1.19	0.98
18 August	1.30	1.21-1.38	1.30
31 August	1.11	1.01-1.21	1.36

In the period 10 May to 16 October 2000, the total amount of rainfall plus sprinkler irrigation was 554 mm. Water evaporation from soil was computed to be 135 mm in this period. Computed transpiration by the crop was 242 mm; it was equal to potential transpiration. Percolation of water through the bottom of the soil system (3 m deep) was computed to be 168 mm in this period.

10 Simulation of bromide-ion in the averaged field

10.1 Bromide-ion in soil

The concentrations of bromide-ion in the averaged Roswinkel soil computed for 29 May are given in Figure 10.1. In this first comparison between computations and measurements, the concentrations measured for the ridges and furrows were pooled. The computed concentrations are compared with the measurements characterised by the SD range: the range of average concentration plus and minus the standard deviation (Appendix C, Table C.2). Negative values of the lower limit of the SD range were set to zero. The SD range of the measurements is very wide; the standard deviations are of the same order of magnitude as the average values. The calculated distribution of bromide-ion in soil is closest to the average plus standard deviation; it is far above the average minus standard deviation.
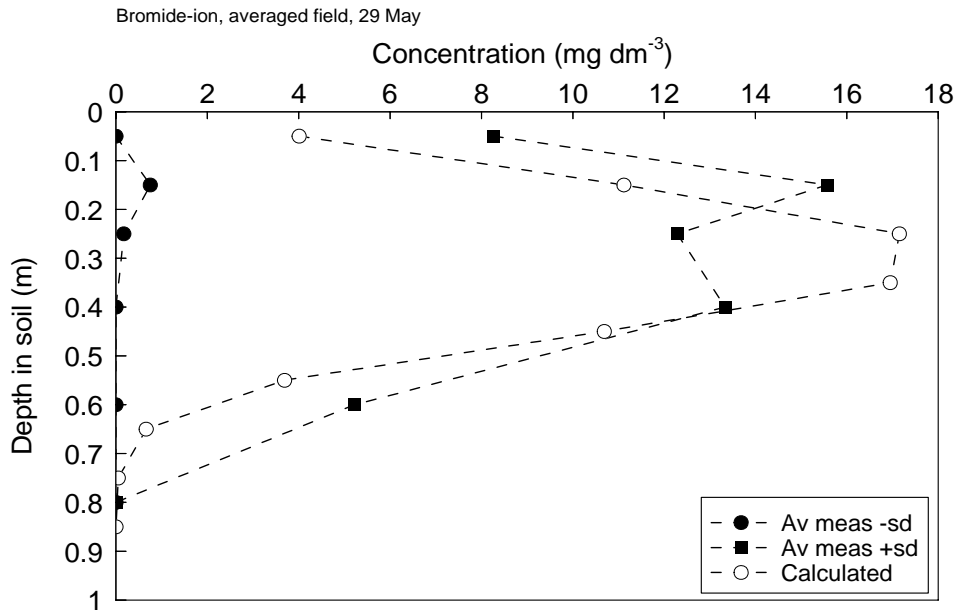
Figure 10.1. Comparison of computed and measured concentrations of bromide-ion in the averaged soil on 29 May. SD range = average ± standard deviation.

The position of the peak of the computed bromide-ion distribution (29 May, Figure 10.1) was in the range of highest measured concentrations in soil. Hardly any bromide-ion was computed to be leached from the top 1 m of the soil at this time. This roughly corresponds to the measured concentrations of bromide-ion in the upper groundwater, which were below or around the quantification limit at that time (Tables 6.1, 6.2 and 6.3). Up to 29 May, computed uptake of bromide by the crop was low, because the plants had just emerged (around 22 May).

The comparison in Figure 10.1 indicates that the measurements for bromide-ion were too low. Almost the complete dosage of bromide-ion is expected to be present in the soil profile at this date. Nevertheless there were many measurements with very low values.

The results of the computations for bromide-ion in the averaged soil on 13 July are presented in Figure 10.2. In the upper 0.7 m of the soil profile, the computed concentrations of bromide are close to the upper side of the SD range. Between 0.7 m and 0.9 m depth, the computed concentrations are roughly midway the SD range, but below that they are closer to the lower side of the SD range. Measured movement of bromide-ion to depths around 1 m was greater than that calculated. In the period from 29 May to 13 July, both the measured and computed distributions of bromide moved to greater depths in soil.

Bromide-ion, averaged field, 13 July
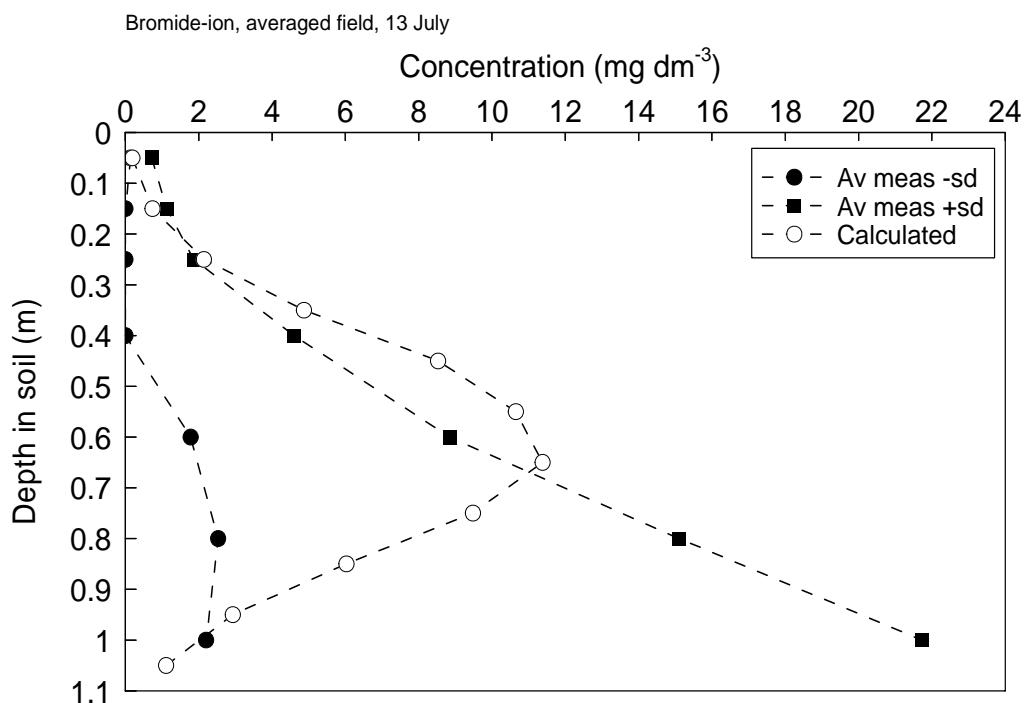
Figure 10.2. Comparison of computed and measured concentrations of bromide-ion in the averaged soil on 13 July.

On average, the concentrations of bromide-ion measured in the groundwater at 1.6 m depth were low on 19 July (Table 6.2). It seems that the peak of the actual distribution in soil was at about 1 m depth in that period. Computed movement of bromide-ion in soil was distinctly less than the average of measured movement (Figure 10.2).

There seems to reasonable agreement between the computed and measured amounts of bromide-ion in the soil profile on 13 July. However, comparison of the concentrations below 1 m depth is not possible.

The concentrations of bromide in the averaged soil computed for 18 September are shown in Figure 10.3. In the upper 0.3 m of the soil profile, the computed concentrations are low in the SD range of the measurements. Possibly, the comparatively high measured concentrations of bromide in this top layer were the result of release of bromide from plant parts dying off. The latter process was not simulated by the model. Below 0.3 m depth, the computed concentrations were mostly near the middle of the SD range. The peak of the computed concentrations was at about 0.8 m depth. The measured bromide peak had moved somewhat deeper into the subsoil.
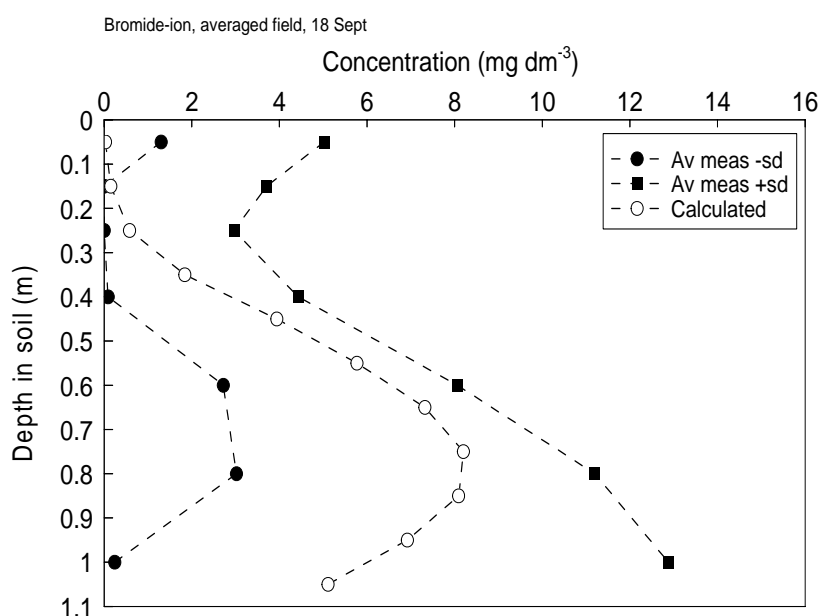
Figure 10.3. Comparison of computed and measured concentrations of bromide-ion in the averaged soil on 18 September.

Low concentrations of bromide-ion were measured in the groundwater at 1.6 m depth on 26 September 2000 (Table 6.2). The computed and measured (average) amounts of bromide-ion in soil seemed to be at the same level (Figure 10.3). However, the concentrations just below 1.1 m cannot be compared (no measurements).

The computed percentages of uptake of bromide-ion by the crop roots are: 0.9% (29 May), 9.6% (13 July), 16.1% (18 September) and 16.5% (end of the crop on 16 October). The amounts of bromide-ion measured in the crop were 16.5% (10 July) and 11.7 % (18 September) of the dosage. At first sight, the computed and measured uptake of bromide-ion by the crop are of the same order of magnitude. However, it should be remembered that the recovery of the measurements was low and uncertain (Chapter 7).

Computed uptake of bromide-ion by the crop does not seem to be so extensive as would be expected. The reason is that much of the bromide was simulated to move below the developing root zone of the crop. This was caused by the high amounts of rainfall + irrigation in the first part of the growing season, with a young crop.

As expected, the calculated volatilisation of bromide-ion and its transformation in soil were nil.

In summary
The SD ranges of the measurements for bromide-ion for the averaged field are very wide. One possible cause is that the measurements for the ridges and furrows were pooled, thus neglecting systematic differences. Hopefully, the more specific comparison between computations and measurements for the ridge and furrow systems separately (Chapter 13) gives narrower SD ranges. The measurements show greater movement to depths around 1 m in soil than that calculated. However, the lower part of the bromide-ion distribution in soil was below measuring depth, which hampers close comparison.

10.2   Bromide-ion in groundwater

The results of the computation of bromide-ion concentration in soil moisture and groundwater at 0.9 m depth in soil are given in Figure 10.4. They represent the breakthrough curve at this depth. The maximum calculated concentration was reached at about 4 months after application of bromide-ion to the soil surface. Within a year after application, the calculated wave of bromide-ion had almost completely passed the 0.9 m depth in soil.
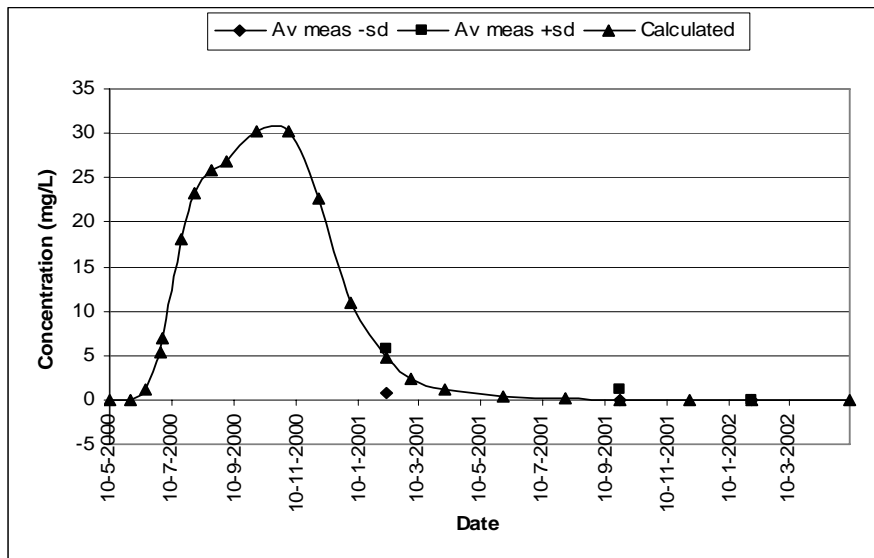
Figure 10.4. Calculated concentrations of bromide-ion in soil moisture and groundwater at 0.9 m depth in soil as a function of time. Measurements in some periods with a shallow groundwater table are represented by their SD range (average ± standard deviation).

Only at times late in the breakthrough period of bromide, groundwater samples could be taken at 0.9 m depth (Table 6.1; Figure 10.4). In the first nine months, groundwater levels were mostly deeper. At the first sampling time of the groundwater (6 February 2001), much of the bromide wave had presumably passed 0.9 m depth in soil. Thus only a small tail of the wave could be measured. The calculated and measured concentrations of bromide in this tail were at the same low level.

The results of the computations and measurements on bromide-ion concentration in groundwater at 1.3 m depth are compared in Figure 10.5. The highest concentrations in groundwater were calculated round the turning of the year (about 8 months after application). In a period of 1.5 year after application, the calculated wave of bromide passed this depth. In the breakthrough period, sampling of groundwater at 1.3 m depth was only possible for some times starting from 6 February 2001 (Table 6.1). Presumably, the greatest part of the wave of bromide had passed this depth by that time. On 4 April 2001, one very high concentration was measured, besides the majority of much lower concentrations. This resulted in a very wide SD range. The negative lower limit of the SD range at this time was drawn at zero. The calculated breakthrough curve seemed to decline somewhat steeper than the part of the curve that could be measured.
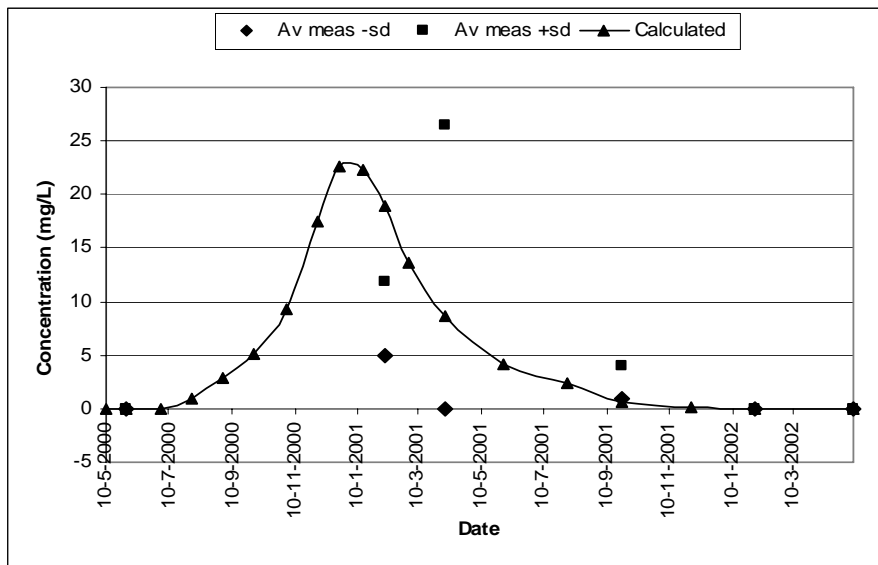
Figure 10.5. Calculated concentrations of bromide-ion in groundwater at 1.3 m depth in soil as a function of time. Measurements in some periods with a shallow groundwater table are represented by their SD range (average ± standard deviation).

The calculated and measured concentrations of bromide-ion in groundwater at 1.6 m depth are given in Figure 10.6. In the first period of about 3 months, incidental concentrations at the mg L^{-1} level were measured, while the vast majority of the concentrations was below the quantification limit (Table 6.2; Figure 10.6). The front of the calculated breakthrough curve lags somewhat behind the measured breakthrough curve. The peak of the calculated concentrations is slightly above the highest value of the SD range of measurements. The tailing of the calculated breakthrough curve declines somewhat steeper than the measured tailing. After a period of 1.7 years, both the calculated and measured breakthrough curves had passed the 1.6 m depth.
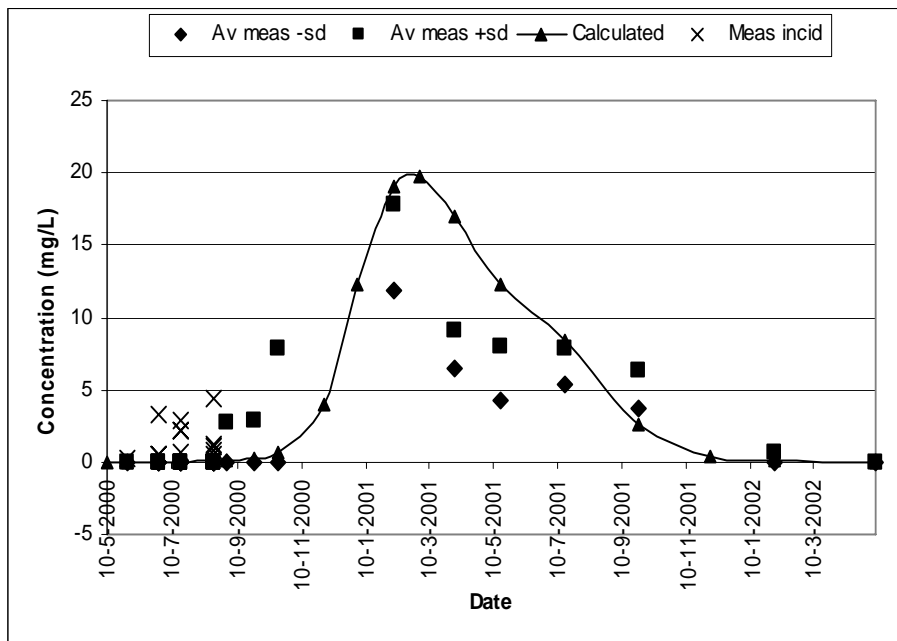
Figure 10.6. Comparison of calculated and measured concentrations of bromide-ion in groundwater at 1.6 m depth. Most measurements are represented by their SD range (average ± standard deviation). Incidental quantifiable concentrations in the first 3 months.

Figure 10.7 shows the calculated and measured concentrations of bromide-ion in groundwater at 2.0 m depth. In the first 5 months after application, there were incidental quantifiable concentrations (up to 2 mg L^{-1}), while the vast majority of the measurements was below the quantification limit (Table 6.3; Figure 10.7). The front of the calculated breakthrough curve tends to be somewhat later than that of the measurements. The calculated maximum concentration is slightly below the top of the SD range of measurements. The tailing of the calculated curve declines somewhat steeper than that of the measurements. In a period of 2 years after application, both the calculated and measured breakthrough curves passed the 2.0 m depth.
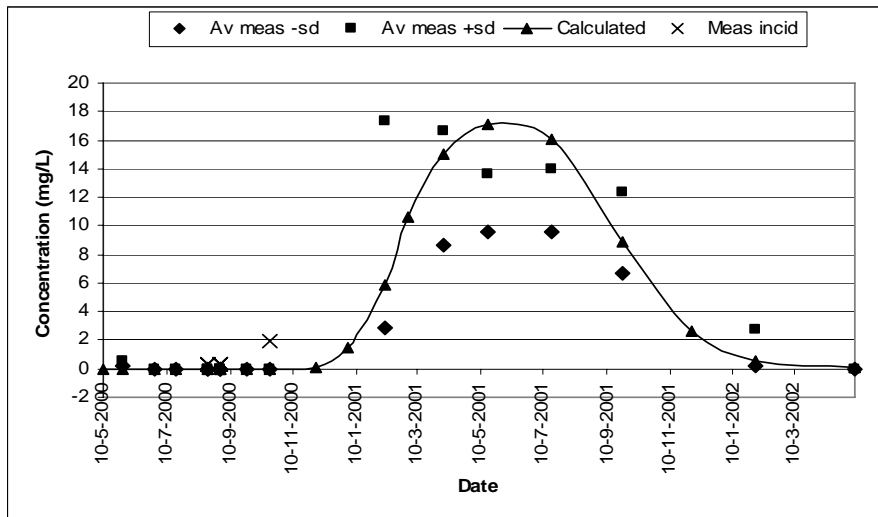
Figure 10.7. Comparison of calculated and measured concentrations of bromide-ion in groundwater at 2.0 m depth. Most measurements are represented by their SD range (average ± standard deviation). Incidental quantifiable concentrations in the first 5 months.

In summary

The measured breakthrough curve of bromide-ion (1.6 and 2.0 m depth) appeared somewhat earlier in the groundwater than the calculated curve. This could be related to comparatively fast movement of bromide-ion below the furrows on the potato field. The flatter tailing of the measured breakthrough curve, as compared to the calculated tailing, could be related to comparatively slow movement below the ridges. The uptake of bromide-ion by the crop and its release from dying plant parts later on can be expected to cause flattening of the measured breakthrough curve.

11 Simulation of carbofuran in the averaged field

11.1 Carbofuran in soil

The concentrations of carbofuran in the averaged Roswinkel soil calculated for 29 May 2000 are given in Figure 11.1. They are compared with the SD range of the measurements, indicated by the lines for 1) average minus standard deviation and 2) average plus standard deviation (Appendix C; Table C.3). In both calculation and measurements, the highest concentrations are still present in the top of the soil profile. The concentration calculated to remain in the top 0.1 m is lower than measured. Further, calculated penetration of carbofuran in the soil profile below 0.3 m is somewhat less than measured.
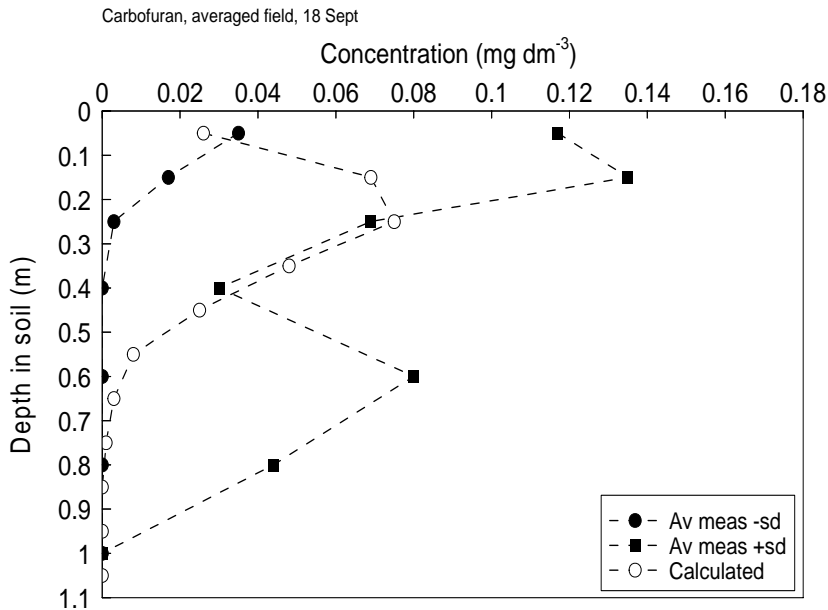
Carbofuran, averaged field, 29 May
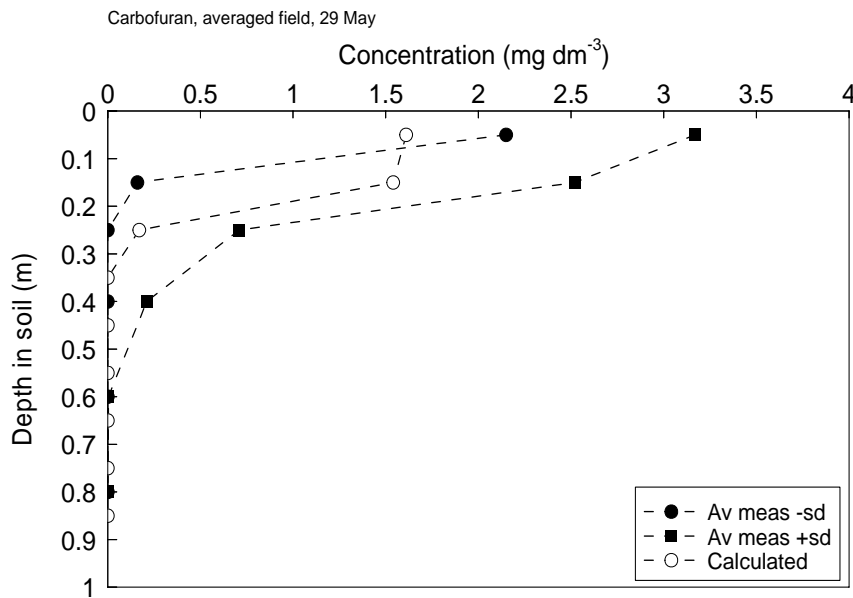
Figure 11.1. Comparison of computed and measured concentrations of carbofuran in the averaged soil on 29 May.

The amount of carbofuran remaining in the soil on 29 May was calculated to be 70.0% of the dosage (measured 97.1% of the dosage; Table 5.6). Transformation in the soil up to this date was calculated to be 29.2% of the dosage. The transformation of carbofuran in soil up to 29 May was slower than would correspond to the first-order kinetics introduced into the computation (Figure 5.2). Uptake by the crop (just emerged) was still very low.

The concentrations of carbofuran calculated for 13 July are shown in Figure 11.2. The value calculated for the top 0.1 m is low in the SD range of measurements. The highest concentrations are calculated for depths around 0.2 m, while the highest measured concentration was still in the top 0.1 m layer. The concentrations calculated for depths below 0.4 m in the soil are low in the SD range of the measurements. So the calculated movement of carbofuran to the subsoil was less than that shown by the average of the measurements.

Carbofuran, averaged field, 13 July
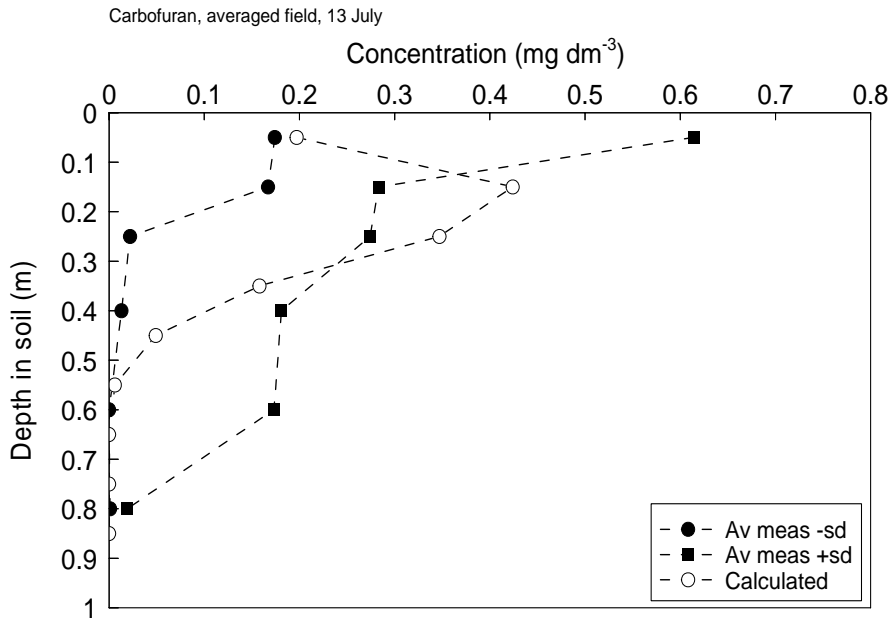
Figure 11.2. Comparison of computed and measured concentrations of carbofuran in the averaged soil on 13 July.

The amount of carbofuran left in the soil on 13 July was calculated to be 25.3% of the dosage (measured 24.7%; Table 5.6). Much of the insecticide had been transformed in the soil (calculated to be 65.7% of the dosage), while 9.1% of the dosage was calculated to be taken up by the crop.

Figure 11.3 presents the results of the carbofuran calculation and measurements for 18 September. Most of the calculated distribution is still present in the upper 0.6 m of the soil profile. The measured distribution has penetrated down to 0.9 m depth. In the top 0.1 m layer, the calculated concentration is near the lower end of the SD range. At 0.35 m depth, the calculated concentration is somewhat above the SD range of the measurements. Calculated movement of carbofuran to the subsoil (low in the SD range) was less than that of the average of the measurements.

Carbofuran, averaged field, 18 Sept

Figure 11.3. Comparison of computed and measured concentrations of carbofuran in the averaged soil on 18 September.

The amount of carbofuran left in the soil on 18 September was calculated to be 5.5% of the dosage (measured 6.6%; Table 5.6). Most of the compound had been transformed in the soil (calculated to be 82.9%), while 11.6% was calculated to be taken up by the crop at this date.

The calculated material balance of carbofuran at the end of the crop growth period (16 October) was: 3.4% left in soil, 11.7% taken up by plant roots and 84.9% transformed in soil. The amount of carbofuran calculated to have volatilised from soil was nil. At this date, calculated leaching of carbofuran to the upper groundwater was still nil.

In summary

The SD range of the measurements for carbofuran in the averaged field are very wide, which hampers close comparison. Hopefully, the SD ranges are smaller when the ridge and furrow systems are distinguished (Chapter 14), thus accounting for systematic differences between the two.

The distributions of carbofuran in soil measured on 13 July and 18 September show a typical pattern:
-    a first fraction of the substance moves slower than computed;
-    a second fraction of the substance moves faster than computed.
Possibly, the first fraction of carbofuran resides in the top of the ridge systems, while the second fraction moves below the furrows. This has to be checked in the more detailed evaluation, in which ridge and furrow systems are distinguished (Chapter 14).

11.2 Carbofuran in groundwater

The concentrations of carbofuran calculated for soil moisture and groundwater at 0.9 m depth are given in Figure 11.4. Carbofuran breakthrough at this depth was computed to start in September 2000 and its maximum concentration was reached in February 2001. At the end of 2001, the calculated wave of carbofuran had passed this depth. Only in a few periods, with a shallow groundwater table, samples could be taken from the groundwater (Table 6.4; Figure 11.4). The concentrations measured for the samples taken on 6 February 2001 are much lower than that calculated.
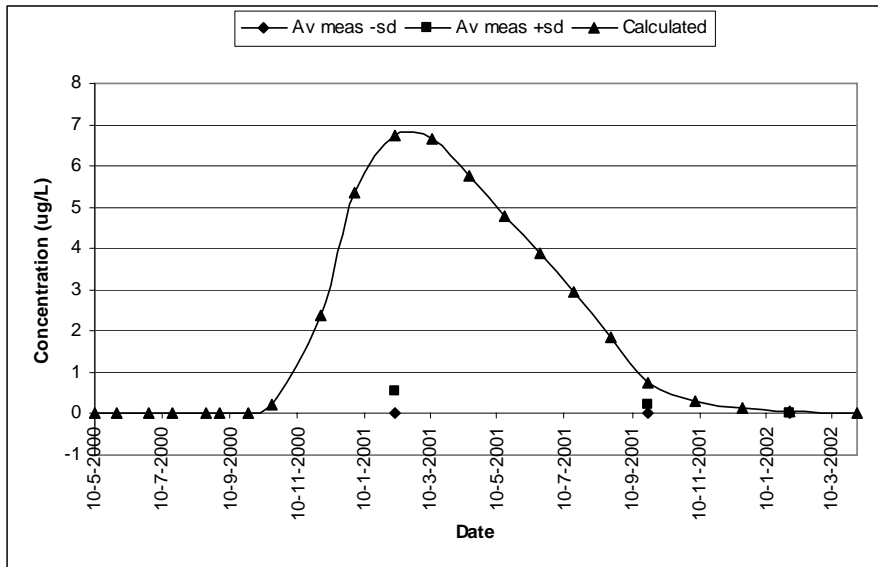
Figure 11.4. Calculated concentrations of carbofuran in soil moisture and groundwater at 0.9 m depth. Comparison with a few measurements (represented by their SD range) which were only possible in periods with a shallow water table.

There are two possible causes for the very low concentrations of carbofuran measured in February 2001:
-   accelerated transformation in the soil profile had started as a result of microbial adaptation (possibility described in Section 3.2);
-   transformation in the water samples during storage before chemical analysis (possibility described in Section 6.2).

The concentrations of carbofuran calculated for the groundwater at 1.3 m depth are given in Figure 11.5. Calculated breakthrough at this depth started in December 2000 and the maximum concentration was reached in May 2001. The calculated wave of carbofuran had passed the depth of 1.3 m in April 2002. The concentrations measured at two times in the main calculated breakthrough period (Table 6.1; Figure 11.5) were much lower than calculated. This may have been caused by accelerated transformation of carbofuran in the soil profile or by transformation during storage of the water samples.
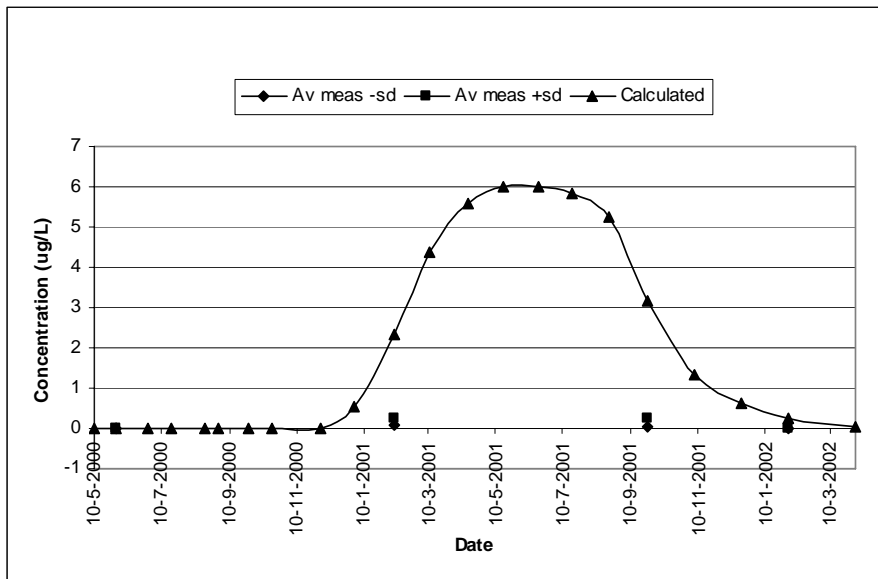
Figure 11.5. Calculated concentrations of carbofuran in groundwater at 1.3 m depth. Comparison with a few measurements (represented by their SD range) which were only possible in periods with a shallow water table.

Figure 11.6 shows the calculated concentration of carbofuran in groundwater at 1.6 m depth as a function of time. Breakthrough at this depth was computed to start in January 2001 and the maximum concentration was reached in August 2001. At the sampling times in the first half of the study period there was a very wide SD range of measurements (Table 6.2; Figure 11.6). This was caused by incidental very high measured values, with the bulk of the measurements at a much lower level. The lower limits of these wide SD ranges were negative; they were drawn at zero in the figure. In the calculated breakthrough period, the measured concentrations were much lower than calculated. This may have been caused by accelerated transformation of carbofuran in the soil profile and/or instability in the experimental procedure.
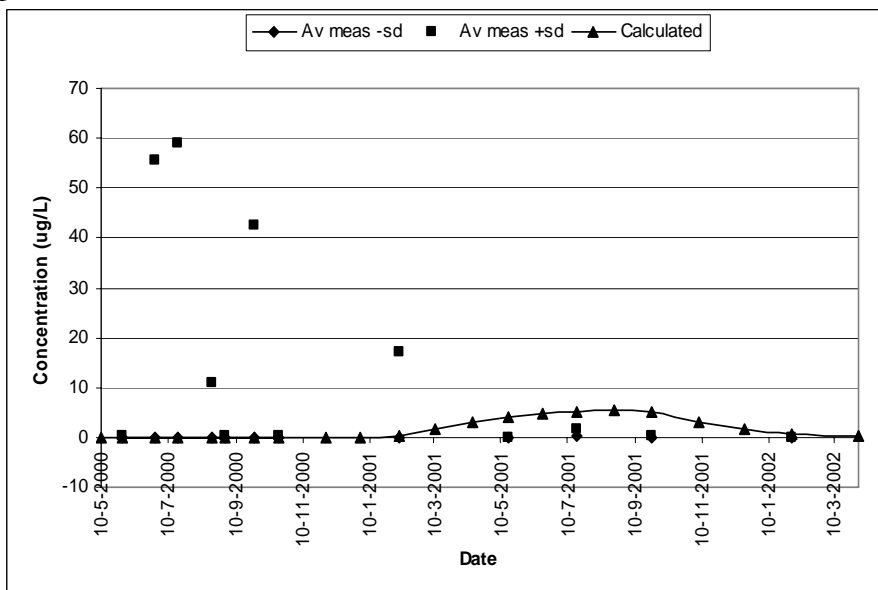
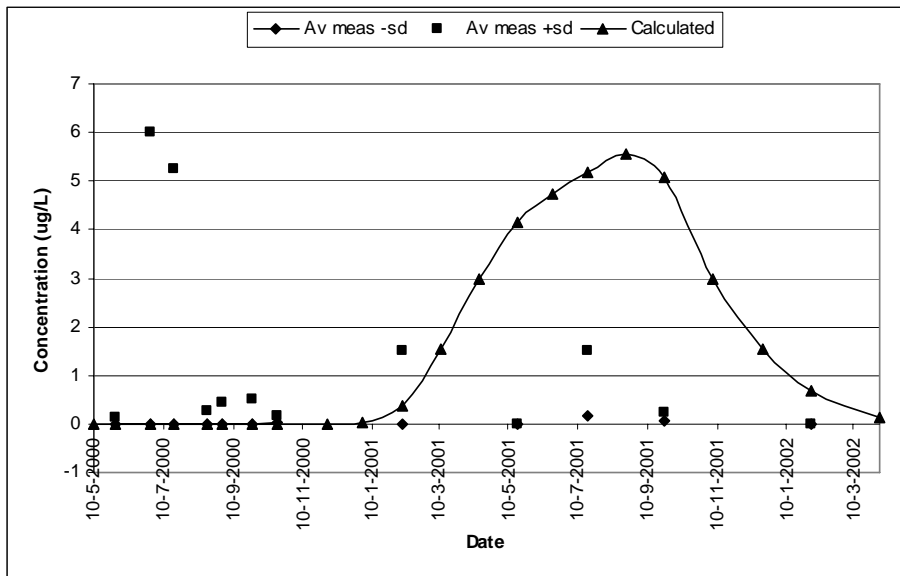*Figure 11.6. Calculated concentrations of carbofuran in groundwater at 1.6 m depth. Comparison with the SD range of measured values, including incidental very high values.*

The concentrations of carbofuran calculated for groundwater at 2.0 m depth are shown in Figure 11.7. Calculated breakthrough started in March 2001 and the maximum concentration was reached in October 2001. The tail of the breakthrough curve still passed this depth in March 2002. At some times, the SD range of measurements was very wide (Table 6.3; Figure 11.7). This was caused by incidental very high values, while the bulk of the measured values was much lower. The lower limits of the wide SD ranges were negative; they were drawn at zero level in the figure. The concentrations measured later in the expected breakthrough period were much less than calculated, which may have been caused by extensive transformation of carbofuran in the soil profile and/or in the experimental procedure.
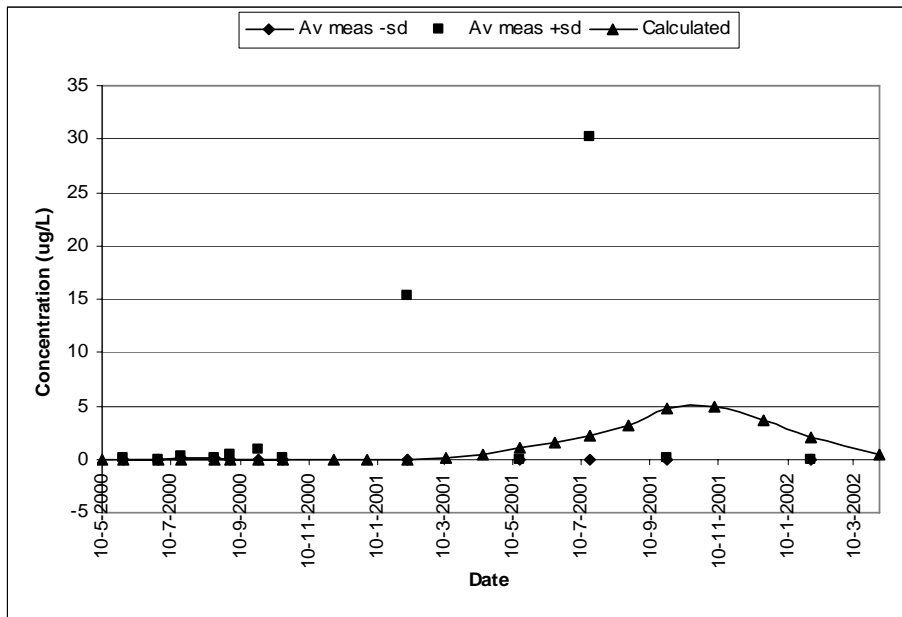
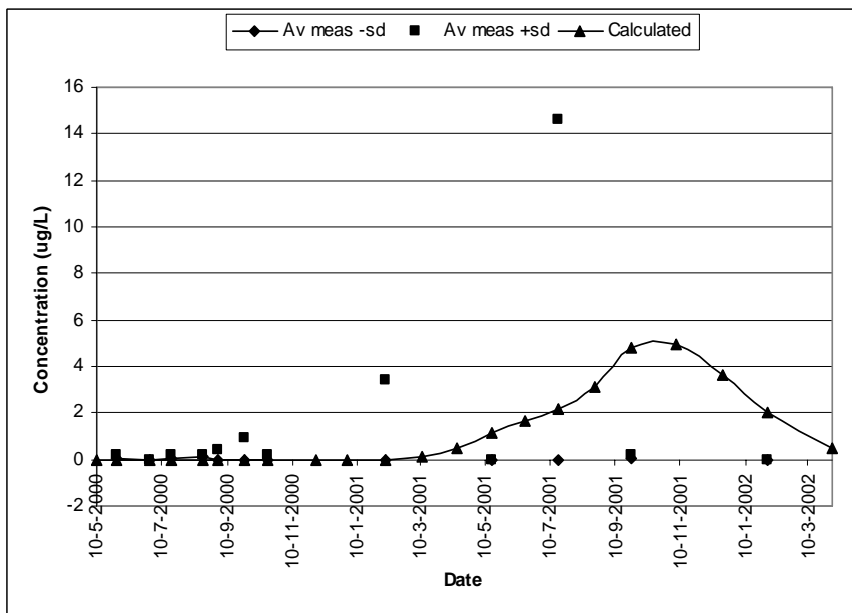*Figure 11.7. Calculated concentrations of carbofuran in groundwater at 2.0 m depth. Comparison with the SD range of measured values, including incidental very high values.*

Possibly, the bulk of the measured concentrations in a series is most representative for chromatographic transport in soil as simulated by the model. Therefore, it is interesting to compare calculations and measurements in a second way, leaving out one or two very high values in a measuring series (if they occur).

The result of the second comparison of calculated and measured concentrations of carbofuran in the groundwater at 1.6 m depth is given in Figure 11.8. As expected, the SD range of measurements is reduced drastically (factor of 10) by excluding the incidental very high values (compare to Figure 11.6). The measurements indicate that some leaching of carbofuran occurred already in the first few months after application. This is much earlier than the start of the calculated wave of leaching. Apparently some early leaching occurred which was not simulated by the model for the averaged field situation. Early leaching from the furrow systems is a possibility to be studied in Chapter 14 etc.

Figure 11.8. Calculated concentrations of carbofuran in groundwater at 1.6 m depth. Comparison with the SD range of measured values, **excluding** *incidental very high values.*

Figure 11.9 shows the second comparison of calculated and measured carbofuran concentrations in groundwater at 2.0 m depth. Again, the SD ranges of the measurements were reduced by the exclusion of the incidental high values (but only a factor of 2 for the widest range). The measurements indicate that the breakthrough of carbofuran at this depth was earlier than simulated by the model, assuming an averaged field situation.

Figure 11.9. Calculated concentrations of carbofuran in groundwater at 2.0 m depth. Comparison with the SD range of measured values, **excluding** *incidental very high values.*

The incidental high concentrations of carbofuran in the initial period are rather high as compared to the top of the calculated breakthrough curve. For bromide-ion, the incidental high concentrations were distinctly lower than the top of its breakthrough curve (Section 10.2). The incidental leaching of carbofuran occurs in a period in which there is still a substantial amount present in the soil profile. In the further time of movement of the main wave, transformation of carbofuran in the soil profile continues, which lowers the concentrations in this wave. No such transformation of bromide-ion in its wave occurs. So the comparatively high incidental concentrations of carbofuran, as compared the top of its breakthrough curve, can be explained from the continued transformation of its main wave in soil.

In summary

The measurements of carbofuran in groundwater present a complicated picture, which seems to reflect complications in its behaviour in soil. These may deal with both, transport and transformation of carbofuran in soil profile and groundwater zone.

The are indications of early leaching (as compared to the computation), possibly from the furrows. Presumably, microbial adaptation resulted in accelerated transformation in soil, but the starting time is unknown. In addition, there may have been complications in the experimental procedure, e.g. with respect to tube installation, sampling and analysis. Summarising, the measurements of carbofuran in groundwater seem to be of limited value for the testing of the simulations by the model.

12 Simulation of water flow in ridge and furrow soil

12.1 Set up of the computations

The next step in the simulation of the Roswinkel potato field is to distinguish ridge and furrow systems (instead of averaging the situation for the whole field). Separate measurements on various quantities of the ridges and furrows are available for the field experiment (Chapters 2 and 5). So comparisons can be made between calculations and measurements for the two systems separately.

In the simulation of the furrow system, the top 0.1 m of the field soil was removed. This layer was added to the top of the ridge system. This simulated the buildup of the ridges with furrow material. Thus the humic sandy top layer of the ridge system was 0.2 m thicker than that of the furrow system. A rather thin humic sandy top layer remained on the low-humic sandy subsoil in the latter system. An outline of the simulated ridge and furrow systems is given in Figure 12.1. The ridge and furrow systems each take up half of the surface area of the field. The detailed input data for each of the soil layers in the ridge and furrow systems, as derived from Table 8.1, are given in Appendix E.
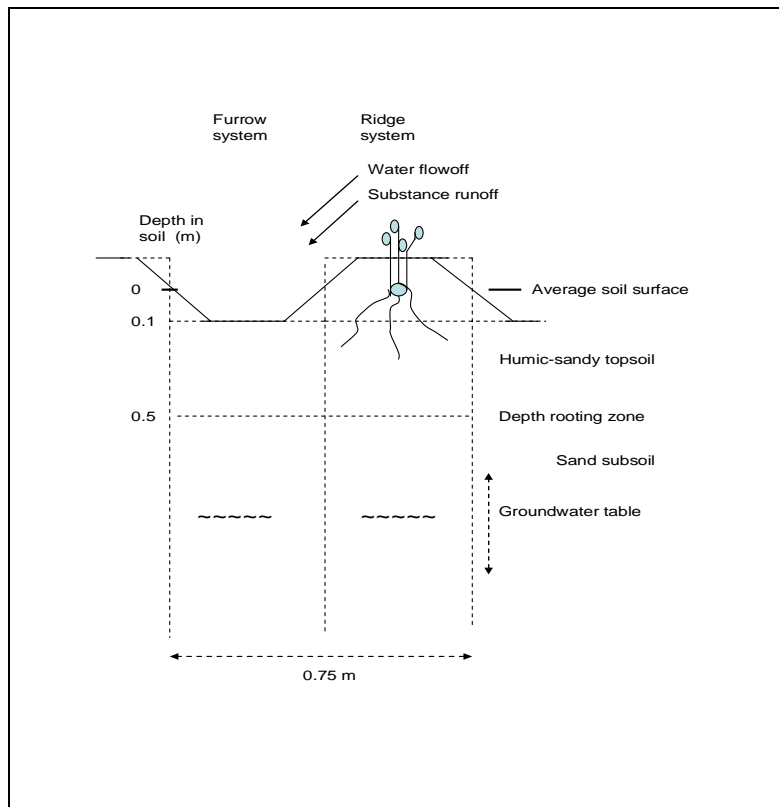
Figure 12.1. Schematisation of the ridge and furrow systems.

In a field with ridges and furrows, part of the water from rainfall and sprinkler irrigation can flow down the surface of the ridges to the furrows. Measurements on the extent of this process on the Roswinkel field are not available. As a first approximation, it is assumed that 20% of the rainfall+irrigation falling on the ridges flows via the soil surface to the furrows. In the calculations this is realised by multiplying the measured rainfall+irrigation by 0.8 for the ridge system and by 1.2 for the furrow system, until harvest. Comparison between computed and measured movement of the substances in the ridge and furrow systems may indicate whether this extent of surface flow-off is plausible.

A fraction of the dosage of the substances can be expected to move with the surface flow of water from the ridges to the furrows. The extent of this movement was estimated from the measurements. On 29 May, the amount of bromide-ion in the ridge soil was measured to be 15% lower than the average for the field (so the amount in the furrow soil was 15% higher) (Table 5.3). At the next sampling time (13 July) some bromide-ion had leached from the soil profile (Table 5.2), so these measurements cannot be used for the present purpose. The amount of carbofuran in the ridge soil on 29 May was 29% lower than the average for the field (so the amount in the furrow soil was 29% higher) (Table 5.6). On 13 July (with hardly any leaching of carbofuran from the soil profile) (Table 5.5), the amount of carbofuran in the ridge soil was 4% lower than that for the averaged field (furrow soil 4% higher). Taking a kind of average value, it is assumed that 15% of the dosage of the substances on the ridges moved with the surface flow of water to the furrows. Supposing that this movement occurred soon after application, the field-averaged dosage was decreased by 15% for the ridge system and it was increased by 15% for the furrow system in the computations.

The plants on the ridge system emerged on 22 May (as before) and soil cover on the ridges was taken to increase linearly until full cover on 20 June (Crum et al., 2004). As a result of the build-up of the ridges (with 0.1 m soil), the depth of the humic-sandy rooting zone was increased from 0.5 m to 0.6 m (Figure 12.1). Rooting depth was taken to increase linearly from 0.2 m on 22 May to the final depth of 0.6 m on 10 July.

As the crop does not grow directly in the furrows, description of crop growth on the furrow system is a bit complicated. It takes some time for the plant roots in the ridges to grow to the soil below the furrows (Figure 12.1). Root development and water uptake in the furrow system was assumed to start on 10 June, at zero depth. From this date on, a potato crop is assigned to the furrow system, with a soil cover increasing linearly from zero (10 June) to full cover (10 July). As 0.1 m of the topsoil had been removed for building up the ridges, only 0.4 m of humic sandy rooting zone remained in the furrow system (Figure 12.1). In this system, the maximum rooting depth of 0.4 m was reached on 10 July.

The other crop data for the ridge and furrow systems were the same as used earlier for the averaged field system (Section 8.3).

The simulation of water flow in the ridge and furrow systems started with the hydraulic relationships obtained in the calibration for the averaged field situation (Section 9.2). The starting parameter values are given in Table 12.1. The parameter values for the top layer were assigned to the top 0.6 m of the ridge system (hilled up) and to the top 0.4 m of the furrow system (soil removed for hilling up) (Figure 12.1). Some specific calibration of the simulation of water flow in the ridge and furrow systems later in the study is an option.

Table 12.1. Values of the parameters in the Van Genuchten-Mualem hydraulic relationships used in the initial simulation of water flow in the ridge and furrow systems.

Layer	Depth (m) in system:		Θres ($m^3 m^{-3}$)	Θsat ($m^3 m^{-3}$)	α (cm^{-1})	n	λ	Ksat ($m\ d^{-1}$)
	ridge	furrow						
Topsoil	0 - 0.6	0 - 0.4	0.02	0.38	0.0234	1.801	0	0.234
Subsoil	> 0.6	> 0.4	0.01	0.31	0.015	1.951	0.168	0.127

In the simulation for the whole (averaged) field, groundwater discharge was described by the "exponential flux function" boundary condition (Section 9.2). The calculated depth of the groundwater table could be compared with the measured depth. In this way the two discharge parameters were obtained by calibration. In the simulated ridge system, water infiltration is lower and water uptake by the crop is higher as compared to the furrow system. It can be expected that the groundwater table for the ridge system is calculated to be deeper than that in the furrow system. This expectation is checked in the first computations for these systems, presented in Appendix F.

The computations reported in Appendix F show that the ratio between computed and measured depth of the groundwater table in the ridge system was on average 1.14 (s.d. = 0.19). Especially at the end of the growing season (August and September), the depth of the groundwater table was computed to be much deeper than measured. The deeper calculated groundwater table is mainly caused by the lower water infiltration into the ridges, caused by flow-off to the furrows.

The depth of the groundwater table computed for the furrows (Appendix F) was on average 0.87 times (s.d. = 0.18) that measured in the field. In practice, water will flow from the furrows to the ridges, especially in and near the water-saturated zone. Therefore, another lower boundary condition for water flow is needed when simulating separate ridge and furrows systems. This should replace the "flux function" boundary condition derived for the whole (averaged) field.

The SWAP-PEARL combination offers the option to introduce measured groundwater levels, as the lower boundary condition for water flow in the soil profile (van Dam et al., 1997). At seven times in and around the growing season of the crop at the Roswinkel field, groundwater level was measured by hand in four tubes (Table 2.6). The average of the four measured values per time was introduced as lower boundary condition for the water flow in the ridge system. The depths of the groundwater table were measured relative to the average soil surface. So the measured depths were increased by 0.1 m to relate them to the top of the ridges

(which were hilled-up 0.1 m). In analogy, the groundwater depths in the furrow system were decreased by 0.1 m, as compared to the measured values. SWAP interpolates the groundwater levels linearly between the seven times.

12.2   Water flow using measured groundwater levels

On 8 May 2000 (2 days before the application of the substances) only the soil below the furrows was sampled for measuring soil moisture content. The results of the computation of the volume fractions of water (VFW's) in the furrow system on 8 May are presented in figure 12.2. In the top 0.5 m of the soil, the computed VFW's are high in the SD range of the measurements. Below that, three values were distinctly above the SD range. It should be noted that the final furrows were formed just before soil sampling, so water flow from the ridges to the furrows is not considered up to this date. The lower limit of the SD range in the subsoil is remarkably low. It seems that some water has been lost from the soil samples taken near the water table. Further, the groundwater table may have been deeper than introduced into the computation (interpolation between 1 January and 29 May).
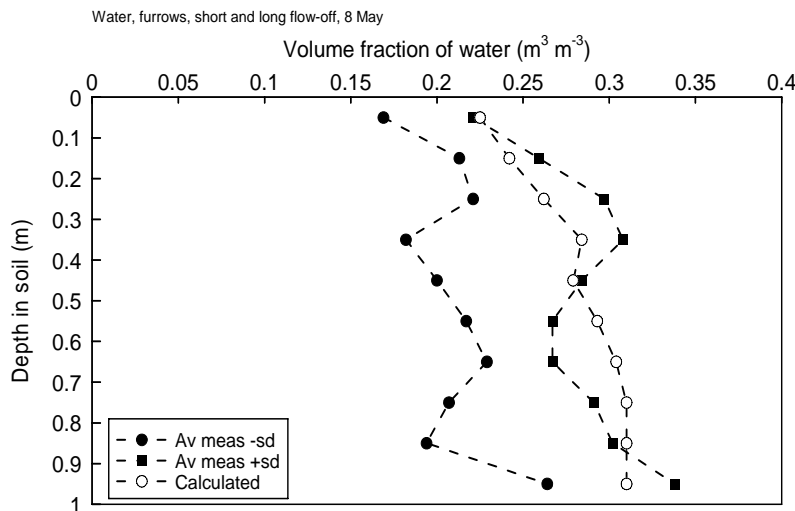
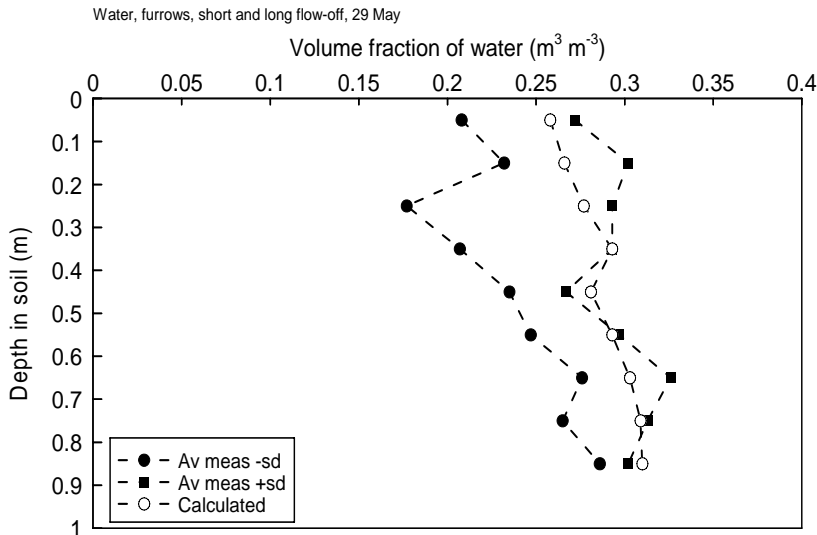*Figure 12.2. Comparison of computed and measured volume fractions of water in the soil of the furrow system on 8 May. The measurements are represented by their SD range.*

In Table 12.2 the VFW values computed for the top of the ridge and furrow systems on 10 May are compared with the measurements on that date (confined to two layers). The computed VFW values are well within the SD range of the measurements.

Table 12.2. Comparison of computed and measured volume fractions of water in the top of the ridge and furrow systems on 10 May. Input of measured groundwater levels.

| Layer (m) | Volume fraction of water ($m^3 m^{-3}$) in: | | | |
| | Ridges | | Furrows | |
	Computed	SD range of measurements	Computed	SD range of measurements
0-0.1	0.19	0.11-0.21	0.22	0.15-0.24
0.1-0.2	0.20	0.15-0.22	0.24	0.18-0.26

The VFW values computed for the ridge system on 29 May are presented in Figure 12.3. Various computed VFW's are close to the upper limit of the SD range of the measurements, while others are well within the SD range.
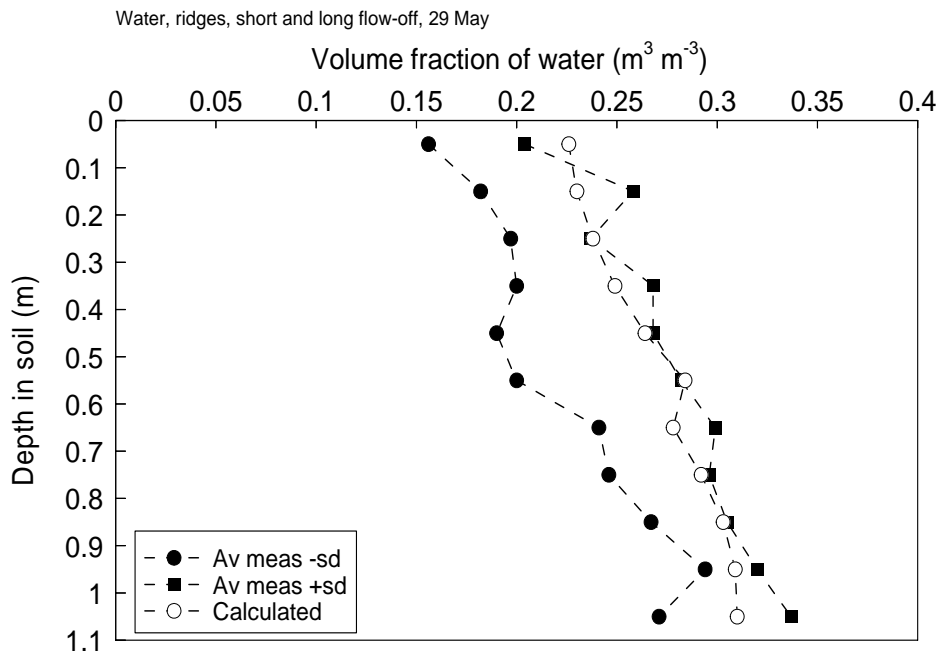
Figure 12.3. Comparison of computed and measured volume fractions of water in the soil of the ridge system on 29 May 2000.

Figure 12.4 shows the results of the computation of VFW's for the furrow system on 29 May. Most computed values were within the SD range of measurements or high in this range, while two values were slightly above the upper limit of this range. The VFW values computed for the furrow system are higher than those computed for the ridge system (Figure 12.3). This corresponds to the type of difference in the measurements.
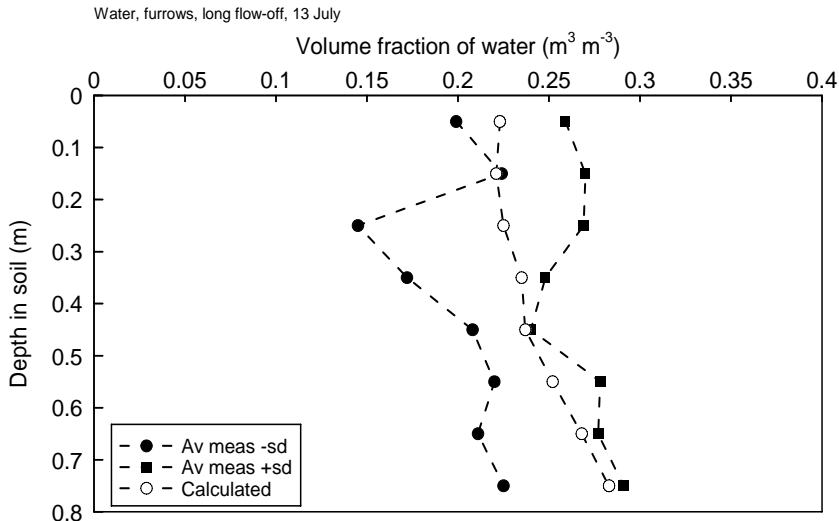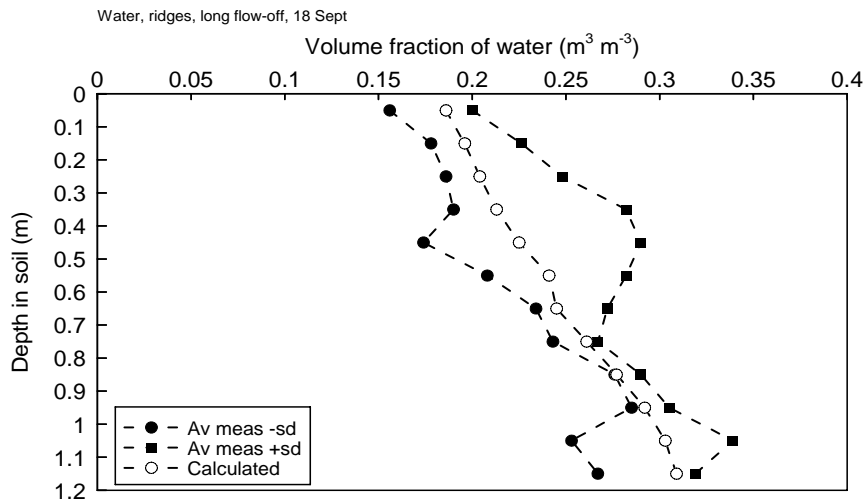
Water, furrows, short and long flow-off, 29 May

Figure 12.4. Comparison of computed and measured volume fractions of water in the soil of the furrow system on 29 May.

Figure 12.5 shows the VFW values in the ridge system computed for 13 July. Most of the computed values are well within the SD range of measurements. Some VFW's in the top layer are close to the upper limit of the SD range.

Water, ridges, long flow-off, 13 July
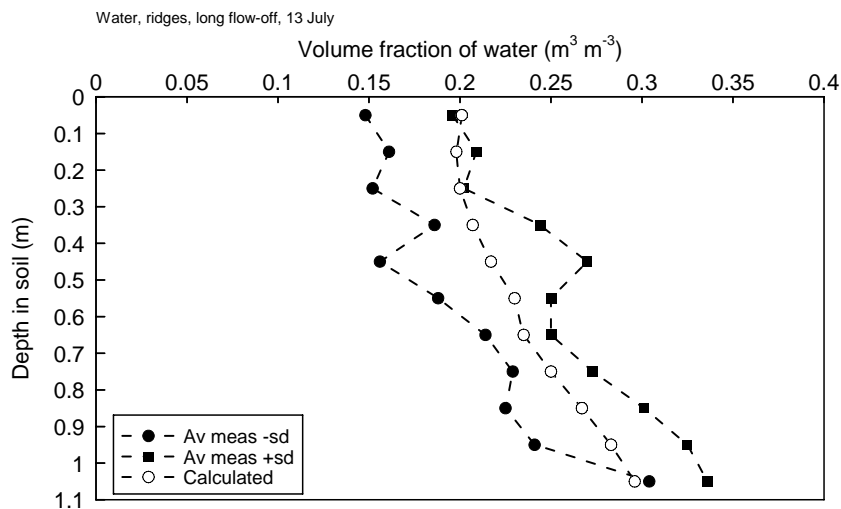
Figure 12.5. Comparison of computed and measured volume fractions of water in the soil of the ridge system on 13 July.

The VFW values computed for the furrow system on 13 July are given in Figure 12.6. They are within the SD range of measurements or near the limits of this range. For this date too, the VFW values computed for the furrow system are higher than those computed for the ridge system (Figure 12.5). This corresponds to the nature of the difference in VFW's measured for the two systems.

Water, furrows, long flow-off, 13 July

Figure 12.6. Comparison of computed and measured volume fractions of water in the soil of the furrow system on 13 July.

The results of the VFW computations for the ridge system on 18 September are compared with the measurements on that date in Figure 12.7. Most computed VFW values are well within the SD range of the measurements.

Water, ridges, long flow-off, 18 Sept

Figure 12.7. Comparison of computed and measured volume fractions of water in the soil of the ridge system on 18 September.

Figure 12.8 shows the results of the computation of VFW's for the furrow system on 18 September. Most computed values are well within the SD range of measurements, while some others are close to the lower or upper limits of this range. The VFW values computed for the furrow system are mostly higher than those computed for the ridge system (Figure 12.7). The measurements for the two systems show the same type of difference.
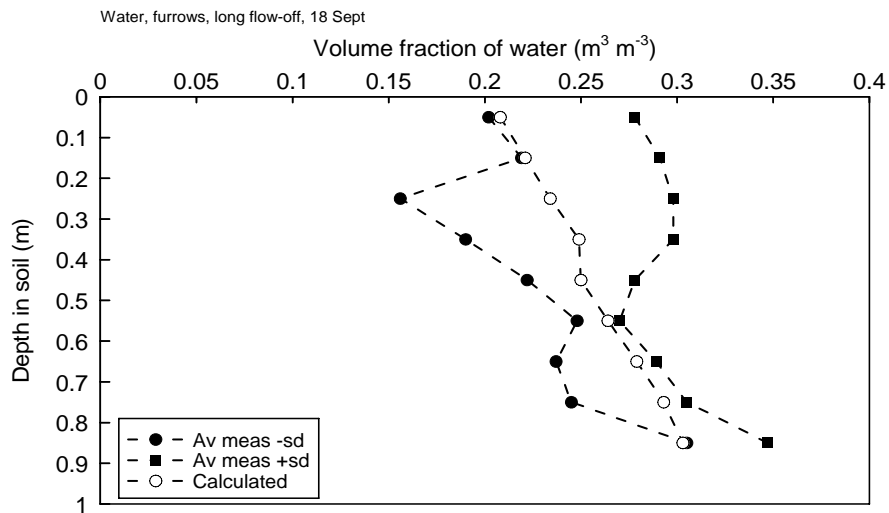
Figure 12.8. Comparison of computed and measured volume fractions of water in the soil of the furrow system on 18 September.

Computed cumulative water transpiration by the crop equalled computed potential transpiration, so no water shortage was simulated for the crop.

In summary
The introduction of measured groundwater levels in the computations results in a substantial improvement of the simulation of water flow in the ridge system (compare to Appendix F). This improvement is most striking in the final part of the growing season. The VFW profiles computed for the furrow system on the sampling dates also correspond reasonably well to the measured profiles. The VFW values computed for the furrow system are mostly higher than those computed for the ridge system, which corresponds to the nature of the difference in the measurements for the two systems. It seems that there is no need for further calibration of the hydraulic relationships (Table 12.1) used for both, the ridge and furrow systems.

13   Simulation of bromide-ion in ridge and furrow soil

It was estimated (Section 12.1) that 15% of the dosage of bromide-ion moved with the water flow over the soil surface from the ridge system to the furrow system shortly after application. In this way, the dosage of bromide-ion for the ridge system became 55.0 kg ha^{-1} and that for the furrow system became 74.4 kg ha^{-1}.

The computed distribution of bromide-ion in the ridge system on 29 May is compared with the measurements for this system in Figure 13.1. In the upper 0.4 m of the soil, the computed movement is somewhat greater than measured. However, computed penetration of bromide-ion below 0.5 m in soil is lower than measured. The average amount of bromide-ion measured in the soil profile is much less than expected on the basis of the computation (no leaching to groundwater yet).
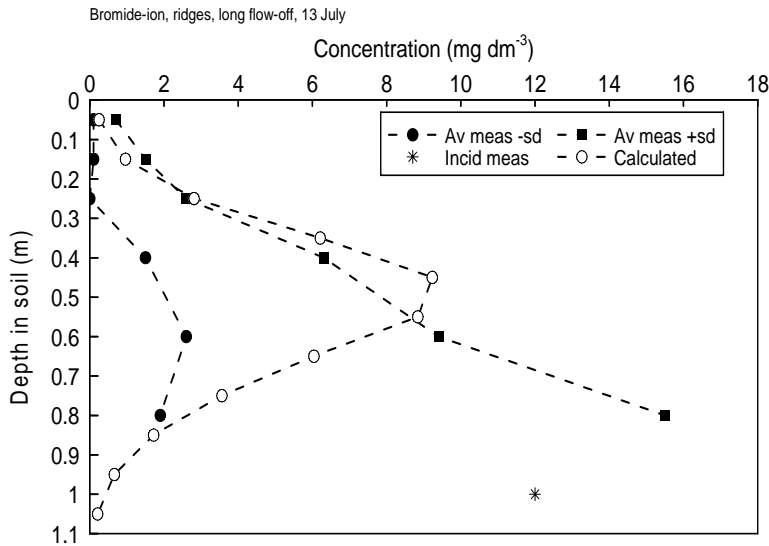
Bromide-ion, ridges long+short flowoff, 29 May
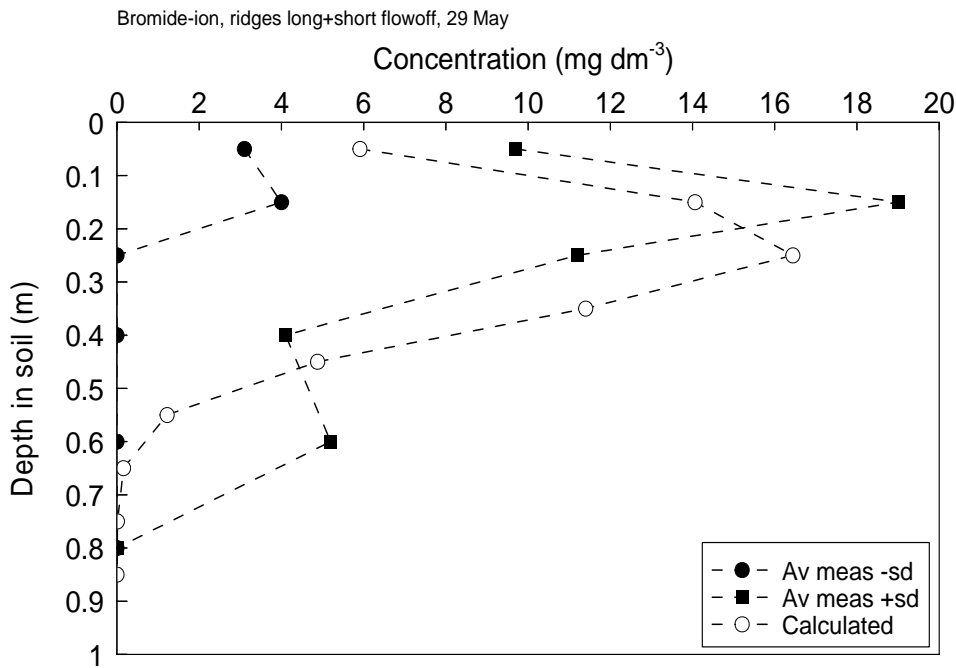
Figure 13.1. Comparison of computed and measured concentrations of bromide-ion in the soil of the ridge system on 29 May. The measurements are represented by their SD range.

Figure 13.2 shows the computed distribution of bromide-ion in the soil of the furrow system on 29 May. The computed concentrations are close to the upper limit of the SD range of the measurements. Computed movement of bromide-ion was almost the same as the measured movement, However, the average amount of bromide-ion measured in soil is much lower than expected on the basis of the computation (no leaching to groundwater yet).
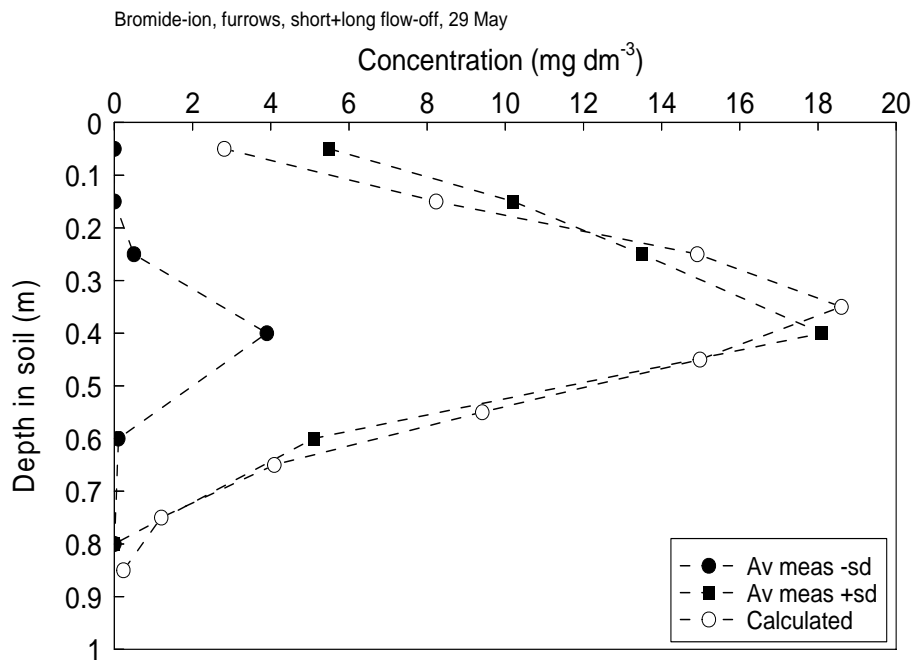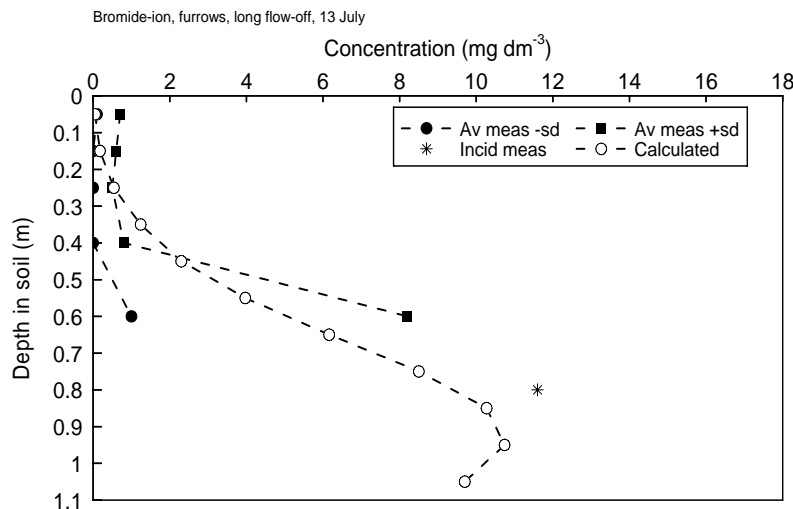

Figure 13.2. Comparison of computed and measured concentrations of bromide-ion in the soil of the furrow system on 29 May.

Computed movement of bromide-ion in the furrow system (peak at 0.35 depth; Figure 13.2) is greater than that in the ridge system (peak at 0.25 m; Figure 13.1). This is mainly caused by the higher amount of water infiltrating in the furrow system.

The concentration profile of bromide-ion computed for the ridge system on 13 July is represented in Figure 13.3. Computed movement in soil (peak at 0.5 m depth) is less than measured movement (peak possibly at 0.8 m). Computed leaching below 1 m depth in soil is small, but according to the measurements leaching had occurred. In relation to this, less bromide-ion was measured in the upper part of the profile than computed.

Figure 13.3. Comparison of computed and measured concentrations of bromide-ion in the soil of the ridge system on 13 July. Asterisks: incidental measurements.

Figure 13.4 shows the computed concentration profile of bromide-ion in the furrow system on 13 July. Here, the computed peak had reached about 0.9 m depth. Only a tail of the bromide distribution in soil was measured. Because of this, computed and measured movement cannot be compared very well. Bromide-ion in the furrow system was computed to move deeper (peak at 0.9 m; Figure 13.4) than in the ridge system (peak at 0.5 m; Figure 13.3).

Figure 13.4. Comparison of computed and measured concentrations of bromide-ion in the soil of the furrow system on 13 July. Asterisks: incidental measurements.

The concentrations of bromide-ion computed for the ridge system on 18 September are given in Figure 13.5. The peak of the distribution was computed to be at 0.45 m depth, while hardly any leaching below 1 m had occurred. According to the measurements, bromide-ion had moved deeper into the soil profile, with distinct leaching to below 1 m. In both the computations and measurements, much of the dosage of bromide-ion was still present in the upper 1 m of the soil at this time.
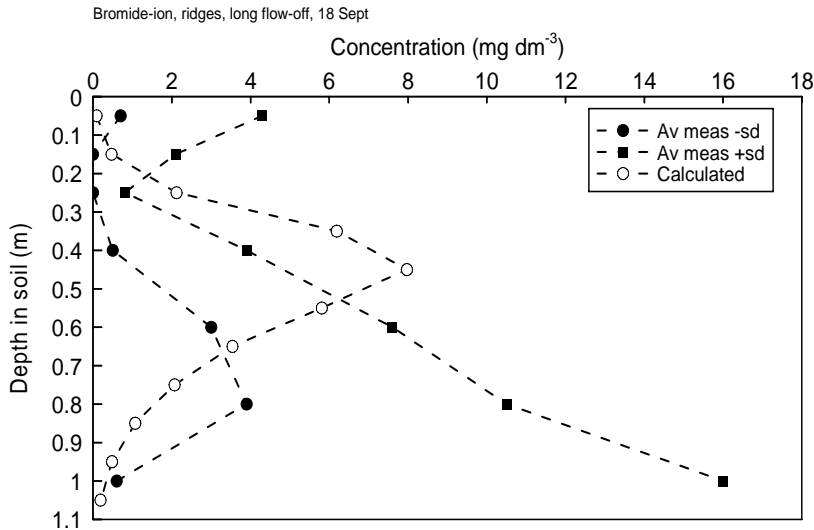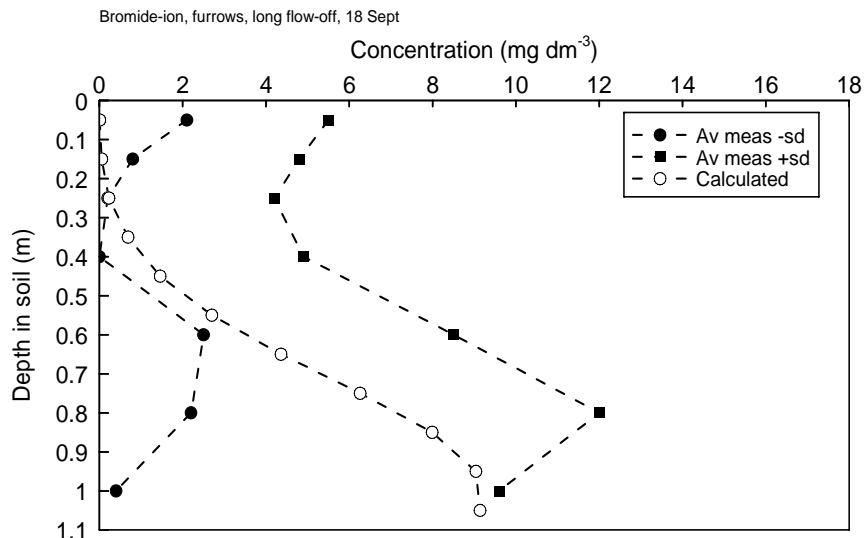

Figure 13.5. Comparison of computed and measured concentrations of bromide-ion in the soil of the ridge system on 18 September.

Figure 13.6 shows the concentrations of bromide-ion computed for the furrow system on 18 September. The peak of the distribution was computed to be at about 1 m depth and substantial leaching below 1 m had occurred. The peak of the measured distribution was at about 0.8 m depth. The concentrations of bromide-ion measured in the top 0.5 m of the soil were on average higher than those computed. This may have been caused by the release of bromide-ion from dying plant parts. Such release (not in the model) confounds the comparison of computed and measured movement of bromide-ion.

Figure 13.6. Comparison of computed and measured concentrations of bromide-ion in the soil of the furrow system on 18 September.

Computed movement in the furrow system (peak at 1 m; Figure 13.6) is much deeper than that in the ridge system (peak at 0.45 m; Figure 13.5). However, such a large difference is not supported by the measurements.

In summary

Even when the ridge and furrow systems are distinguished, the variation in the measured concentration of bromide-ion in soil is great. This is shown by the wide SD ranges in the Figures. In some cases, a substantial fraction of the distribution of bromide-ion in soil had moved below the measuring depth. At the end of the growing season, bromide-ion was probably released from the dying plant parts to the top layers. These factors hamper a close comparison between computed and measured results. Consequently, only tendencies in the comparison can be given.

On the first sampling date (29 May), downward movement of bromide-ion in the furrow system was measured to be substantially greater than that in the ridge system. According to the computations, such a difference can be roughly explained by the greater infiltration of water in the furrows. On 13 July and 18 September, the computed movement of bromide-ion in the ridge soil was less than that measured. Further, the difference in bromide-ion movement in the ridge and furrow systems was computed to be much greater than measured. This indicates that more water infiltrated into the ridges than was simulated in the computation. It seems that the flow-off of water from the ridges was restricted to a first period of e.g. a month after application of the substances. Then the soil is bare or grown with a small plants. When the plants have grown up, other processes can be expected to play a more important part. Flow of rain water along certain pathways through the canopy followed by local infiltration into the soil is then a possible process. This may explain the comparatively deep penetration of some bromide into the subsoil of the ridges measured on 13 July. After the crop has grown up, the occurrence of local pathways of flow through the canopy followed by local infiltration into the soil may be quite similar for the ridge and furrow systems.

14 Simulation of carbofuran in ridge and furrow soil

Surface transport of carbofuran from the ridges to the furrows was estimated to be 15% of the dosage (Section 12.1). So the dosage of carbofuran was taken to be 3.94 kg ha^{-1} for the ridge system and 5.32 kg ha^{-1} for the furrow system.

The concentrations of carbofuran in the ridge soil computed for 29 May are presented in Figure 14.1. The substance is computed to be still present in the top layer of the soil. Computed movement of the main part of the distribution is somewhat greater than that measured.
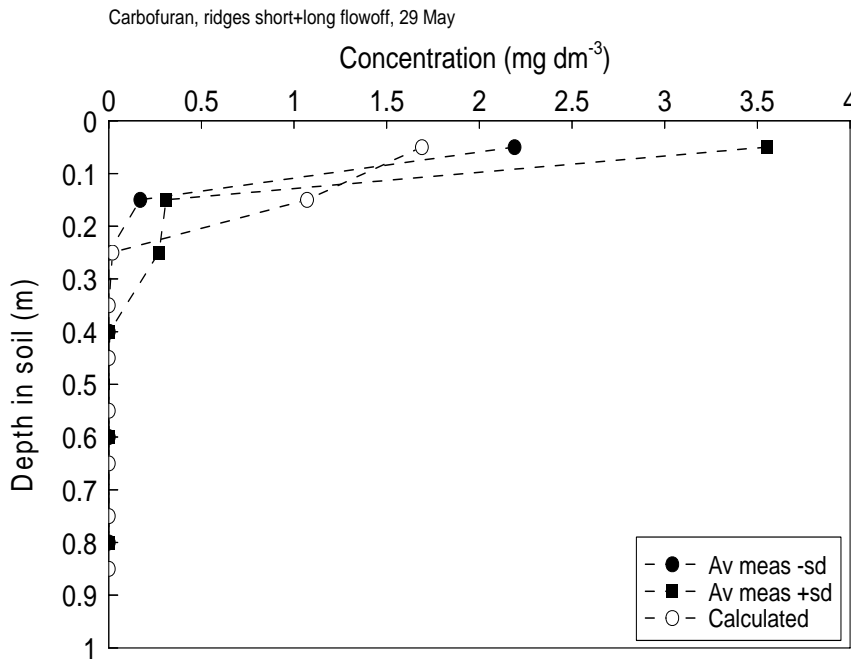
Figure 14.1. Comparison of computed and measured concentrations of carbofuran in the soil of the ridge system on 29 May. The measurements are represented by their SD range.

Figure 14.2 shows the distribution of carbofuran computed for the furrow system on 29 May. The highest concentrations are still present in the top layer of the soil. The measurements show the same type of distribution, but the amount of carbofuran in soil is remarkably high. It should be noted that the rate of transformation of carbofuran in the field soil up to 29 May was lower than corresponded to the first-order kinetics for the whole measuring period (Section 5.2) introduced in the computation. Both computed and measured movement of carbofuran in the furrow soil on 29 May (Figure 14.2) are distinctly greater than that in the ridge soil (Figure 14.1).
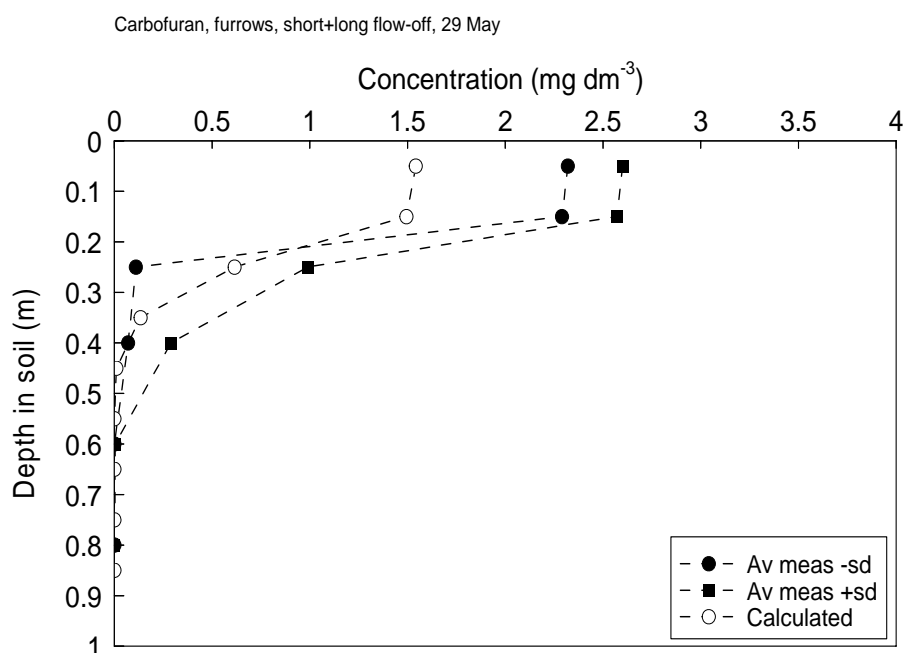
Figure 14.2. *Comparison of computed and measured concentrations of carbofuran in the soil of the furrow system on 29 May.*

The distribution of carbofuran in soil computed for the ridge system on 13 July is shown in Figure 14.3. The peak of the computed distribution is at 0.15 m depth. However, the highest measured concentrations were still present in the top 0.1 m of the soil. The computation showed less movement below 0.4 m depth than the measurements.
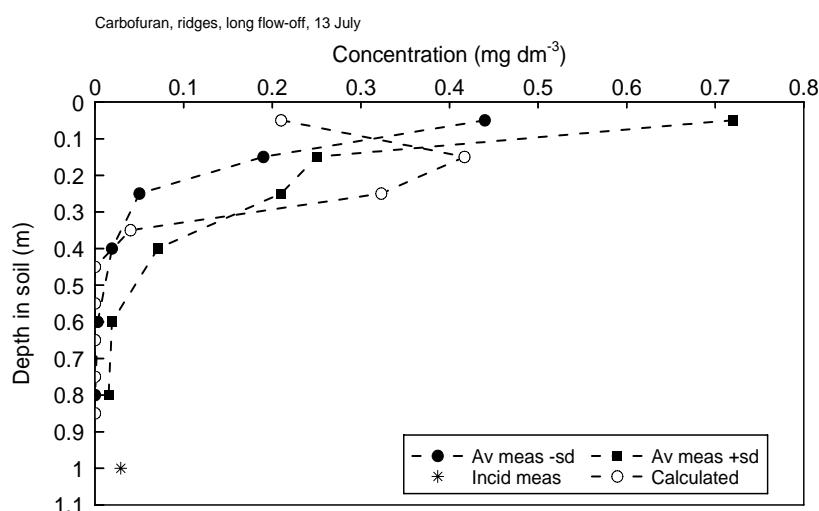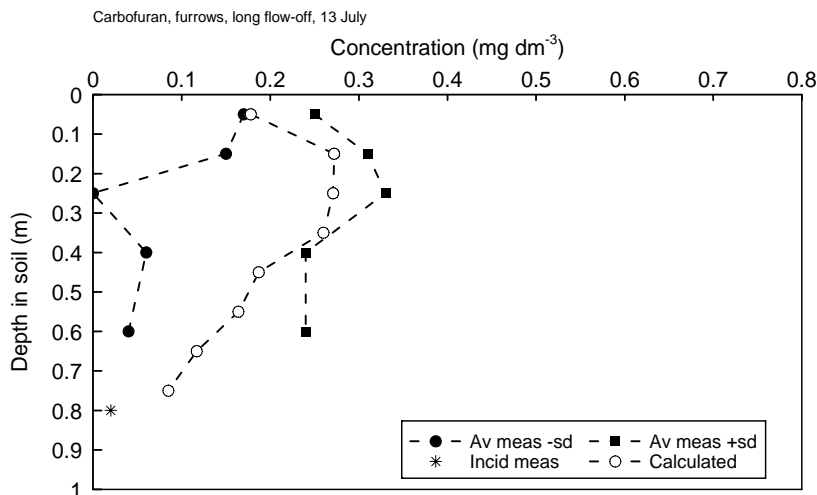

Figure 14.3. *Comparison of computed and measured concentrations of carbofuran in the soil of the ridge system on 13 July.*

Figure 14.4 shows the distribution of carbofuran computed for the furrow system on 13 July. A broad peak was computed to be present around 0.25 m depth. Some movement of carbofuran to depths below 0.8 m was simulated by the computation. The measurements showed a very wide SD range, with the highest average concentrations still present in the top 0.2 m of the soil. There was a distinct measured movement to 0.65 m depth and possibly deeper. Computed movement of carbofuran in the furrow system up to 13 July (Figure 14.4) was distinctly greater that that in the ridge system (Figure 14.3). The measurements show the same type of difference.

Figure 14.4. Comparison of computed and measured concentrations of carbofuran in the soil of the furrow system on 13 July.

The distribution of carbofuran in soil computed for the ridge system on 18 September is given in Figure 14.5. The peak of the computed distribution is at 0.25 m depth and the substance is computed to be retained in the top 0.5 m of the soil profile. The highest average of the measured concentrations (very wide SD range) was still present at 0.15 m depth. Measured movement of carbofuran to depths below 0.5 m was greater than computed movement. By this time the amount of carbofuran measured in the field soil had decreased to 6.6% of the dosage (Section 5.2).
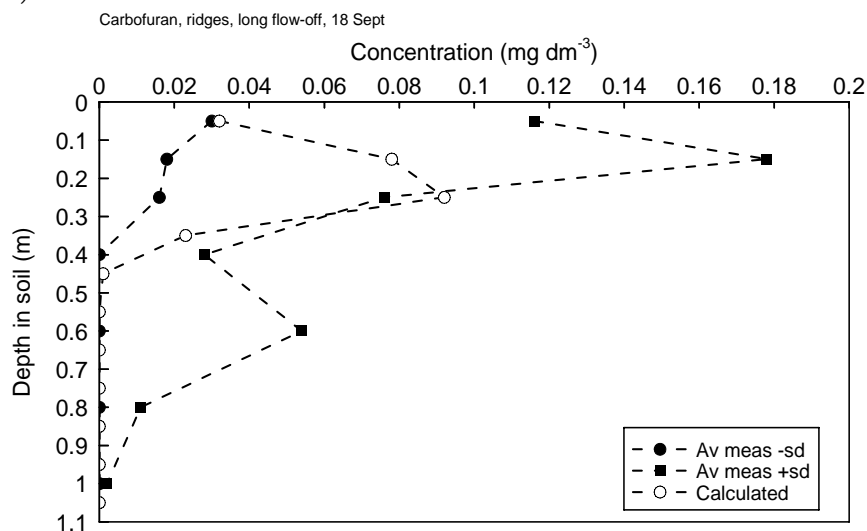

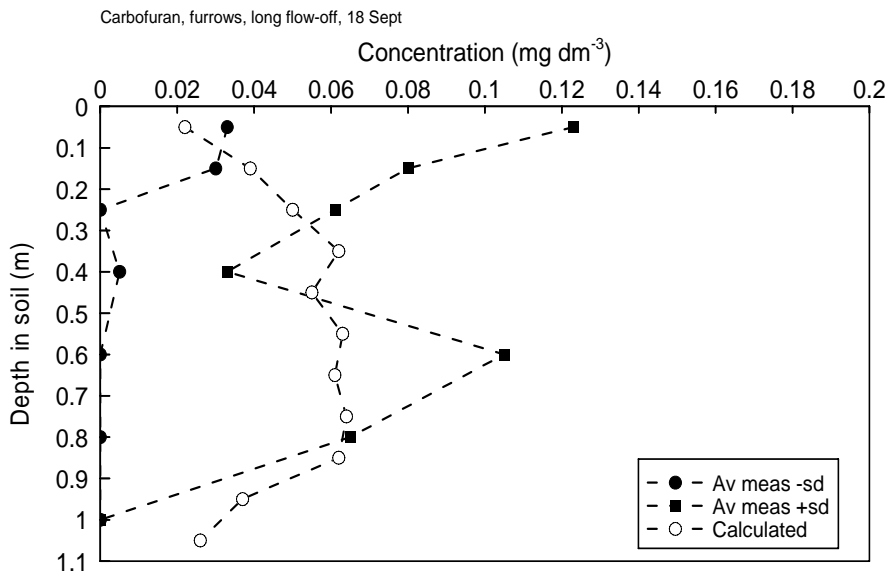*Figure 14.5. Comparison of computed and measured concentrations of carbofuran in the soil of the ridge system on 18 September.*

Figure 14.6 shows the computed distribution of carbofuran in the furrow system on 18 September. The substance was computed to be spread out over the soil profile, with a very broad peak between 0.3 and 0.9 m depth. Measured movement of carbofuran (very wide SD range) was less than that computed, both in the top layer of the soil and in the subsoil. Computed movement of carbofuran in the furrow system (Figure 14.6) was distinctly greater than that computed for the ridge system (Figure 14.5). The measurements showed the same tendency, but to a much smaller extent.

Carbofuran, furrows, long flow-off, 18 Sept

Figure 14.6. Comparison of computed and measured concentrations of carbofuran in the soil of the furrow system on 18 September.

In summary

It was hoped that, by distinguishing ridge and furrow systems, the variation in the measurements for a certain depth would decrease substantially. However, the figures indicate that this variation, represented by the SD range, is still great. This is an obstacle in the close comparison of computed and measured results. As a consequence, only tendencies in the comparison can be given.

The measurements for carbofuran on 29 May support the idea that a fraction of the water and the carbofuran dosage moves along the soil surface from the ridges to the furrows. The deeper movement of the substance in the furrow system is still visible in the measurements for 13 July. However, the assumption of a continuous surface flow (20%) from the ridge to the furrows leads to overestimation of the movement in the furrows system on 18 September. So it seems that the assumption of surface water flow from the ridges to the furrows only holds for an initial part of the cropping period. This could be the period with bare soil (before emergence of the crop) and with the presence of a small crop. A somewhat deeper distribution of the substance in furrow soil in July may be an after-effect from the first period. In a second part of the cropping period, the crop may have a large impact on water infiltration into the soil of both ridges and furrows.

15 Simulation of ridges and furrows with short flow-off period

The results presented in Chapters 13 and 14 indicate that the period in which water flows-off from the ridges to the furrows was shorter than the growing season. Now it is assumed that flow-off is restricted to the first month after application of the substances to the field (10 May). In this period, the field is bare or only a small crop is present. The idea is that, in the presence of a well-developed crop, flow along pathways through the canopy followed by local infiltration into both ridges and furrows plays a dominant part.

15.1 Water flow

The first date for comparing the computed and measured VFW's (29 May) was within the shortened flow-off period. So the computed VFW's are the same as for the ridge and furrow systems with the long flow-off period. See in Section 12.2 Figure 12.3 for the ridge system and Figure 12.4 for the furrow system.

The VFW's computed for the ridge system on 13 July, with flow-off restricted to the first month, are given in Figure 15.1. The VFW's computed for the top 0.3 m of the soil are close to the upper limit of the SD range of the measurements. Below that, they are mostly well within the SD range. The VFW's computed for the top 0.5 m of the soil profile are slightly higher than those computed for the ridge system with long flow-off period (Figure 12.5). This results from the higher water infiltration in the ridges after the first month in the present simulation.
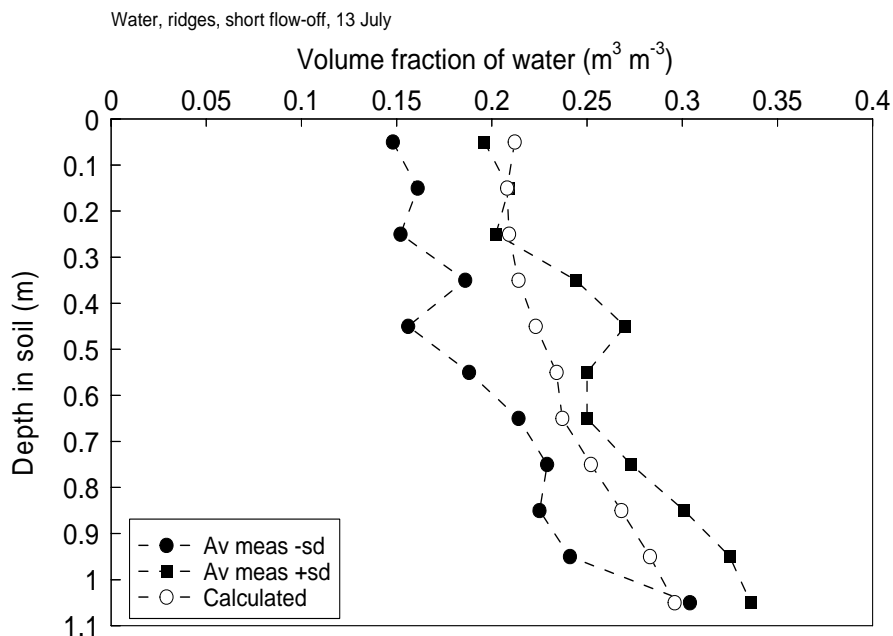

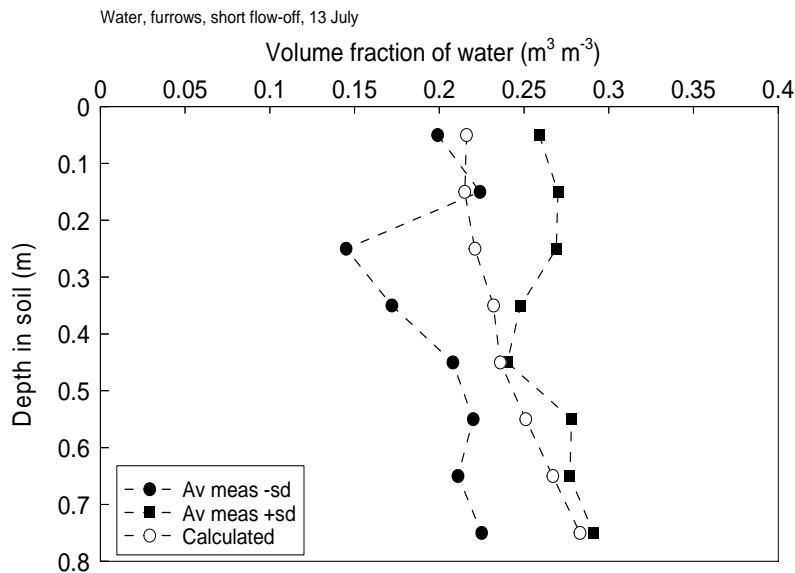*Figure 15.1. Comparison of computed and measured volume fractions of water in the soil of the ridge system on 13 July. Short period with flow-off.*

The VFW's for the furrow system with short flow-off period computed for 13 July are shown in Figure 15.2. Most computed VFW's are well within the SD range of measurements. The VFW's computed for the top 0.4 m of the soil profile are slightly lower than those for the furrow system with long flow-off period (Figure 12.6). This can be explained from the lower water infiltration in the present case of a short flow-off period. Below 0.4 m depth the differences in VFW for the short and long flow-off periods are very small.

Figure 15.2. Comparison of computed and measured volume fractions of water in the soil of the furrow system on 13 July. Short period with flow-off.

Figure 15.3 shows the VFW's computed for the ridge system with short flow-off period, on 18 September. The computed VFW's are well within the SD range of measurements. Over the whole soil profile, the VFW's are slightly higher than those computed for the ridge system with long flow-off period (Figure 12.7).
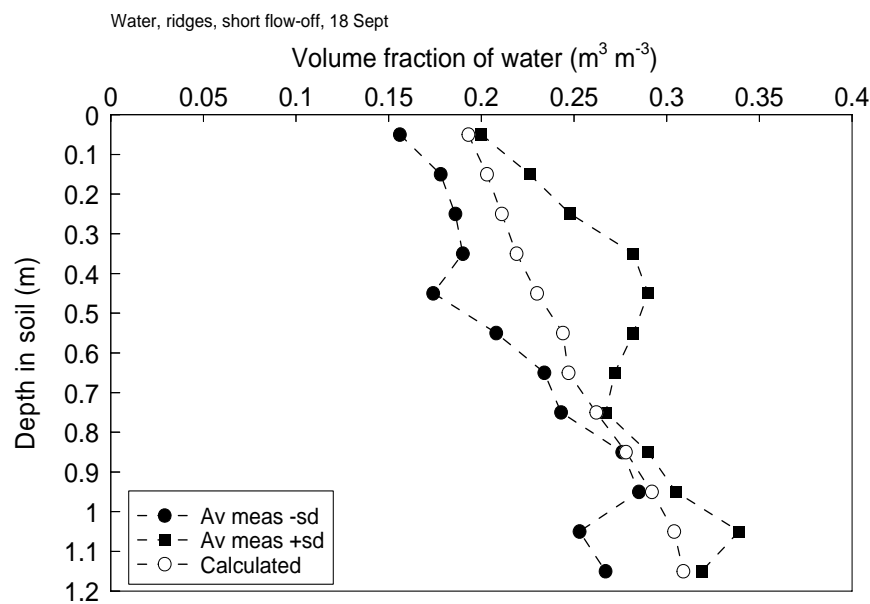

Figure 15.3. Comparison of computed and measured volume fractions of water in the soil of the ridge system on 18 September. Short period with flow-off.

Figure 15.4 shows the VFW's for the furrow system with short flow-off period, computed for 18 September. Most computed VFW's are well within the SD range of measurements. The VFW's are slightly lower than or almost the same as those for the long flow-off period (Figure 12.8). So the effect of the lower water infiltration in the present case on the VFW's in the furrow system is computed to be small.
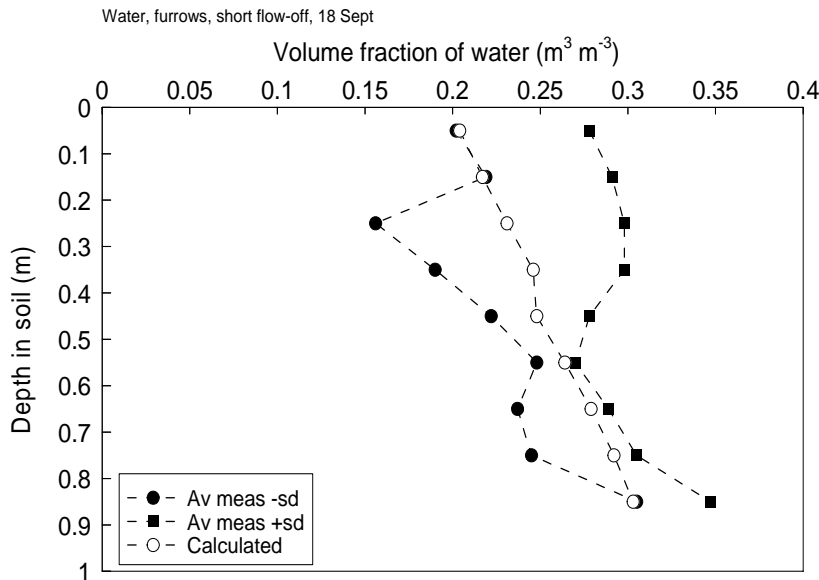

Figure 15.4. Comparison of computed and measured volume fractions of water in the soil of the furrow system on 18 September. Short period with flow-off.

In summary

The present computations show the expected effect: a) comparatively high VFW's in the soil of the ridge system in the period without flow-off and b) comparatively low VFW's in the soil of the furrow system in the period without flow-off. However, the effect of shortening the flow-off period on the VFW's in both systems was only small.

It should be noted that the VFW's computed for the ridge and furrow systems are mostly well within the SD range of the measurements. This is a distinct improvement over the computations for the averaged field (ridges and furrows pooled; Section 9.3), in which many of the computed VFW's were close to the upper or lower boundaries of the SD range of measurements.

15.2   Movement of bromide-ion

The first date for comparing the computed and measured concentrations of bromide-ion (29 May) was within the shortened flow-off period (1 month). So the computed concentrations are the same as for the ridge and furrow systems with the long flow-off period. See in Chapter 13 Figure 13.1 for the ridge system and Figure 13.2 for the furrow system.

The concentrations of bromide-ion in the ridge system with short flow-off period computed for 13 July are given in Figure 15.5. Computed movement is less than measured movement. Movement computed here for a short flow-off period (peak at about 0.6 m) is slightly deeper than that for a long flow-off period (Figure 13.3; peak at about 0.5 m depth). This can be explained from the higher water infiltration in the ridges in the present case with a short flow-off period.
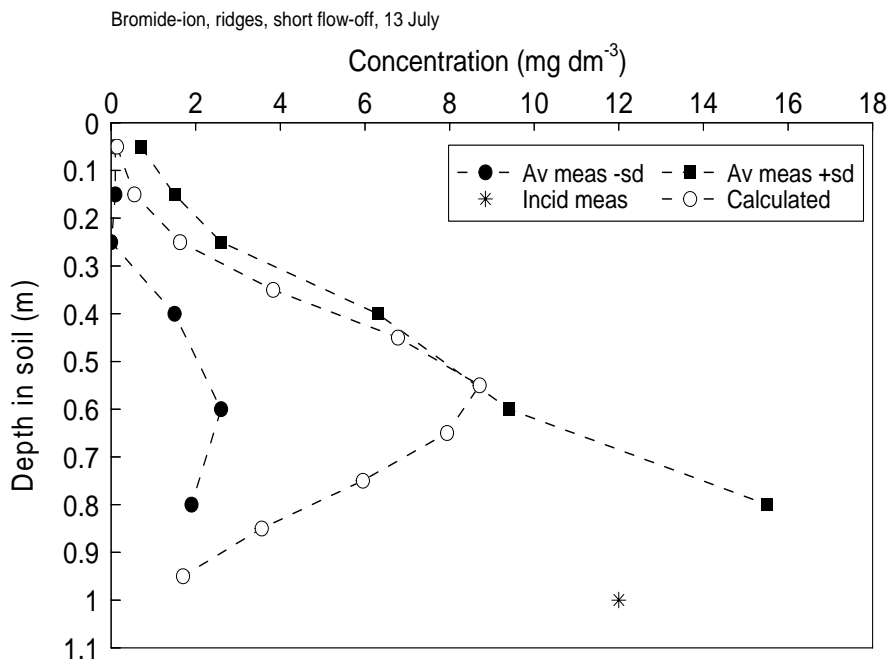

Figure 15.5. Comparison of computed and measured concentrations of bromide-ion in the soil of the ridge system on 13 July. Short period with flow-off.

Figure 15.6 shows the concentrations of bromide-ion in the furrow system with short flow-off period, computed for 13 July. Computed movement of the tail of the distribution was somewhat less than measured movement. Much of the measured distribution was below the measuring depth, which hampers a close comparison. Computed movement in this case of a short flow-off period (peak at about 0.85 m) is somewhat less than that computed for a long flow-off period (Figure 13.4; peak at about 0.95 m). This can be explained from the lower water infiltration into the furrow system in the case of a short flow-off period.
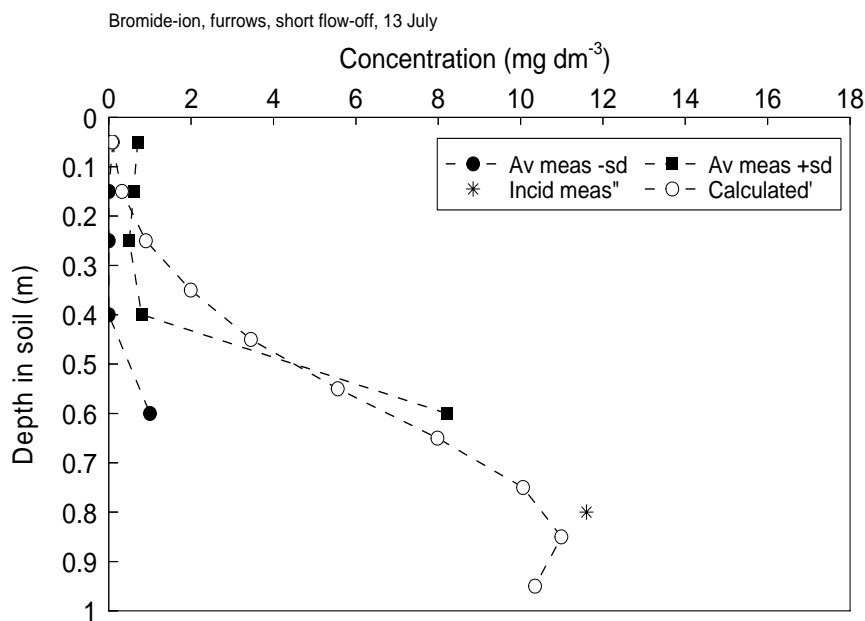
Concentration (mg dm^{-3})

Figure 15.6. Comparison of computed and measured concentrations of bromide-ion in the soil of the furrow system on 13 July. Short period with flow-off.

The concentrations of bromide-ion in the ridge system with short flow-off period, computed for 18 September, are given in Figure 15.7. Computed movement in ridge soil is less than that measured. The release of bromide-ion from dying plant parts (see measurements in topsoil) is not simulated by the computation. Computed movement in the ridge system with short flow-off period is deeper (peak at about 0.6 m) than that in the system with a long flow-off period (Figure 13.5; peak at about 0.45 m). This can be explained from the higher water infiltration into the ridge system in the present case of a short flow-off period.

Figure 15.8 shows the distribution of bromide-ion in the furrow soil system with short flow-off period, computed for 18 September. Comparison with the measurements is complicated by the release of bromide-ion from dying plant parts (see measurements for the topsoil), which was not simulated. Computed movement of bromide-ion in the furrow system with short flow-off (peak at about 0.8 m) was less deep than with a long flow-off period (Figure 13.6 ; peak at about 1 m). This is related to the lower amount of water infiltrating into the furrow system in the present case with a short flow-off period.
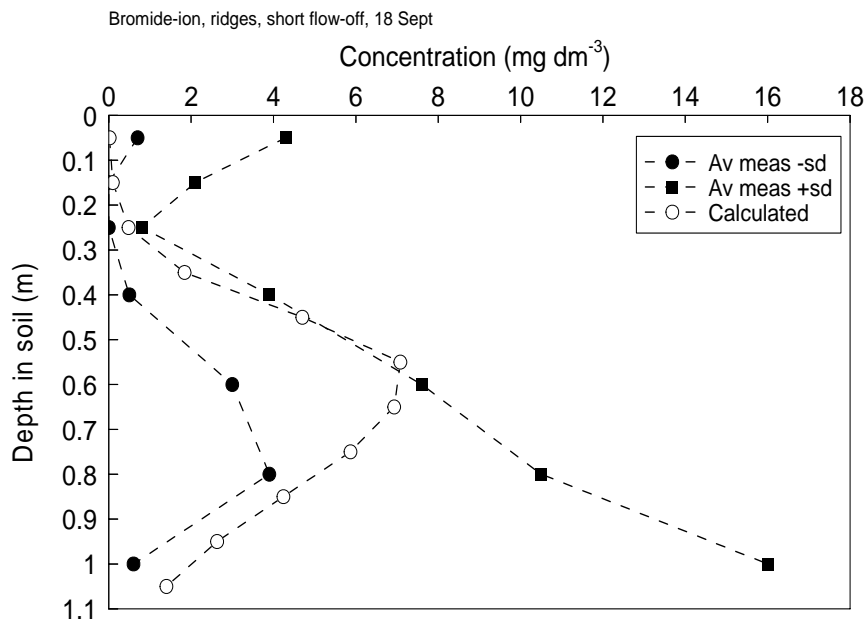
Figure 15.7. Comparison of computed and measured concentrations of bromide-ion in the soil of the ridge system on 18 September. Short period with flow-off.
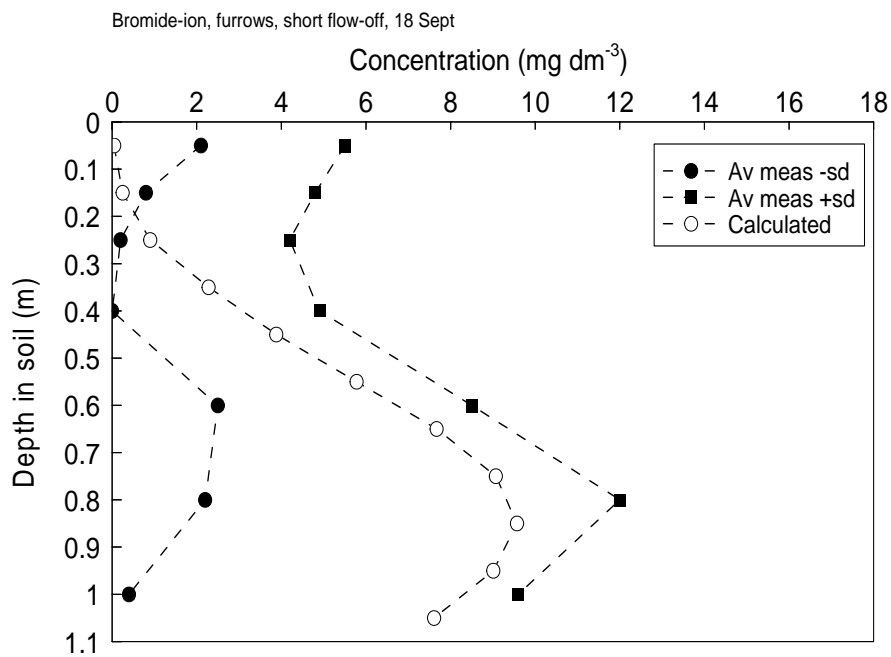

Figure 15.8. Comparison of computed and measured concentrations of bromide-ion in the soil of the furrow system on 18 September. Short period with flow-off.

In summary

The introduction of a short period (1 month) of water flow-off from the ridges to the furrows gives an improvement of the correspondence between the computations and measurements. A fraction of the bromide-ion distribution in soil seems to move faster than was computed by the model. This was found for both, the ridge and furrow systems. This means that only a fraction of the soil system participated in bromide-ion transport. This may be caused by the occurrence of certain flow pathways through the canopy, resulting in local water infiltration into the soil. A factor like soil surface condition may contribute to localised water infiltration.

It is remarkable that bromide-ion was measured to move to a large extent out of the top layer in July. This can be explained if the pattern of water infiltration changed in time. Such a pattern could be the result of variation in rainfall intensity and duration, wind direction and speed, crop development and soil surface conditions. Nevertheless, there was fast transport of a fraction of the bromide-ion distribution in soil. It seems that non-uniform water flow is not restricted to the soil near the surface, but that it also occurs deeper in the soil.

The measurements of September show comparatively high bromide-ion concentrations in the top layer, that were not present in July. Probably, a distinct amount of bromide-ion was released from dying plant parts in the later part of the growing season.

15.3   Movement of carbofuran

The first date for comparing the computed and measured concentrations of carbofuran (29 May) was within the shortened flow-off period (1 month). So the computed concentrations are the same as for the ridge and furrow systems with the long flow-off period. See in Chapter 14 Figure 14.1 for the ridge system and Figure 14.2 for the furrow system.

The concentrations of carbofuran in the ridge system with short flow-off period, as computed for 13 July, are given in Figure 15.9. Computed movement in the top layer was greater than measured, but penetration into the subsoil was computed to be somewhat less than measured. The movement computed for the short flow-off period (peak at about 0.2 m) was somewhat deeper than that for the long flow-off period (Figure 14.3; peak at about 0.15 m). This is related to the higher water infiltration into the ridge system with the short flow-off period.
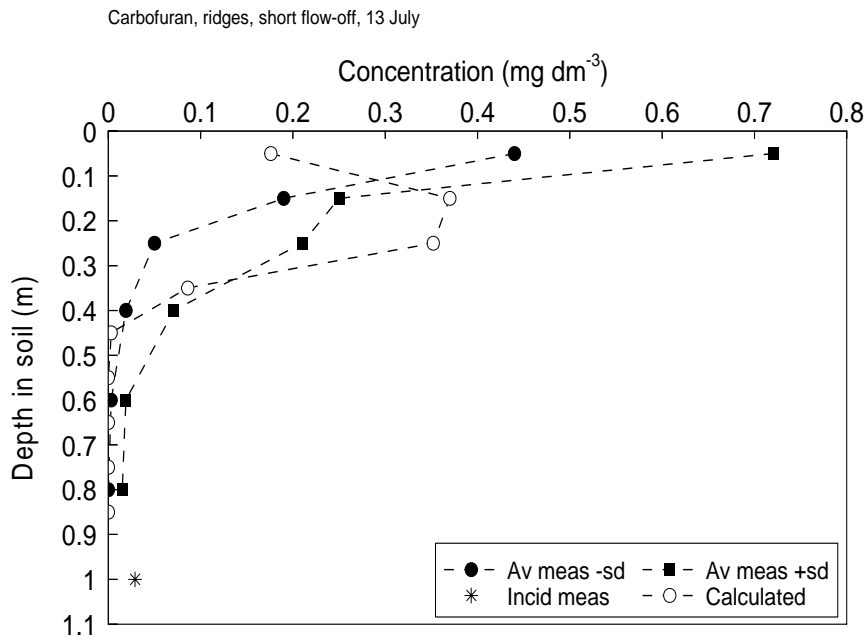
Carbofuran, ridges, short flow-off, 13 July

Concentration (mg dm^{-3})

Figure 15.9. *Comparison of computed and measured concentrations of carbofuran in the soil of the ridge system on 13 July. Short period with flow-off.*

Figure 15.10 shows the distribution of carbofuran in the furrow system with short flow-off period, computed for 13 July. Computed movement to the subsoil seems to be less than measured (extrapolated). Computed movement for short flow-off (peak at about 0.2 m) is somewhat less than that for the long flow-off period (Figure 14.4; peak around 0.25 m). This is related to the lower water infiltration in the furrow system with the short flow-off period.
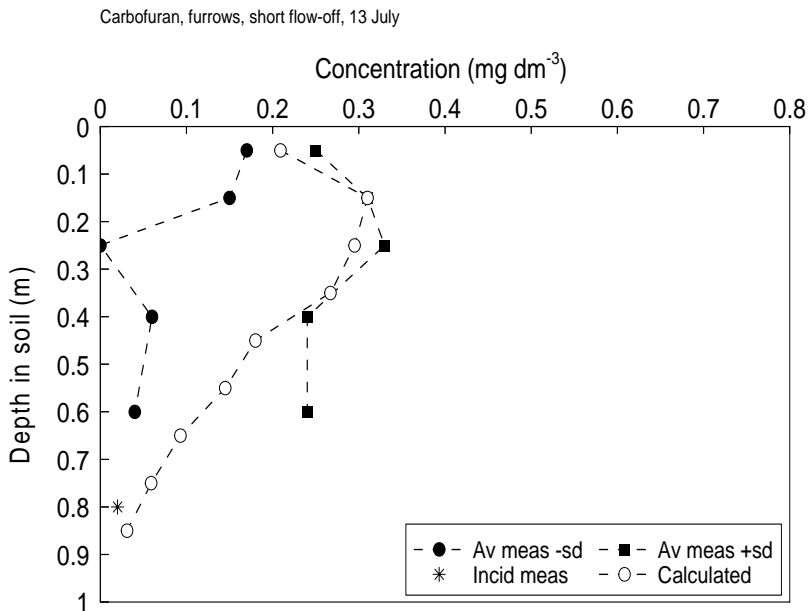
Carbofuran, furrows, short flow-off, 13 July

Concentration (mg dm^{-3})

Figure 15.10. *Comparison of computed and measured concentrations of carbofuran in the soil of the furrow system on 13 July. Short period with flow-off.*

The distribution of carbofuran in the ridge system with short flow-off period, computed for 18 September, is given in Figure 15.11. Movement from the top layer was computed to be greater than measured, but computed penetration into the subsoil was less than measured. The movement computed for the short flow-off period (peak at about 0.3 m) was somewhat greater than that for the long flow-off period (Figure 14.5; peak around 0.25 m). This can be explained from the greater water infiltration in the ridge system with the short flow-off period.

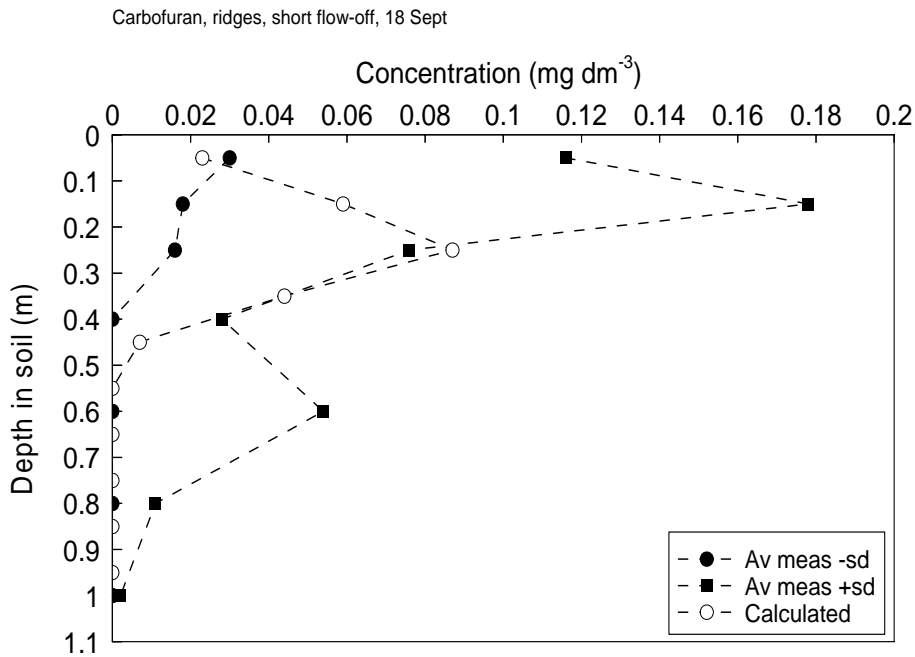Carbofuran, ridges, short flow-off, 18 Sept

Figure 15.11. Comparison of computed and measured concentrations of carbofuran in the soil of the ridge system on 18 September. Short period with flow-off.

Figure 15.12 shows the concentrations of carbofuran in the furrow system with short flow-off period, as computed for 18 September. In both computations and measurements, carbofuran was spread out in the soil profile, with the computed movement from the top layer being greater than measured. The peak of the distribution is computed to be at 0.35 m depth, which is less than computed for the long flow-off period (Figure 14.6; wide peak between 0.35 and 0.85 m). The lower movement is related to the lower water infiltration into the furrow system with the short flow-off period.
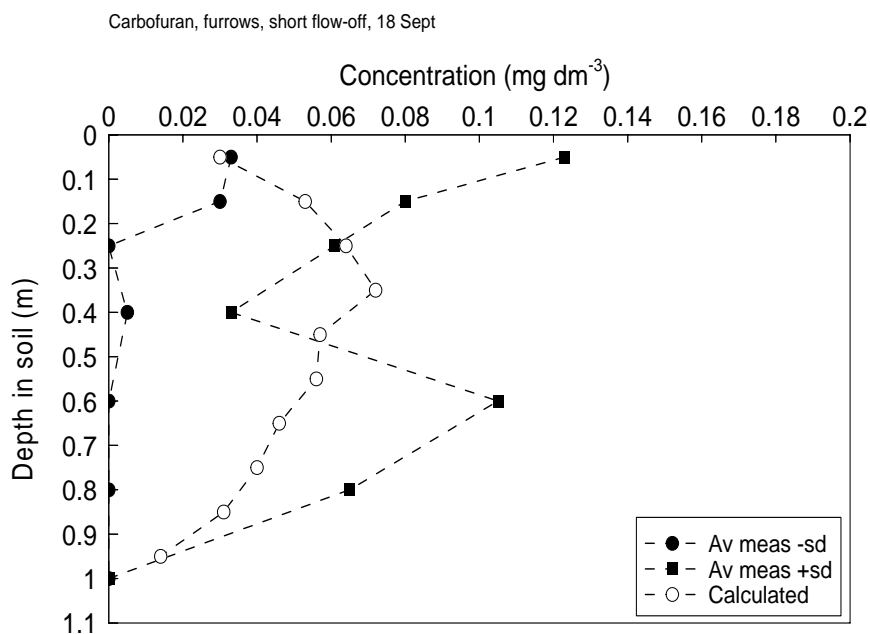
Carbofuran, furrows, short flow-off, 18 Sept

Figure 15.12. Comparison of computed and measured concentrations of carbofuran in the soil of the furrow system on 18 September. Short period with flow-off.

The amount of carbofuran computed to be present in the furrow system on 18 September (Figure 15.12) is distinctly greater than that in the ridge system on this date (Figure 15.11). This is the result of: 1) the surface run-off of 15% of the dosage from the ridges to the furrows, 2) the lower uptake of carbofuran by the smaller root system in the furrows, and 3) the faster movement of carbofuran in the furrow system to soil depths with comparatively low transformation rates.

In summary
The assumption of a short flow-off period for the ridge and furrow systems gives a better correspondence between computed and measured distributions of carbofuran in soil. The average movement of carbofuran in soil is now described reasonably well by the model. However, the following tendencies remain: a) the computed movement from the top layer is greater than measured and b) the computed penetration into the subsoil is less than measured.

The retention of carbofuran in the top layer of the ridge and furrow systems was greater than simulated in the computation. This indicates that there was uneven water infiltration and flow in both systems. Probably, a fraction of the substance in the top layer was outside the main pathways of water flow. The resulting retardation can be expected to be stronger for the adsorbed carbofuran than for the non-adsorbed bromide-ion.

In some cases, measured movement of carbofuran to the subsoil is greater than computed. A fraction of the substance seems to be present in the main flow pathways of the water. Differences in the extent to which soil zones participate in water flow and substance transport also explain the very wide variation in the concentrations measured at a certain depth in soil.

16 Breakthrough at 1 m depth in soil

Computation procedure

The course of the concentration of the substances in the water phase with time (breakthrough curve) was computed for 1 m depth in soil. This was done to illustrate the effect of distinguishing ridges and furrows on the computed leaching to the upper groundwater. The computation was carried out for both bromide-ion and carbofuran in a) the all-time averaged field system, b) the ridge system and c) the furrow system. In the all-time averaged-field system, all quantities were averaged (no ridges and furrows distinguished) (Chapter 8). The ridge system had been build up with 0.1 m topsoil, which resulted in a 0.6 m thick humic-sandy rooting zone (Section 12.1). The top 0.1 m of soil was taken from the furrow system, so that 0.4 m of humic-sandy rooting zone remained.

In the first month after application of the substances, 20% of the rainfall plus sprinkler irrigation was taken to flow via the soil surface from the ridge system to the furrow system (called "short flow-off" in Chapter 15). Just like in Chapters 13 and 14, it was assumed that 15% of the dosage of the substances was transported via the soil surface from the ridge system to the furrow system. The description of crop development was adapted to the ridge and furrow systems, as described in Section 12.1.

Harvest date for the potatoes was set at 30 November 2000. From that date on the separate ridge and furrow systems no longer existed, so the computation was interrupted. The soil surface was taken to be levelled. The distribution of the substances in the ridge and furrow systems at harvest was assigned to the corresponding layers of the post-harvest averaged field. The top 0.2 m of the ridge system was assigned to the top 0.1 m of the post-harvest field system. The concentrations computed for the other layers at harvest were averaged (ridge 0.2-0.3 m layer with furrow 0-0.1 m layer gives post-harvest 0.1 to 0.2 m layer, etc). The averaged concentrations on 30 November were introduced as initial distribution of the substances in soil in the post-harvest computation.

Breakthrough of bromide-ion

The results of the computation of bromide-ion breakthrough from the all-time averaged field are given in Figure 16.1. Breakthrough from the top metre of this averaged field system already started in June. A peak concentration of 28 mg dm^{-3} was reached in the beginning of November 2000. In the next 10 months, the breakthrough concentration decreased gradually to a very low level.
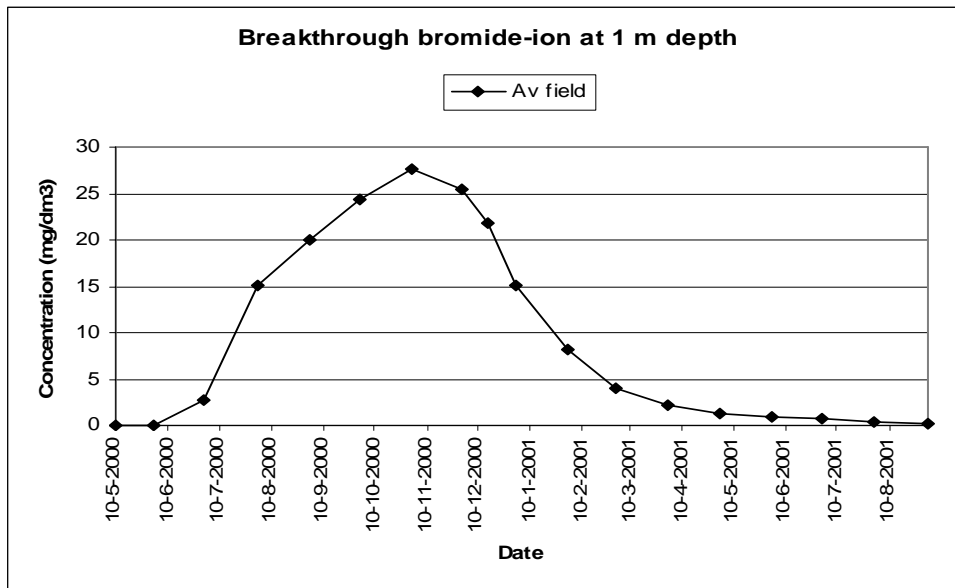
Figure 16.1. Concentrations of bromide-ion in the water phase passing at 1 m depth in soil (breakthrough curve) computed for the all-time averaged field system.

Figure 16.2 shows the results of the computation of bromide-ion breakthrough at 1 m depth for the ridge and furrow systems. Breakthrough of bromide-ion from the furrow system already started within a month after application. A comparatively high peak concentration around 35 mg dm^{-3} was reached in July 2000. After that, breakthrough concentration decreased gradually until harvest (30 November; end of furrow system).
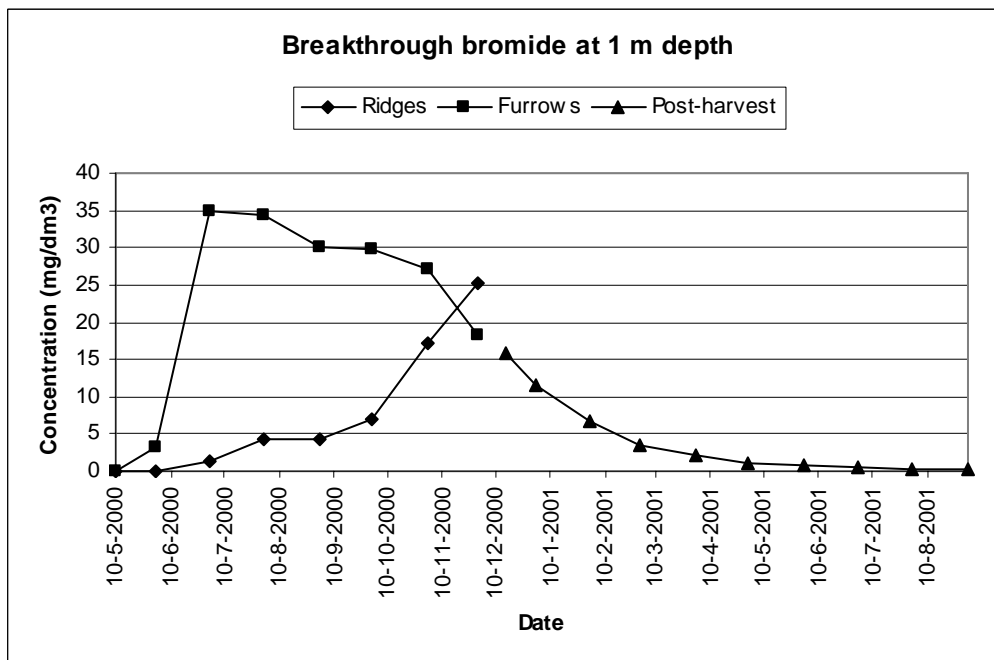

Figure 16.2. Concentrations of bromide-ion in the water phase passing at 1 m depth in soil (breakthrough curve) computed for 1) ridge system until harvest, 2) furrow system until harvest and 3) post-harvest averaged field (follow-up of ridge and furrow systems).

Breakthrough of bromide-ion from the ridge system (Figure 16.2) started comparatively late (beginning of July 2000) and the concentration increased continuously until harvest time.

Breakthrough of bromide-ion computed for the post-harvest averaged field (follow-up of ridges and furrows) is also shown in Figure 16.2. The concentration at 1 m depth decreased gradually until low values 9 months later. The concentrations in this breakthrough tail were somewhat lower than those computed for the all-time averaged field system (Figure 16.1).

Breakthrough of carbofuran

The concentrations of carbofuran computed for the water passing at 1 m depth in soil, for the all-time averaged field system, are shown in Figure 16.3. Breakthrough started in November 2000 and a maximum concentration of about 7.5 µg dm^{-3} was reached in March 2001. In the next period of 7 months, the breakthrough concentration of carbofuran decreased gradually to a low level.
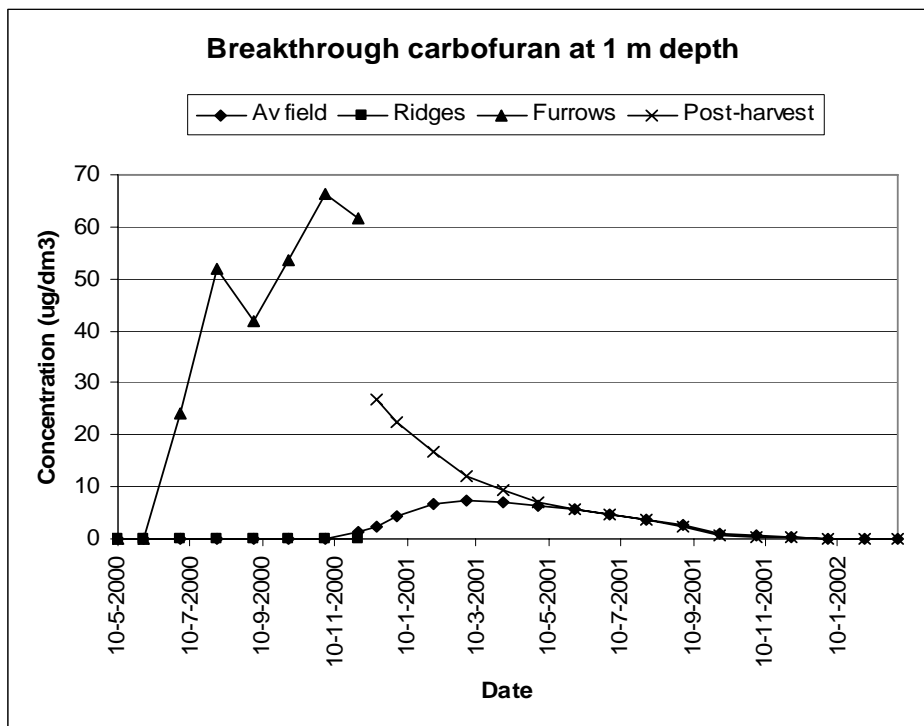

Figure 16.3. Concentrations of carbofuran in the water phase passing at 1 m depth in soil (breakthrough curve). Four systems: 1) all-time averaged field system, 2) ridge system until harvest, 3) furrow system until harvest and 4) post-harvest averaged field system (follow-up of ridge and furrow systems).

The concentration of carbofuran breaking through from the furrow system increased rapidly in June 2000 (Figure 16.3). The maximum concentration of 66 µg dm^{-3} was reached around 1 November 2000, shortly before harvest time (30 November).
Carbofuran in the ridge system did not reach the 1 m depth in soil before harvest time (Figure 16.3; all values zero).

The computation for the post-harvest averaged field (follow-up of ridges and furrows) resulted in a tail of the breakthrough curve (Figure 16.3). In the course of 10 months after harvest, the concentration in water at 1 m depth decreased gradually to a low level.

In summary
Breakthrough of bromide-ion from the furrow system occurs much earlier than that from the ridge system. However, the maximum concentrations leaching from the soil are of the same order of magnitude for ridges, furrows and all-time averaged field. As there is no transformation of bromide-ion in soil, the residence time has hardly any effect on the concentration leached.

Breakthrough of carbofuran from the furrow system occurs early and the leached concentrations are comparatively high. On the contrary, carbofuran in the ridge system did not leach at all within the cropping period. The much longer residence time in the ridge system provides ample time for transformation of carbofuran. The short residence time results in the leaching concentrations of carbofuran from furrow soil to be much higher than that from the all-time averaged field.

17 General discussion

An enormous amount of measuring data was collected in the framework of the Roswinkel potato-field experiment in the years 2000 to 2002. These data had to elaborated for input into the PEARL computations and for comparison between the computed and measured results. Supplementary data had to collected, e.g. from weather stations and from the literature. The main question in this report is what can be learned from a) the results of the field experiment as such, b) the comparison of computed and measured results, and c) possible extrapolations on the basis of the results.

There was a wide range of measured values for the concentration of bromide-ion and carbofuran at a certain depth in soil. This can be due to variation in the field, but there may be a contribution of variation in the measurements. E.g. the measurements for bromide-ion in the soil on 29 May contained many zero values and the averaged amount in the soil profile was much lower than expected (still hardly any uptake and leaching). When measuring low concentrations of a pesticide, e.g. in groundwater, there is a risk of contamination in the field and in the lab. This may have contributed to the incidentally measured high values.

There are clear indications that some precipitation water flowed along the soil surface from the ridges to the furrows. It was assumed that 20% of the water (rainfall plus sprinkler irrigation) flowed from the ridges to the furrows, but that this was restricted to the first month after application. This could roughly explain the greater movement of the substances in the furrow system, as compared to that in the ridge system. It should be investigated whether the surface flow can be related to precipitation intensity and duration. Based on the measurements, it was estimated that 15% of the dosage of the substances moved along the soil surface from the ridges to the furrows. More information on the extent of this process is welcome.

The presence of a well-developed crop is expected to have much effect on the pattern of water infiltration into the soil. The intercepted precipitation can follow certain flow pathways through the canopy, such as stem flow and local dripping from leaves. The infiltration of water in soil could be variable in time due to changes in crop development, intensity and duration of rainfall, wind direction and speed, soil surface condition, etc. So the effect of a crop on the dispersion of a substance in soil could be less than expected for permanent flow pathways. More information on the infiltration pattern of water in a cropped field and on the variation of this pattern with time is needed.

Comparisons between computed and measured results on substance behaviour in soil-plant systems can provide interesting information. Close correspondence would give confidence in the model, whereas clear deviations ask for resumed thinking, experimentation and modelling. It was found that close comparison between computations and measurements is hampered for various reasons such as:

- the necessity of calibrating water flow in soil;
- the very wide ranges in the concentrations measured for bromide-ion and carbofuran;
- the incomplete profiles of bromide-ion in soil;
- the complication of the uptake/release of bromide ion in/from the plants;
- the probable onset of accelerated transformation of carbofuran in soil later in the experiment;
- some unexpected and contradictory measuring results.

The present study shows that a close test of a computation model is difficult to attain. Even so when testing against the Roswinkel data set, which is much more detailed than those from most other studies. So the computations have to be compared with tendencies in the wide ranges of the measurements.

The PEARL model is intended to be used for one-dimensional (vertical) systems dealing with the behaviour of pesticides in (cropped) soils. For this purpose, the conditions have to be averaged on field scale. Models for two-dimensional soil-plant systems are scarce and poorly developed. Therefore it is interesting to see to what extent the use of a one-dimensional model can be adapted to two dimensional systems. Distinguishing separate ridge and furrow systems, and the use of the PEARL model for each of them, is an example of a feasible two-dimensional analysis with a one-dimensional model.

The average movement of the substances in the ridge and furrow systems could be described reasonably well (in wave form) by the computations. However, according to the measurements, a fraction of the substances tended to stay behind in the top layer. This effect seemed to be stronger for carbofuran (adsorbed) than for bromide-ion (not adsorbed). Another fraction of the substances was measured to move faster into the subsoil than simulated. One can imagine that there are three zones with respect to water flow and substance transport in the ridge and furrow soils: 1) a zone with water flow and substance transport faster than the average, 2) a zone with average (chromatographic) transport and 3) a zone with slow transport outside the main flow pathways of the water. Such non-uniform transport in soil also explains the wide variation in the concentrations measured for the substances at a certain depth in soil.

The effect of distinguishing ridge and furrow systems on the breakthrough of the substances at 1 m depth in soil is computed to be much greater for carbofuran than for bromide-ion. This is mainly related to the transformation of carbofuran in soil. In the furrow system the residence time of carbofuran is comparatively short, which provides limited time for transformation in soil. On the contrary, the comparatively long residence time in the ridge system provides ample time for transformation in soil. This results in much lower breakthrough concentrations. The early leaching from the furrow system increases the risk of leaching of a pesticide, as compared to the leaching from the averaged field.

References

Bakker, H. de, J. Schelling, D.J. Brus & C. van Wallenburg (1989). Systeem van bodemclassificatie voor Nederland. De hogere niveaus (System of soil classification in the Netherlands. The higher levels). Centrum voor Landbouwpublikaties en Landbouwdocumentatie, Wageningen, The Netherlands.

Briggs, G.G., R.H. Bromilow & A.A. Evans (1982). Relationships between lipophilicity and root uptake and translocation of non-ionised chemicals by barley. Pestic. Sci. 13: 495-504.

Crum, S.J.H., K. Trouwborst, J.H. Smelt, L.J.T. van der Pas, K. Oostindie & L.W. Dekker (2004). Transport of water, bromide and the pesticide carbofuran in the unsaturated zone and subsurface groundwater on a ridged potato field. A summary of measured data for computations. Field experiment on a sandy soil at Roswinkel, The Netherlands. Internal Report, with CD. Alterra, Wageningen UR, The Netherlands.

Dam, J.C. van, J. Huygen, J.G. Wesseling, R.A. Feddes, P. Kabat, P.E.W. van Walsum, P. Groenendijk & C.A. van Diepen (1997). SWAP version 2.0. Theory. Simulation of water flow, solute transport and plant growth in the Soil-Water-Atmosphere-Plant environment. Report 71, Department of Water Resources, Wageningen Agricultural University, Wageningen, The Netherlands.

EU (2007). Review report for the active substance carbofuran. SANCO/10054/2006 final. 7 September 2007.
http://www.efsa.europa.eu

FAO (1988). FAO-UNESCO Soil Map of the World. Revised Legend. World Resources Report 60. Food and Agricultural Organisation of the United Nations, Rome, Italy.

Feddes, R.A. (1987). Crop factors in relation to Makkink reference-crop evapotranspiration. In: Evaporation and weather. Proceedings and Information 39: 33-45. J.C. Hooghart (ed). TNO Committee on Hydrological Research, The Hague, The Netherlands.

Gregory, P.J. & L.P. Simmonds (1992). Water relations and growth of potatoes. In: The potato crop. The scientific basis for improvement. Chapter 5. Pages 214-246. P Harris (ed.). Chapman & Hall, London.

Karpouzas, D.G., A. Walker, D.S.H. Drennan & R.J. Froud-Williams (2001). The effect of initial concentration of carbofuran on the development and stability of its enhanced biodegradation in top-soil and sub-soil. Pest Manag. Sci. 57: 72-81.

KNMI (2000a, 2001a). Maandoverzicht neerslag en verdamping in Nederland (Monthly survey of precipication and evaporation in the Netherlands). Royal Netherlands Meteorological Institute, De Bilt, The Netherlands.

KNMI (2000b, 2001b). Maandoverzicht van het weer in Nederland (Monthly survey of the weather in The Netherlands). Royal Netherlands Meteorological Institute, De Bilt, The Netherlands.

Leistra, M., A.M.A. van der Linden, J.J.T.I. Boesten, A. Tiktak & F. van den Berg (2001). PEARL model for pesticide behaviour and emissions in soil-plant systems. Description of the processes in FOCUS PEARL v 1.1.1. Alterra–rapport 013; RIVM report 711401 009. Alterra, Green World Research, Wageningen, The Netherlands.

Lide, D.R. (1999). CRC Handbook of chemistry and physics. 80th ed. CRC Press, Boca Raton FL, USA.

Linden, A.M.A., van der, J.J.T.I. Boesten, A.A. Cornelese, R. Kruijne, M. Leistra, J.B.H.J. Linders, J.W. Pol, A. Tiktak & A.J. Verschoor (2004). The new decision tree for the evaluation of pesticide leaching from soils. RIVM report 601450019/2004. National Institute of Public Health and the Environment, Bilthoven, The Netherlands.

Massop, H.T.L. & P.A.J.W. de Wit (1994). Hydrologisch onderzoek naar de drainageweerstanden van het tertiair ontwateringsstelsel in Oost-Gelderland. Report 373, Winand Staring Centre, Wageningen, The Netherlands.

NL-Ctgb (2007). Toelatingen. Bestrijdingsmiddelendatabank. Carbofuran. Board for the Authorization of Plant Protection Products and Biocides, Wageningen, The Netherlands. http://www.ctgb.nl

Pinto, P.J.C.A. (1988). Computer simulation modeling of the growth and development of the potato crop under different water regimes. PhD thesis, University of California, Davis CA, USA.

Scorza Júnior, R.P., J.H. Smelt, J.J.T.I. Boesten, R.F.A. Hendriks & S.E.A.T.M. van der Zee (2004). Preferential flow of bromide, bentazon and imidacloprid in a Dutch clay soil. J. Environ. Qual. 33: 1473-1486.

Tiktak, A., F. van den Berg, J.J.T.I. Boesten, D. van Kraalingen, M. Leistra & A.M.A. van der Linden (2000). Manual of FOCUS PEARL version 1.1.1. RIVM report 711401 008, Alterra report 28. National Institute of Public Health and the Environment, Bilthoven, The Netherlands.

Tomlin, C.D.S. (2003) The pesticide manual. A world compendium. 13th Ed. British Crop Protection Council, Alton, Hampshire, UK.

Tucker, W.A. & L.H. Nelken (1982). Diffusion coefficients in air and water. In: W.J. Lyman, W.F. Reehl & D.H. Rosenblatt (eds). Handbook of chemical property estimation methods. Environmental behavior of organic compounds. Chapter 17. McGraw-Hill, New York, USA, pp1-25.

Wösten, J.H.M., G.J. Veerman, W.J.M. de Groot & J. Stolte (2001). Waterretentie- en doorlatendheidskarakteristieken van boven- en ondergronden in Nederland: de Staringreeks (Water retention and conductivity characteristics of topsoils and subsoils in The Netherlands: the Staring Series). Alterra Rapport 153, Alterra, Wageningen, The Netherlands.
http://www.alterra.wur.nl/NL/publicaties+Alterra

Appendix A Adsorption of carbofuran to Roswinkel topsoil at 5 and 25 ºC.
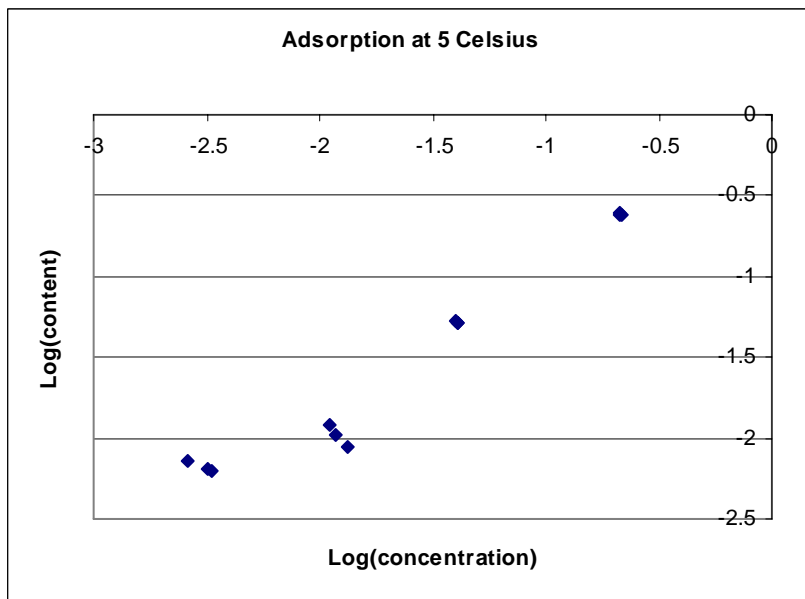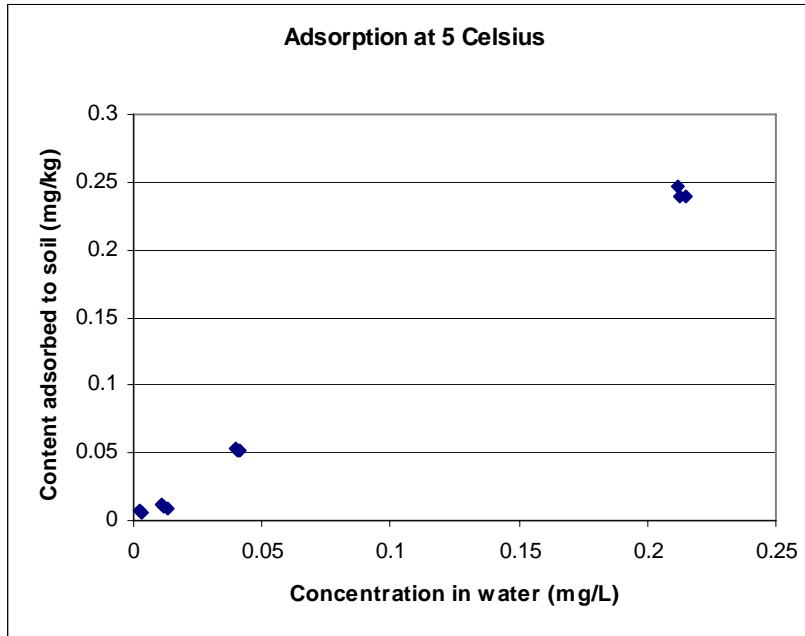

Figure A.1. Measuring points for the adsorption of carbofuran to Roswinkel topsoil at 5 ºC. Linear and log scales, respectively.
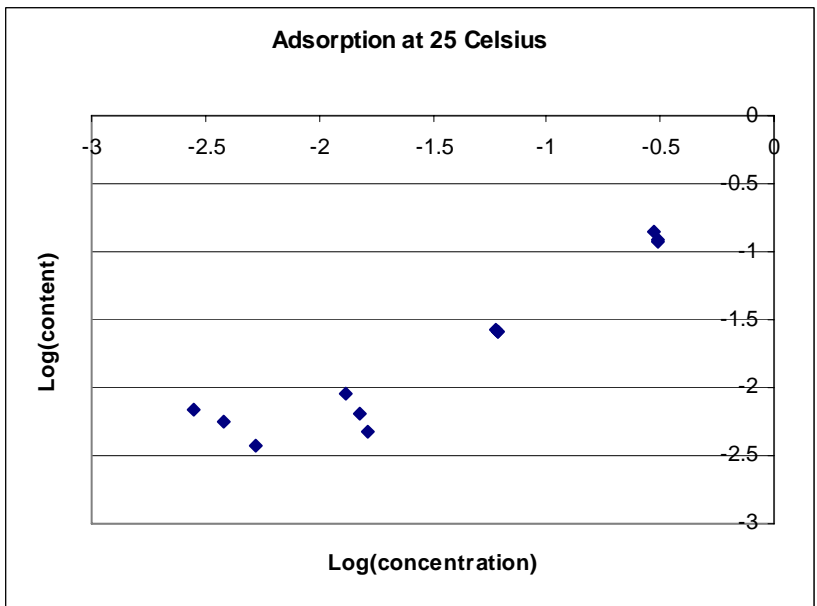
Figure A.2. Measuring points for the adsorption of carbofuran to Roswinkel topsoil at 25 °C. Linear and log scales, respectively.

Appendix B   Rate of transformation of carbofuran in Roswinkel topsoil at 5 and 25 °C.

Figure B.1. Rate of transformation of carbofuran in Roswinkel topsoil at 5 °C. Linear-linear and log-linear scales, respectively.
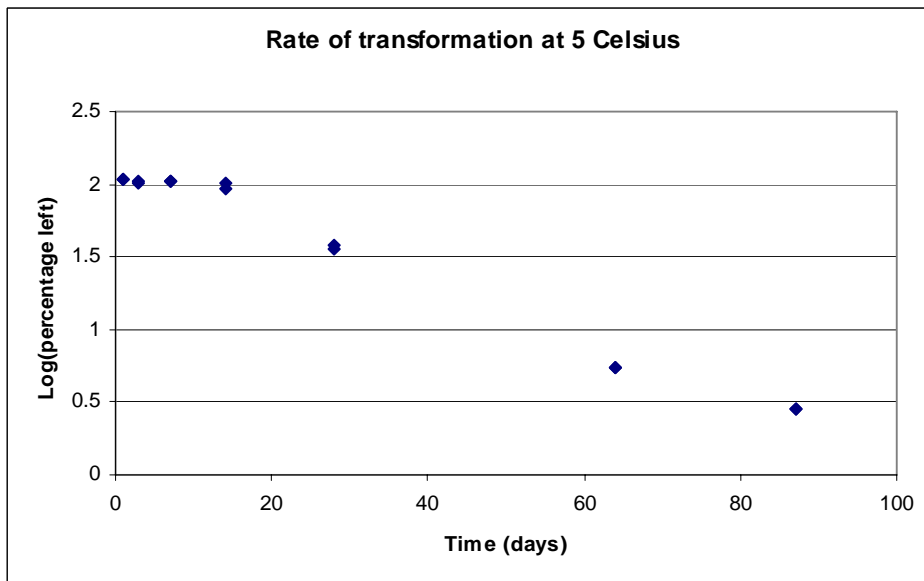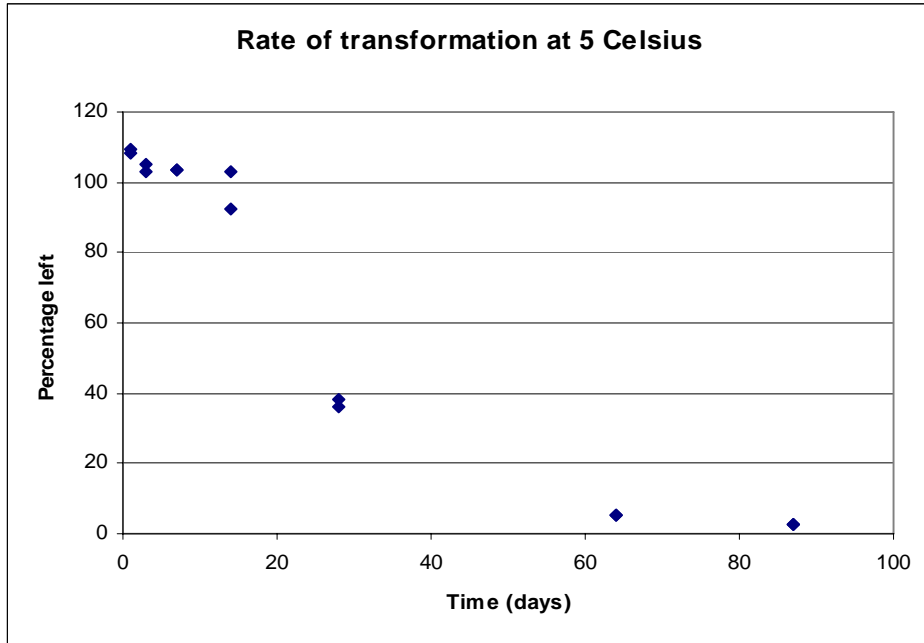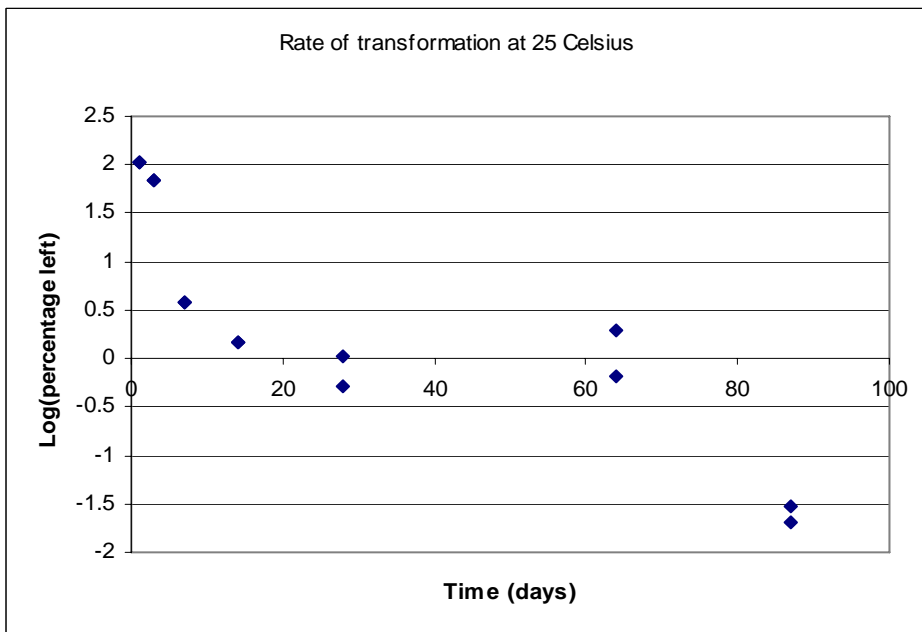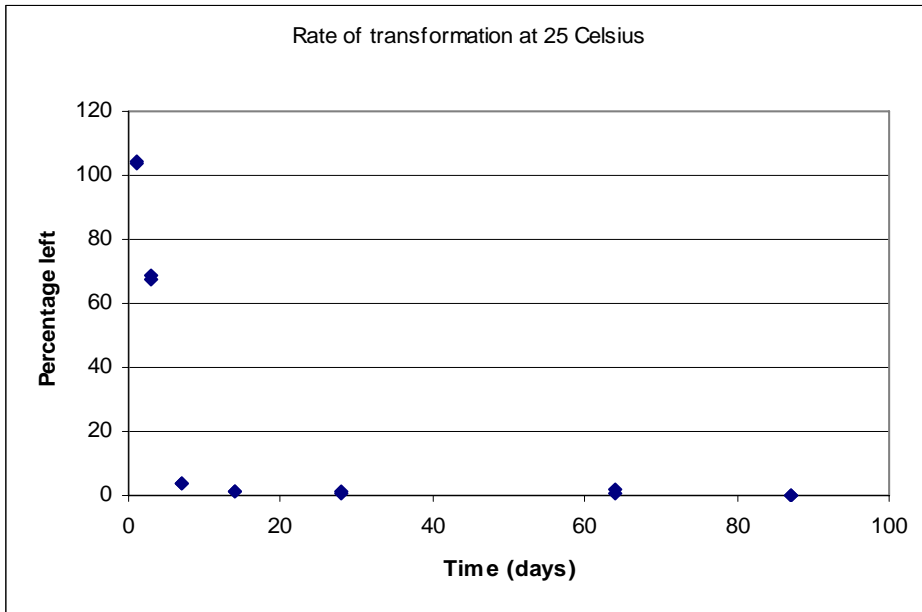
Figure B.2. Rate of transformation of carbofuran in Roswinkel topsoil at 25 ºC. Linear-linear and log-linear scales, respectively.

Appendix C Measured quantities averaged for the whole Roswinkel field.

The main text presents the averages of the measured quantities for the ridge and furrow systems separately (with their standard deviation) (Chapters 2 and 5). The first series of computations, however, was carried out for the whole field system (ridges and furrows pooled). These computations have to be compared with the measured quantities averaged for the whole field. These whole-field averages, with their standard deviation, are presented in this Appendix.

Table C.1. Averages and standard deviations of the measured volume fractions of water (VFW's) in soil for the whole Roswinkel field (ridges and furrows pooled).

Layer (m)	10 May		29 May		13 July		18 September	
	Average VFW ($m^3 m^{-3}$)	Standard deviation ($m^3 m^{-3}$)	Average VWF ($m^3 m^{-3}$)	Standard deviation ($m^3 m^{-3}$)	Average VFW ($m^3 m^{-3}$)	Standard deviation ($m^3 m^{-3}$)	Average VFW ($m^3 m^{-3}$)	Standard deviation ($m^3 m^{-3}$)
0-0.1	0.177	0.050	0.210	0.041	0.200	0.039	0.209	0.044
0.1-0.2	0.203	0.040	0.244	0.044	0.216	0.039	0.229	0.040
0.2-0.3			0.226	0.043	0.192	0.049	0.222	0.054
0.3-0.4			0.242	0.039	0.213	0.033	0.240	0.050
0.4-0.5			0.240	0.031	0.219	0.042	0.241	0.046
0.5-0.6			0.256	0.037	0.234	0.033	0.251	0.029
0.6-0.7			0.283	0.031	0.237	0.026	0.256	0.022
0.7-0.8			0.279	0.026	0.252	0.024	0.260	0.020
0.8-0.9			0.288	0.017	0.270	0.041	0.295	0.023
0.9-1.0			0.308	0.011	0.283	0.042	0.302	0.015

Table C.2. Averages and standard deviations of the measured concentrations of bromide-ion in soil for the whole Roswinkel field (ridges and furrows pooled).

Layer (m)	29 May		13 July		18 September	
	Average concentration ($mg\ dm^{-3}$)	Standard deviation ($mg\ dm^{-3}$)	Average concentration ($mg\ dm^{-3}$)	Standard deviation ($mg\ dm^{-3}$)	Average concentration ($mg\ dm^{-3}$)	Standard deviation ($mg\ dm^{-3}$)
0-0.1	4.03	4.23	0.43	0.29	3.16	1.86
0.1-0.2	8.16	7.41	0.52	0.61	1.84	1.87
0.2-0.3	6.23	6.06	0.78	1.08	1.22	1.74
0.3-0.5	6.06	7.28	2.15	2.45	2.26	2.17
0.5-0.7	2.04	3.19	5.31	3.53	5.39	2.67
0.7-0.9	< 0.7		8.81	6.28	7.11	4.09
0.9-1.1			11.96	9.76	6.56	6.32

Table C.3. Averages and standard deviations of the measured concentrations of carbofuran in soil for the whole Roswinkel field (ridges and furrows pooled).

Layer (m)	29 May		13 July		18 September	
	Average concentration (mg dm^{-3})	Standard deviation (mg dm^{-3})	Average concentration (mg dm^{-3})	Standard deviation (mg dm^{-3})	Average concentration (mg dm^{-3})	Standard deviation (mg dm^{-3})
0-0.1	2.66	0.51	0.394	0.220	0.076	0.041
0.1-0.2	1.34	1.18	0.225	0.058	0.076	0.059
0.2-0.3	0.32	0.39	0.148	0.126	0.036	0.033
0.3-0.5	0.09	0.12	0.097	0.084	0.015	0.015
0.5-0.7	0.001	0.002	0.076	0.097	0.030	0.050
0.7-0.9	0		0.010	0.009	0.014	0.030
0.9-1.1					0	

Appendix D Preliminary computations on water flow in Roswinkel soil

<u>Moisture retention</u>
Preliminary computations on the water flow in Roswinkel soil were carried out with the hydraulic relationships measured for one column of some soil layers by Crum et al. (2004). The experiences are reported in this Appendix. These relationships were not used in the computations for the main part of the study. Instead, the averaged relationships for a similar topsoil and subsoil presented by Wösten et al. (2001) were used as starting point in the main study (Section 9.1).

A first point of consideration is the saturated volume fraction of water in soil. This volume fraction is obtained by measurement/extrapolation in the laboratory experiment on the moisture retention curve. It can be compared with the total pore volume in soil, which can be calculated from the dry bulk density of the soil and the densities of the solid phases. Many measurements of the bulk density of the Roswinkel soil layers are available and these were averaged (Tables 2.3 and 8.1). Density of the mineral parts is taken to be 2650 kg m^{-3} and that of the organic matter to be 1470 kg m^{-3}.

The saturated volume fractions of water derived from the laboratory measurements (Table 2.4) and the calculated total pore volumes are compared in Table D.1. In all cases, the calculated total pore volume is (much) higher than the saturated volume fraction of water derived from the moisture retention measurement in the lab (Crum et al., 2004). Even in laboratory experiments, with ample wetting of the soil columns, there seems to be a rather high pore volume without water (e.g. because of hysteresis and entrapped air).

Table D.1. Comparison of saturated volume fractions of water, derived from laboratory measurement of moisture retention, with the calculated total pore volumes for layers of the Roswinkel soil.

Layer (m)	Dry bulk density (kg m^{-3})	Organic matter content (kg kg^{-1})	Total pore volume, calculated (m^3 m^{-3})	Saturated volume fraction water, lab (m^3 m^{-3})
Ridge, 0-0.1	1080	0.049	0.58	0.40
Furrow, 0-0.1	1210	0.049	0.53	0.37
0.3-0.4	1540	0.017	0.41	0.31
0.6-0.7	1810	0.006	0.31	0.27

An interesting question is what happens if the calculated total pore volumes are introduced as the water-saturated fractions into the moisture retention equations for the top layers (Table 2.4). Doing so results in volume fractions of water at field capacity (pressure head – 1.0 m; pF = 2) of 0.35 m^3 m^{-3} (ridges 0-0.1 m) and 0.37 m^3 m^{-3} (furrows 0-0.1 m). This is much higher than the field capacity in the field which is expected from the soil moisture measurements to be between 0.20 and 0.25 m^3 m^{-3} (Table 2.5). Thus the use of the total pore volumes in the moisture retention equation leads to a drastic over-estimation by the computation of moisture retention in the field.

The residual volume fraction of water Θres in very dry Roswinkel topsoil was reported by Crum et al. (2001) to be 0.045 $m^3\,m^{-3}$ (Table 2.4), which is higher than expected. Wösten et al. (2001) presented averaged moisture retention curves for several soil groups. They give a typical Θres value of 0.02 $m^3\,m^{-3}$ for humic sandy top layers and of 0.01 $m^3\,m^{-3}$ for sandy subsoils. We assume that the latter values are more reliable, because they were obtained by averaging many measurements.

On the basis of the measurements of soil moisture in the field samples (Table 2.5), the volume fraction of water Θ(-1.0) in the top soil at a pressure head of –1.0 m (pF=2) is expected to be in the range of 0.20 to 0.25 $m^3\,m^{-3}$. The question is now whether the moisture retention curves measured in the laboratory (Table 2.4) can be expected to describe the field situation. To check this, the moisture retention at pressure head $h_p = - 1.0$ m was calculated using the parameters for the retention curves obtained for ridge (0-0.1 m), furrow (0-0.1 m) and layer 0.3-0.4 m in the laboratory (Table 2.4). The only modification is that Θres is set at 0.02 $m^3\,m^{-3}$ (see above). This yields volume fractions of water Θ(-1.0) of 0.24 $m^3\,m^{-3}$ (ridge, 0-0.1 m), 0.25 $m^3\,m^{-3}$ (furrow, 0-0.1 m) and 0.17 $m^3\,m^{-3}$ (layer 0.3-0.4 m). The first two values are high in the range expected from the field measurements, but the third value is lower than expected on the basis of Table 2.5.

Wösten et al. (2001) also presented continuous translation equations, to derive moisture retention from soil composition. Introduction of the composition of the Roswinkel top layer (0.2 m) in the software tool "Staringreeks" gave a Θsat value of 0.52 $m^3\,m^{-3}$ and a Θ(-1.0) value of 0.38 $m^3\,m^{-3}$. These values are much too high in view of both lab measurements and field measurements for the Roswinkel topsoil.

Hydraulic conductivity
The saturated hydraulic conductivity Ksat measured for the Roswinkel soil layers (Crum et al., 2004; Table 2.4) ranges from 0.25 m d^{-1} in the topsoil to 0.10 m d^{-1} in the subsoil. These values can be compared with the values given for similar soils in the Staring Series (Wösten et al., 2001). For topsoil class B1 the latter gives Ksat = 0.23 m d^{-1} and for topsoil class B2 it gives Ksat = 0.13 m d^{-1}. A Ksat value of 0.15 m d^{-1} is assigned to subsoil O1. So the Ksat values obtained for the Roswinkel soil layers in the lab (Crum et al., 2004) are at the level expected on the basis of the Staring Series for similar soils (Wösten et al., 2001).

Wösten et al. (2001) also present continuous translation functions for Ksat on the basis of soil composition. This gives Ksat = 0.33 m d^{-1} for the top 0.2 m of the Roswinkel soil and Ksat = 1.35 m d^{-1} for the 0.6 to 1.0 m layer. The latter value seems to be too high. Bulk density is under-estimated and Θsat is over-estimated, as compared to the Roswinkel subsoil.

Simulation of water flow
Run PW1 with the SWAP-PEARL combination was carried out with the parameters of the hydraulic relationships obtained in the laboratory (Table 2.4). The only modification was to set the residual volume fraction of water Θ_{res} in the 0.3 m top layer to 0.02 $m^3\,m^{-3}$ and that of the deeper layers to 0.01 $m^3\,m^{-3}$ (Wösten et al., 2001). The parameters measured for the top 0.1 m (ridges and furrows) were averaged and assigned to the top 0.3 m of the soil profile. The parameters measured for the 0.3 to 0.4 m layer were assigned to the 0.3 to 0.5 m layer, while those measured for the 0.6 to 0.7 m layer were assigned to the soil below 0.5 m. Groundwater flux q_b from the bottom of the soil system was described with the option of an exponential function. The starting values of coefficient a_{fb} = - 0.0112 $m^3\,m^{-2}\,d^{-1}$ and exponent b_{fb} = - 2.5 m^{-1} were taken from the Dutch Standard scenario.

The volume fractions of water computed in Run PW1 for the upper part of the soil profile (not shown) were substantially higher than those measured in the growing season of 2000 (Table 2.5). Further, the groundwater table was computed to be distinctly shallower than measured on 29 May and 13 July 2000. First of all, enhancement of the downward groundwater discharge seemed to be needed.

In Run PW2, the coefficient a_{fb} for downward groundwater flow was doubled to 0.0224 $m^3\,m^{-2}\,d^{-1}$. The depth of the groundwater table was described better now (not shown). As an example, when the groundwater table is at 0.5 m depth, the used combination of a_{fb} = 0.0224 $m^3\,m^{-2}\,d^{-1}$ and b_{fb} = - 2.5 m^{-1} gives a downward groundwater flux of 6.4 mm d^{-1}, which is rather high. When the groundwater table is at 1.0 m depth, the downward bottom flux q_{bot} is calculated to be 1.8 mm d^{-1}. In most cases, volume fraction of water in the top 0.3 m of the soil profile (not shown) was still over-estimated in Run PW2.

The parameters for the hydraulic relationships in the top layer are considered now in more detail. The top 0.1 m of the ridges contains comparatively loose soil (hilled up). The top 0.1 m of the furrows can be considered to be more representative for the overall top 0.3 m of the soil profile. So in Run PW3, the parameter values obtained for the top of the furrow (Table 2.4) were assigned to the top 0.3 m of the profile.

In Run PW3, the volume fractions of water in the top 0.3 m layer of the soil profile (not shown) were still over-estimated. This is expected to be caused by the hysteresis in soil moisture retention behaviour. In the laboratory, soil moisture retention at drying (starting from wet soil) is measured. In the field, soil moisture retention follows a set of scanning curves, in between the drying curve and the wetting curve as extremes. A possible approach to approximate the scanning curves by a single retention curve is to set Θsat at a lower value in the computations.

At some comparison times, the volume fraction of water in the 0.3 to 0.5 m layer was under-estimated by the PW3 calculation. The measured moisture profiles did not show a dip in the volume fraction of water at these depths. It seems that the single-column measurement (0.3 to 0.4 m) of moisture retention in the laboratory under-estimates average moisture retention in the field. In view of the gradual course of soil

moisture with depth it is preferred to have a single moisture retention curve for the upper 0.5 m of the soil profile.

In Run PW4, moisture retention in the top 0.5 m of the soil was described by a single retention curve. A lower value of Θsat = 0.32 $m^3 m^{-3}$ was used to approximate the scanning curves of moisture retention. The value of Θres in this layer was set at 0.02 $m^3 m^{-3}$. The other parameter values were taken from the lab measurement for furrow (0 to 0.1 m) (Table 2.4). In the layer 0.5 to 0.8 m, Θsat was set at the lower value of 0.28 $m^3 m^{-3}$, to account for hysteresis, while Θres was maintained at 0.01 $m^3 m^{-3}$. The other parameter values were taken from the lab measurement for 0.6 to 0.7 m depth (Table 2.4). It was assumed that hysteresis did not have an effect below 0.8 m depth (Θsat maintained at 0.31 $m^3 m^{-3}$).

The volume fractions of water (VFW's) calculated with Run PW4 for the four soil measuring times in the summer of 2000 are given in Figures D.1 to D.4. They are compared with a range of measured values, represented by 1) the average minus the standard deviation and 2) the average plus the standard deviation (called SD range).

The VFW's calculated for 8 May (Figure D.1) are mostly close to the lower boundary of the SD range. There is a dip in calculated VFW at 0.55 m depth. Some VFW's measured for the deepest layers are remarkably low; possibly some water was lost from the wet subsoil during sampling (this may hold for all sampling times).
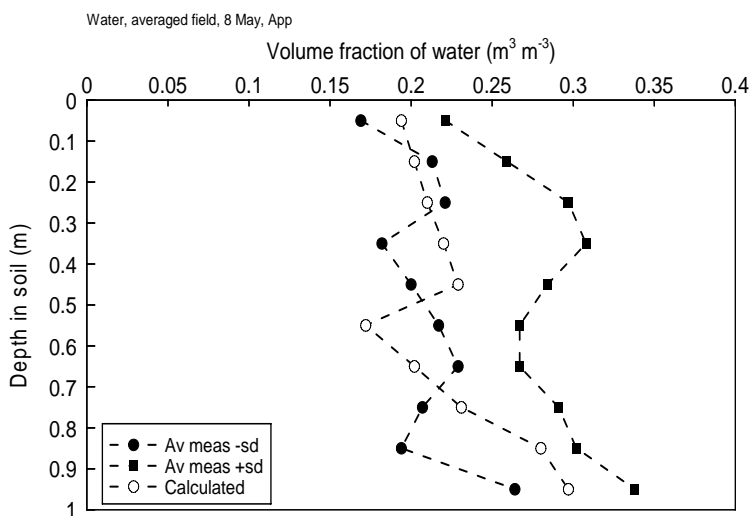

Figure D.1. Comparison of computed (averaged field) and measured (furrows) volume fractions of water in soil on 8 May 2000. The measurements are represented by their SD range.

The comparison of VFW values in soil for 10 May, given in Table D.2, shows that the calculated values (Run PW4) are well within the SD range of the measurements.

Table D.2. Comparison of computed (Run PW4) and measured volume fractions of water in the top of the averaged soil for 10 May 2000.

Layer (m)	Volume fraction of water ($m^3\,m^{-3}$)	
	Computed	SD range of measurements
0-0.1	0.20	0.13-0.23
0.1-0.2	0.21	0.16-0.24

For 29 May the calculated VFW's (Figure D.2) are mostly well within the SD range of the measurements. However, some values are close to the upper limit of the range.
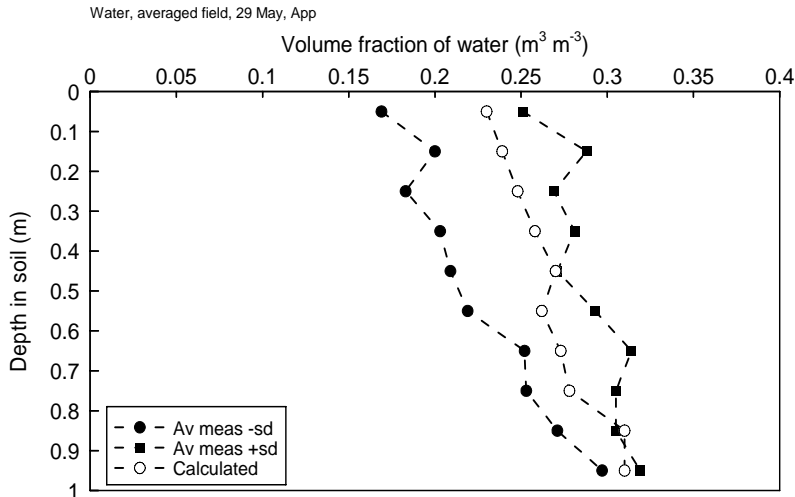

Figure D.2. Comparison of computed and measured volume fractions of water in the averaged soil on 29 May 2000.

The VFW's calculated for 13 July (Figure D.3) are close to the upper limit of the SD range of measurements or even somewhat above this limit.
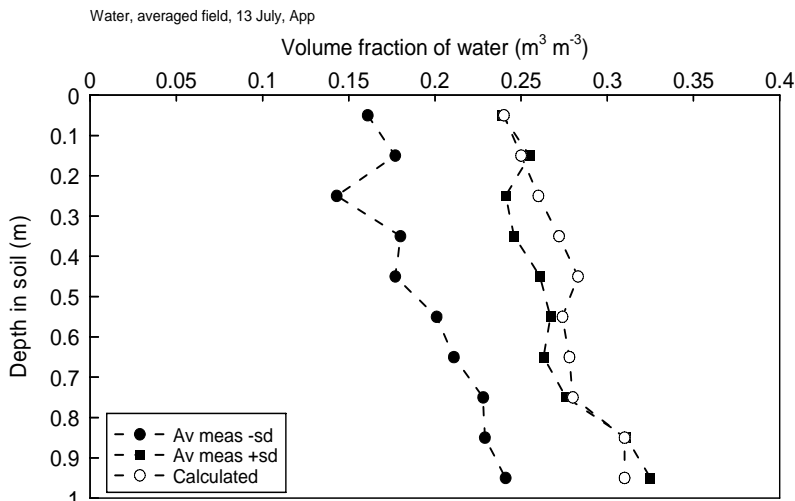

Figure D.3. Comparison of computed and measured volume fractions of water in the averaged soil on 13 July 2000.

The calculation for 18 September (Figure D.4) gave VFW values for the top and bottom layers well within the SD range of the measurements. However, there is a clear dip in the calculated VFW at 0.55 m depth.
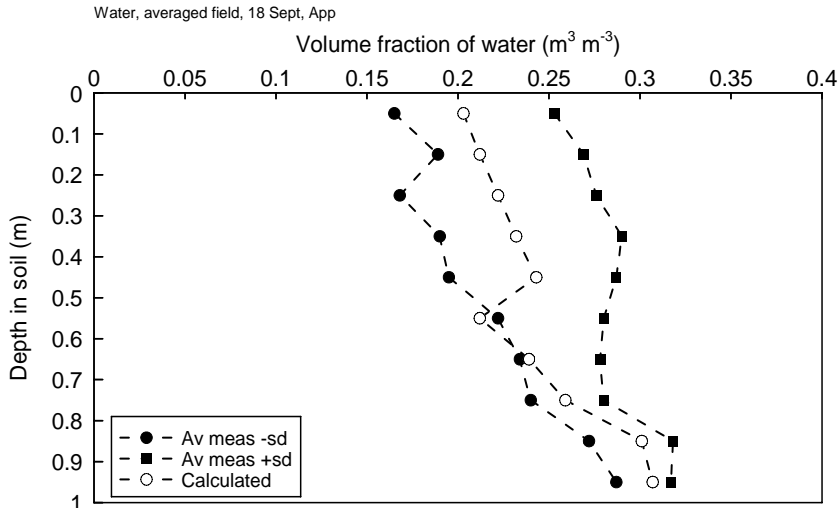

Figure D.4. Comparison of computed and measured volume fractions of water in the averaged soil on 18 September 2000.

In summary, there were wide ranges of VFW values measured at a certain depth in the Roswinkel soil. The calculated VFW's were 1) well within the SD range, 2) close to its lower limit, 3) close to its upper limit or 4) somewhat outside the SD range (both above and below).

The calculated depths of the groundwater table can be compared with the ranges of measured depths. The comparison for the summer of 2000 is given in Table D.3. At three times, calculated groundwater level is within or close to the SD range of measured levels. At one time, calculated depth is distinctly shallower and also at one time it is distinctly deeper than the SD range of measurements.

Table D.3. Comparison of the computed (Run PW4) and measured depths of the groundwater table in the summer of 2000. Four hand measurements at each time. SD range: average ± standard deviation.

Date in 2000	Depth of groundwater table (m)		Computed	Ratio measured/computed
	Hand-measured			
	Average	SD range		
29 May	0.90	0.80-0.99	1.03	0.87
28 June	1.29	1.22-1.36	0.96	1.34
19 July	1.10	1.01-1.19	1.00	1.10
18 August	1.30	1.21-1.38	1.35	0.96
31 August	1.11	1.01-1.21	1.30	0.85

There are some arguments for not using the soil moisture retention curves measured for Roswinkel soil layers (Crum et al., 2004; Table 2.4):

- only one measurement per (type of) soil layer has been made;
- the values stated for the residual volume fraction of water are likely to be too high;
- the soil moisture profiles measured in the field do not show the dip expected from the retention curve for the intermediate layer;
- averaged relationships derived from many measurements for topsoils and subsoils similar to those for Roswinkel are available;
- irrespective of the use of the starting relationships, calibration against the measured moisture profiles seems to be needed.

The saturated hydraulic conductivities Ksat reported by Crum et al. (2004) for the single Roswinkel soil columns are close to the averaged values presented by Wösten et al. (2001). The calculated soil moisture profile in soil may not be very sensitive to the Ksat value.

Appendix E   Detailed input data for the soil layers of the ridge and furrow systems.

Several measurements for the Roswinkel soil were carried out for the level field (no ridges and furrows) (Section 2.2). These were elaborated to detailed input data for the averaged field (Table 8.1). This Appendix presents the translation of level-field soil data to those for the separate ridge and furrow systems.

*Table E.1. Properties of each soil horizon of the **ridge system**, most of them derived from the measurements for the soil of the Roswinkel field.*

Depth soil horizon (m)	Sand (> 50 μm) (%)	Silt (2-50 μm) (%)	Clay (< 2 μm) (%)	Organic matter (%)	Bulk density (kg m^{-3})	pH	Depth factor f_z (-)
0-0.1	87.9	8.5	3.6	4.9	1080	4.5	1.0
0.1-0.2	87.9	8.5	3.6	4.9	1190	4.5	1.0
0.2-0.3	87.9	8.5	3.6	4.9	1260	4.5	1.0
0.3-0.4	87.9	8.5	3.6	3.1	1450	4.5	1.0
0.4-0.5	92.0	5.4	2.6	1.7	1620	4.7	0.98
0.5-0.6	93.1	4.6	2.3	1.2	1690	4.8	0.91
0.6-0.7	94.5	3.5	2.0	0.6	1790	4.8	0.80
0.7-0.8	95.1	2.9	2.0	0.5	1810	5.0	0.67
0.8-0.9	95.7	2.3	2.0	0.3	1810	5.0	0.50
0.9-1.0	95.7	2.3	2.0	0.3	1810	5.0	0.33
1.0-1.1	95.7	2.3	2.0	0.3	1810	5.0	0.10
1.1-2.2	95.7	2.3	2.0	0	1810	5.0	0
2.2-3.1	95.7	2.3	2.0	0	1810	5.0	0

*Table E.2. Properties of each soil horizon of the **furrow system**, most of them derived from the measurements for the soil of the Roswinkel field.*

Depth soil horizon (m)	Sand (> 50 μm) (%)	Silt (2-50 μm) (%)	Clay (< 2 μm) (%)	Organic matter (%)	Bulk density (kg m^{-3})	pH	Depth factor f_z (-)
0-0.1	87.9	8.5	3.6	4.9	1210	4.5	1.0
0.1-0.2	87.9	8.5	3.6	3.1	1360	4.5	1.0
0.2-0.3	92.0	5.4	2.6	1.7	1550	4.7	0.98
0.3-0.4	93.1	4.6	2.3	1.2	1630	4.8	0.91
0.4-0.5	94.5	3.5	2.0	0.6	1720	4.8	0.80
0.5-0.6	95.1	2.9	2.0	0.5	1780	5.0	0.67
0.6-0.7	95.7	2.3	2.0	0.3	1810	5.0	0.50
0.7-0.8	95.7	2.3	2.0	0.3	1810	5.0	0.33
0.8-0.9	95.7	2.3	2.0	0.3	1810	5.0	0.10
0.9-2.0	95.7	2.3	2.0	0	1810	5.0	0
2.0-2.9	95.7	2.3	2.0	0	1810	5.0	0

Appendix F Water flow in ridge and furrow systems with flux function for groundwater discharge, applied to the systems separately

In the present computations for the ridge and furrow systems, the flux boundary condition for groundwater flow was used as calibrated for the whole (averaged) field (Section 9.2). Thus the coefficients for the exponential flux function were taken to be a_{fb} = - 0.03 m^{3}m^{-2} d^{-1} and b_{fb} = - 3.0 m^{-1}. The "long flow-off" option was used here: the 20% flow-off of water from the ridges to the furrows was simulated to occur in the whole measuring period.

The volume fractions of water (VFW's) calculated for the top of the ridge systems on 10 May are compared with the measurements (confined to two layers) in Table F.1. The calculated VFW values are well within the SD range of the measurements.

Table F.1. Comparison of calculated and measured volume fractions of water in the top of the ridges on 10 May. Groundwater discharge described with exponential function.

Layer (m)	Volume fraction of water (m^3 m^{-3})	
	Calculated	SD range of measurements
0-0.1	0.16	0.11-0.21
0.1-0.2	0.17	0.15-0.22

The volume fractions of water (VFW's) computed for the ridge system on 29 May are compared with the measurements in Figure F.1. Nearly all the computed VFW's are well within the SD range of the measurements.
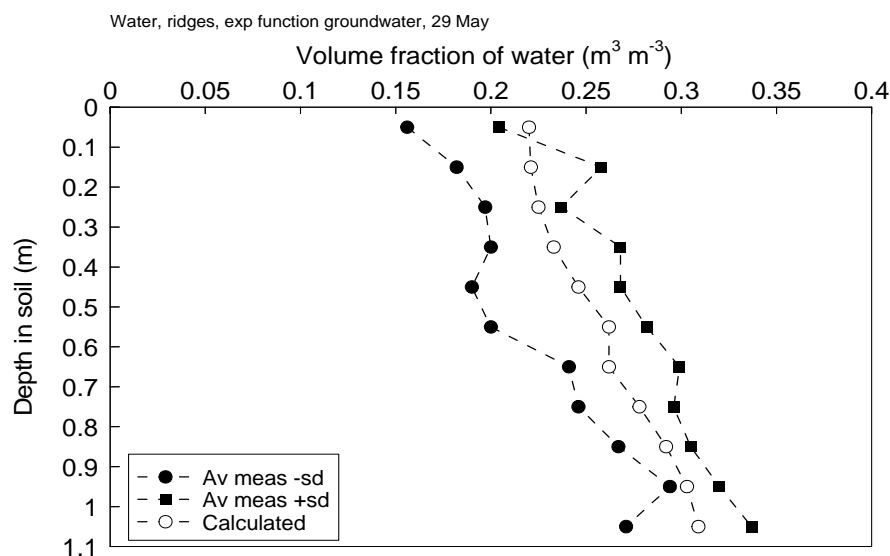

Figure F.1. Comparison of computed and measured volume fractions of water in the soil of the ridge system on 29 May. The measurements are represented by their SD range.

Figure F.2 shows the computed and measured VFW's for the ridge systems on 13 July. Most of the computed VFW values are close to the upper limit of the SD range of the measurements, while others are well within this range. Only the VFW value for the greatest depth is at the lower limit of the SD range.
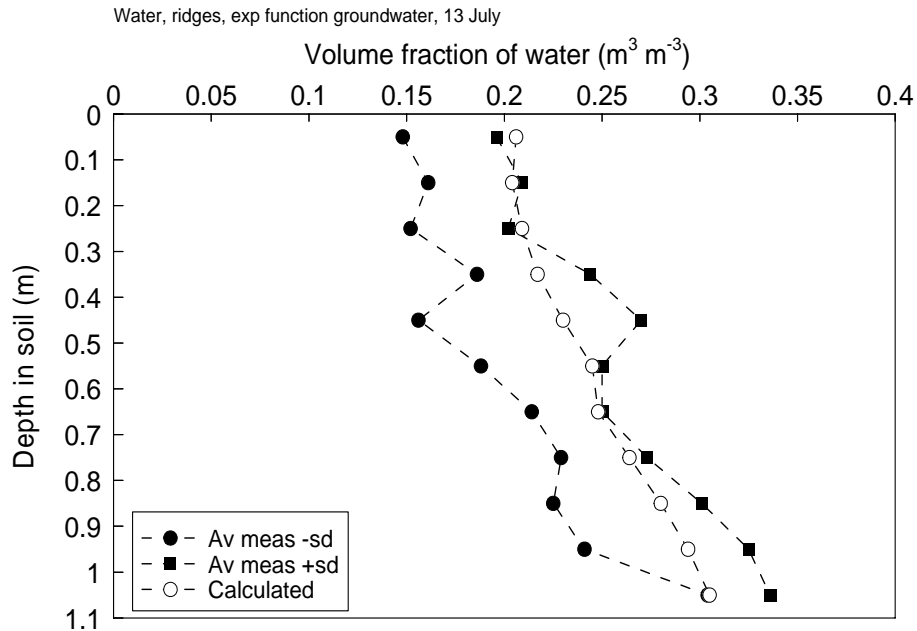
Water, ridges, exp function groundwater, 13 July

Figure F.2. Comparison of computed and measured volume fractions of water in the soil of the ridge system on 13 July.

The VFW's computed for the ridge system on 18 September are shown in Figure F.3. In the top 0.5 m of the soil, the computed VFW's are close to the lower limit of the SD range of measurements. Below that depth, the computed VFW's are lower than the SD range of measurements.
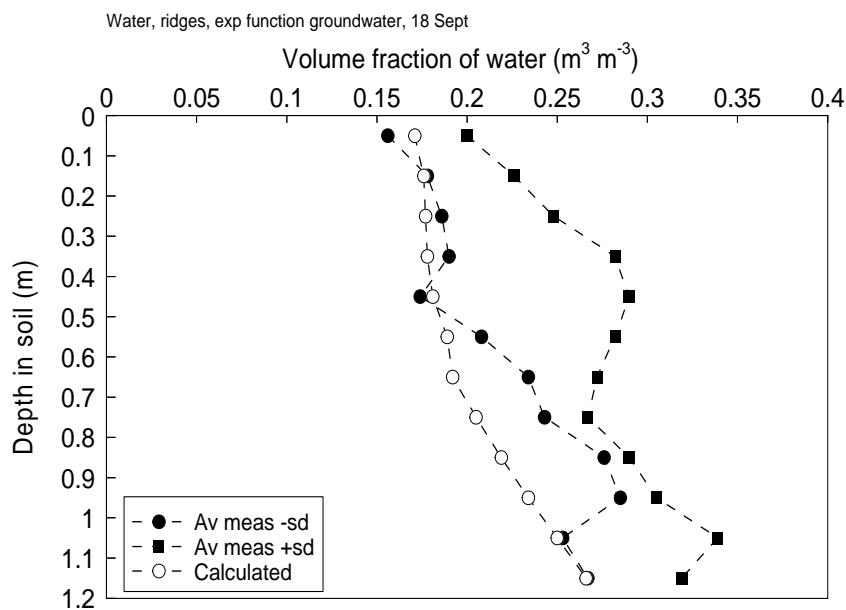
Water, ridges, exp function groundwater, 18 Sept

Figure F.3. Comparison of computed and measured volume fractions of water in the soil of the ridge system on 18 September.

Alterra-rapport 1750

The ratio between computed and measured depth of the groundwater table in the ridge system was on average 1.14 (s.d. = 0.19). Especially at the end of the growing season (August and September), the depth of the groundwater table was computed to be much deeper than measured. This explains the low VFW values calculated for the subsoil of the ridge system on 18 September (Figure F.3). The deeper calculated groundwater table is mainly caused by the lower water infiltration into the ridges, caused by flow-off to the furrows.

The depth of the groundwater table computed for the furrows was on average 0.87 times (s.d. = 0.18) that measured in the field. In practice, water will flow from the furrow systems to the ridge systems, especially in and near the water-saturated zone. Therefore, another lower boundary condition for water flow is needed when simulating separate ridge and furrows systems (Section 12.2). This should replace the "flux function" boundary condition derived for the whole (averaged) field.